Stabilizing and Equalizing Mechanisms Alter Community Coexistence and Macroevolutionary Diversity Patterns

By

Lauren G. Shoemaker

B.A., Colorado College, 2011

A thesis submitted to the

Faculty of the Graduate School of the

University of Colorado

in partial fulfillment of the requirement for the degree of

Doctor of Philosophy

Department of Ecology and Evolutionary Biology

2017

This thesis entitled:

Stabilizing and Equalizing Mechanisms

Alter Community Coexistence and Macroevolutionary Diversity Patterns

Written by Lauren G. Shoemaker

has been approved for the Department of Ecology and Evolutionary Biology

_____

Prof. Brett A. Melbourne

_____

Prof. Aaron Clauset

_____

Prof. Kendi Davies

_____

Prof. Daniel F. Doak

_____

Prof. Christy M. McCain

Date _____

The final copy of this thesis has been examined by the signatories, and we find that both the content and the form meet acceptable presentation standards of scholarly work in the above mentioned discipline.

Shoemaker, Lauren G. (Ph.D., Ecology and Evolutionary Biology)

Stabilizing and equalizing mechanisms alter community coexistence and macroevolutionary diversity patterns

Thesis directed by Prof. Brett A. Melbourne and Prof. Aaron Clauset

Ecological variability, both across space and through time, plays a critical role in maintaining the incredible range of biodiversity observed in nature and is foundational to coexistence theory. Using a combination of analytical techniques, simulation models, and novel paleobiology databases, I examine how ecological variability contributes to coexistence, or how competing species are able to persist in a given environment. I quantify the strength of coexistence in spatially structured communities and the relative importance of species similarities (equalizing mechanisms) and species differences (stabilizing mechanisms) in maintaining biodiversity across space and time. I find that trait-tradeoffs among species, abiotic heterogeneity, stochasticity, and dispersal limitation within spatially structured communities all have unique signatures of coexistence mechanisms. I additionally show that coexistence theory allows us to analyze more complex communities with multiple assembly mechanisms. While coexistence theory exhibits robust, unique signatures across assembly mechanisms, other, more commonly used methods, such as the beta-null deviation measure, are unable to infer community assembly processes from patterns in beta-diversity. This is especially evident for the presence-absence based measure when compared to the abundance-based measure. Finally, I extend the stabilizing and equalizing framework of coexistence theory beyond its use in community ecology to examine macroecological patterns in mammalian diversity. I show that body mass diversity

and its evolution can be well-approximated using primarily equalizing mechanisms. This trend holds across terrestrial mammals, a mammalian sub-clade (Equidae), and even across vastly different environments. Both marine (cetaceans) and terrestrial mammals exhibit similar body mass distributions and evolution, where environmental constraints determine the minimum size above which equalizing processes interact in a predictable way to create a right-skewed body mass distribution. Across this work, I find that stabilizing mechanisms are critical for coexistence in spatially structured communities, but equalizing mechanisms effectively predict patterns in mammalian body mass diversity across evolutionary time scales. Generally, the equalizing and stabilizing framework of coexistence theory provides a mechanistic understanding of patterns in biodiversity, both at the community and macroecological scale.

Dedication

To all of my incredibly supportive family and friends.

Acknowledgements

I am so thankful to my wonderful family—Topher Weiss-Lehman, Jennifer Shoemaker, Tom Shoemaker, and Mark Shoemaker—for their support and encouragement along the way. Thanks to my advisors, Brett A. Melbourne and Aaron Clauset, for their support and guidance throughout this process. I have been fortunate to work with many wonderful collaborators throughout my dissertation, including Mauricio Cantor, Lauren Sullivan, Karen Abbott, Kevin Bracy Knight, Reniel Cabral, Jonathan Chase, Kendi Davies, César Flores, Stan Harpole, Caroline Havrilla, Andreas Huth, Diana Nemergut, Carter Tillquist, Franziska Taubert, Melinda Varga, Hal Whitehead, the sNiche working group, the 2016 EBIO Writing Cooperative, Metacommunity 2.0 working group, and the Nutrient Network. Thank you to my lab members and to the incredibly supportive Ecology and Evolutionary Biology Department, including the Writing Co-op, Modeling Reading Group, and QDT for brainstorming, help with analyses, and reading numerous manuscript drafts. Many faculty have been very gracious with their time including Nichole Barger, Deane Bowers, Bill Bowman, Kendi Davies, and Ginger Ferguson. Thank you to my fellow ecology graduate students Amy Churchill, Carrie Havrilla, Amanda Hund, Allison Louthan, and Helen McCreery for the laughter, runs, ski days, and support along the way.

Contents

Chapters

Tables

Table

Figures

Figure

Chapter 1

Introduction

The remarkable range of biodiversity observed in the natural world has, paradoxically, long served as a source of both unification and tension within ecology. Attempts to explain patterns of species diversity have led to the heated debate of niche versus neutral theory (Hubbell 2001, Chase and Leibold 2003, Leibold and McPeek 2006), the creation of coexistence theory (Tilman 1982, Chesson 2000a,b), and an appreciation of the importance of scale in structuring communities (Hutchinson 1959, Chase and Knight 2013). Common among these research fields is the acknowledgement that ecological communities are highly complex systems. They consist of diverse assemblages of species, all with potentially unique pair-wise and higher-order interactions, nonlinear population dynamics, and feedbacks both among different species and between species and the abiotic environment.

Attempts to make sense of the vast amount of complexity inherent in communities have led ecologists down disparate paths in search of solutions. For example, in niche theory, biodiversity is generally hypothesized to be the outcome of a 'niche space' consisting of multiple dimensions, such as species' water, light, and nutrient requirements (Hutchinson 1959). Species are hypothesized to segregate in this high-dimensional niche space, yielding diverse communities of species, where each species occupies its own, unique region (i.e. niche) of this ecospace. While niche theory provides an intuitive explanation for explaining the vast complexity we observe in ecological communities, it is difficult to disprove niche theory in a given ecosystem—or even define an underlying null model for communities—because of the inherent complexity and high-dimensionality assumed by the theory. Neutral theory (Hubbell 2001) arose as a direct response to these challenges inherent in niche theory. In direct contradiction to niche theory,

neutral theory begins by assuming that all species are ecologically identical to one another, and hypothesizes that patterns in species assemblages are statistical products of random sampling and dynamical random walks through space and time (Hubbell 2001, Vellend et al. 2014). Neutral theory has commonly been evoked in highly diverse communities with relatively minor environmental variation, such as rainforests (Chave and Leigh 2002; Wiegand et al. 2012) and coral reefs (Hubbell 1997, Volkov et al. 2007, though see Dornelas et al. 2006). It currently serves as both an explanation of observed patterns and, alternatively, as a null model (or base null model, altered to include more realistic and complex scenarios) against which to test aspects of niche theory (Rosindell et al. 2012).

Within the disparate niche and neutral views of communities, a unifying concept is the idea of ***coexistence*** (Tilman 1982, Chesson 2000b), which examines how competing species persist in a given environment. While the niche versus neutral framework was originally presented as a dichotomy, community ecology now embraces that these frameworks instead represent two ends of a spectrum (Leibold and McPeek 2006, Adler et al. 2007). Co-occurrence of seemingly ecologically equivalent species does not necessarily imply neutral dynamics, as niche dynamics also can yield such patterns (Leibold and McPeek 2006). Species may also be ecological equivalent in a given trait, but divergent in other critical traits, satisfying different elements of both niche and neutral theory.

Coexistence theory provides a framework for analyzing communities along the niche to neutral spectrum, without having to classify communities within a dichotomous framework. Instead, in coexistence theory, the relative importance of niche and neutral processes can be partitioned and directly compared. Regardless of the underlying complexity inherent in communities, the stable biodiversity is quantified as the number of species coexisting in a

community. Stable coexistence is defined as the inherent dynamical tendency of species to recover from low population density while in the presence of the other species in the community (Armstrong and McGehee 1980, Turelli 1981). Without this tendency, coexistence is not stable, and species within a community may be trending towards **competitive exclusion**, as other species in the community outcompete them. Or, alternatively, coexistence may be unstable—as occurs in neutral theory (Hubbell 2001). In this case, no species is outcompeting one another, but rather, species drift towards extinction and are unable to recover when at low densities (Vellend et al. 2014).

Regardless if a community exhibits stable coexistence, competitive exclusion, or unstable coexistence, the magnitude of change in population size for a species at low-density quantifies the **coexistence strength** of a species. If a species tends to recover fast from low-density, then it is said to coexist strongly (Shea and Chesson 2002). Alternatively, if a species decreases quickly from low-density, then it is strongly outcompeted in the community. Coexistence strength can be further partitioned into two general categories to examine the relative importance of niche and neutral processes: ***stabilizing*** and ***equalizing mechanisms*** (Chesson 2000a,b; Adler et al. 2007). Stabilizing mechanisms, which are niche differences between species, minimize interactions between competitors by increasing intraspecific competition relative to interspecific competition (Adler et al. 2007). They include differences in species' optimal abiotic conditions, nonlinear competitive dynamics, and the covariance between a species' intrinsic fitness and its population size across a landscape (Chesson 2000a, Snyder and Chesson 2003, Snyder et al. 2005, Chesson 2008). For example, spatial heterogeneity in abiotic conditions, dispersal limitation that mediates the amount of spatial overlap between species, or trait-tradeoffs causing species to have higher fitness in different habitats all increase spatially stabilizing mechanisms of coexistence

(Amarasekare and Nisbet 2001, Yu and Wilson 2001). Taken together, stabilizing mechanisms quantify the strength of the **spatial niche** in a spatially varying environment, and alternatively, the **temporal niche** in a temporally varying environment (Shea and Chesson 2002).

In contrast, equalizing mechanisms measure the degree of neutrality in a community. For example, if a community were fully neutral on the niche-to-neutral spectrum, than only equalizing mechanisms would be present and the community would exhibit unstable coexistence. Equalizing mechanisms are calculated by determining the fitness differences between species if all environmental variability was averaged. If equalizing fitness differences between species are large (species are not ecologically equivalent), strong stabilizing mechanisms are required for coexistence. For example, if one species has a much higher intrinsic growth rate than a second species, strong stabilizing mechanisms (e.g. niche differences) are required such that the first species does not competitively outcompete the second. This may occur in a highly heterogeneous environment with dispersal limitations, in which case the spatial niche would yield coexistence of both species. Conversely, if equalizing differences are small (species are more equal, e.g. if they have similar intrinsic growth rates), only weak stabilizing mechanisms are necessary for coexistence (Chesson 2000, Adler et al. 2007).

Despite the flexibility of coexistence theory and its popularity within community ecology, it has not been directly linked with other major theories of biodiversity, such as metacommunity theory (i.e. a theory for spatially structured communities consisting of discrete habitat patches). Furthermore, most studies of coexistence theory do not directly quantify coexistence strength and partition it into its mechanistic components, nor compare its ability to infer diversity patterns from community assembly processes against more commonly used measures. Finally, the equalizing and stabilizing framework of coexistence theory was originally

created for communities, but can be extended beyond communities to examine macroecological patterns of diversity, as I present in my dissertation.

1.1 Overview of Chapters

My dissertation focuses on quantifying coexistence strength across ecosystems and determining the relative roles of equalizing and stabilizing mechanisms in maintaining biodiversity both in communities and at the larger macroecological scale. I combine theoretical and empirical analyses to explore coexistence in relatively simple simulated two-species metacommunities, more complex simulated metacommunities of 25 species, and novel empirical databases of diverse assemblages of species within a single clade (e.g. organisms that evolved from a common ancestor) spanning millions of years.

Specifically, in chapters two and three, I focus on the role of spatial structure and variation across space in maintaining species richness (defined as the total number of species at both the local and regional scale, i.e. alpha- and gamma-diversity). My second chapter links four commonly considered 'paradigms' of spatial structure from metacommunity theory (Leibold et al. 2004, Holyoak et al. 2005) to the equalizing and stabilizing framework of coexistence theory (published as Shoemaker and Melbourne 2016 in *Ecology*). The four paradigms encompass multiple key community assembly processes, including dispersal, trait-tradeoffs, neutral theory, and habitat heterogeneity (Leibold et al. 2004), and I explore the connection between these processes, coexistence strength, and the relative importance of equalizing and stabilizing mechanisms. To do so, I create a single modeling framework, simulate spatial community dynamics through time, and derive analytical solutions for stabilizing and equalizing coexistence mechanisms for each of the four paradigms. Using this framework, I subsequently explore how

spatial heterogeneity in habitat quality, trait-tradeoffs, dispersal, and stochasticity alter the relative contributions of equalizing and stabilizing mechanisms to coexistence. I additionally demonstrate how coexistence theory provides a single framework for comparing metacommunities of varying complexity, including metacommunities that are too complex to fit within the 'paradigm' framework.

Chapter three combines mechanistic modeling with a commonly-used empirical diversity measure to connect the conceptual framework from chapter two to empirical measures of diversity across space (Chase et al. 2011). I focus on the beta-null deviation measure, which is commonly evoked when determining the relative role of niche (stabilizing) and neutral (equalizing) assembly mechanisms in community structure (published as Tucker and Shoemaker et al. 2016 in *Oikos*). Using simulations of metacommunities with known assembly mechanisms—both with and without biological stochasticity, I show that the beta-null deviation measure is unreliable in its ability to correctly infer underlying community assembly mechanisms and stabilizing and equalizing structure. The abundance-based metric (Kraft et al. 2011, Stegen et al. 2013) is more robust, however, than the presence-absence based metric (Chase et al. 2011).

While chapters two and three rely on analytical, simulation, and statistical methods to examine coexistence in spatially varying habitats, chapters four and five explore patterns in diversity across temporal—rather than spatial—scales. I extend the equalizing and stabilizing framework commonly used in community ecology to examine macroevolutionary patterns of mammalian taxonomic and body mass diversity. To do so, I combine extant data on species body masses with novel databases I construct of extinct species' masses and first- and last-appearances. I then fit a partial differential equation model to extant body size data and patterns

in mammalian body size diversity across evolutionary time. Using this model, I infer the relative importance of equalizing and stabilizing mechanisms in maintaining diversity in body masses. The model is nearly-neutral and composed of two equalizing processes shared among species: 1. a physiological minimum body size and 2. Cope's rule, or the tendency for lineages to increase in body size through time (Alroy 1998, Hone and Benton 2005). The model also includes a stabilizing, species-specific extinction risk, as larger species have higher risks of stochastic extinction events (Clauset and Erwin 2008, Clauset et al. 2009).

In chapter four, I measure the relative importance of these processes versus species richness in predicting body size diversity through time in the Equidae sub-clade (published as Shoemaker and Clauset 2014 in *Ecology Letters*). I find that patterns of body size previously observed in terrestrial mammals more generally (Clauset and Erwin 2008) follow similar patterns in the Equidae sub-clade. Furthermore, over 90 percent of the maximum size of Equidae through time can be predicted using only the simple stabilizing and equalizing mechanisms described above. These changes in maximum size are, surprisingly, largely independent of taxonomic diversity. Chapter five compares marine (cetaceans) and terrestrial mammals to examine the universality of these processes, exploring commonalities and divergences in patterns across environments. I find that patterns in mammalian body size evolution are remarkably environmentally independent at the macroevolutionary scale. Environment dictates the minimum physiological size above which body size diversity evolves in a manner that can be well approximated by equalizing mechanisms (e.g. a random-walk of body sizes biased by Cope's rule) along with a size-dependent extinction risk.

Finally, in chapter six, I summarize my key results examining processes that maintain and promote biodiversity across both space and time. I highlight how ecological and

evolutionary processes, such as dispersal, trait-tradeoffs, stochasticity, and speciation relate to the equalizing and stabilizing framework of coexistence theory and briefly discuss future directions for examining the relative importance of equalizing and stabilizing mechanisms in maintaining diversity across both space and time.

Chapter 2

Linking Metacommunity Paradigms to Spatial Coexistence Mechanisms

Lauren G. Shoemaker and Brett A. Melbourne

Published as: Shoemaker, L. G. and Melbourne, B. A. (2016), Linking metacommunity paradigms to spatial coexistence mechanisms. Ecology, 97: 2436–2446. doi:10.1002/ecy.1454.

Four metacommunity paradigms—usually called neutral, species sorting, mass effects, and patch dynamics, respectively—are widely used for empirical and theoretical studies of spatial community dynamics. The paradigm framework highlights key ecological mechanisms operating in metacommunities, such as dispersal limitation, competition-colonization tradeoffs, or species equivalencies. However, differences in coexistence mechanisms between the paradigms and in situations with combined influences of multiple paradigms are not well understood. Here, we create a common model for competitive metacommunities, with unique parameterizations for each metacommunity paradigm and for scenarios with multiple paradigms operating simultaneously. We derive analytical expressions for the strength of Chesson's spatial coexistence mechanisms and quantify these for each paradigm via simulation. For our model, fitness–density covariance, a concentration effect measuring the importance of intraspecific aggregation of individuals, is the dominant coexistence mechanism in all three niche-based metacommunity paradigms. Increased dispersal between patches erodes intraspecific aggregation, leading to lower coexistence strength in the mass effects paradigm compared to species sorting. Our analysis demonstrates the potential importance of aggregation of individuals (fitness–density covariance) over co-variation in abiotic environments and competition between

species (the storage effect), as fitness–density covariance can be stronger than the storage effect and is the sole stabilizing mechanism in the patch dynamics paradigm. As expected, stable coexistence does not occur in the neutral paradigm, which requires species to be equal and emphasizes the role of stochasticity. We show that stochasticity also plays an important role in niche-structured metacommunities by altering coexistence strength. We conclude that Chesson's spatial coexistence mechanisms provide a flexible framework for comparing metacommunities of varying complexity.

2.1 Introduction

Metacommunity theory has significantly increased our understanding of the role of spatial heterogeneity, spatial scales, and dispersal in community structure (Amarasekare 2003, Leibold et al. 2004, Holyoak et al. 2005, Moritz et al. 2013). Local communities (patches) connected via dispersal form metacommunities, meaning metacommunities may take a multitude of forms depending on patch structure, ease of dispersal between patches, environmental heterogeneity, and species-specific traits. Metacommunity models, and the natural systems they represent, thus could encompass an arbitrarily large parameter space. However, many metacommunities exhibit similar dynamics, leading to a theoretical and empirical focus on four metacommunity types, which were formalized and termed the metacommunity paradigms by Leibold et al. (2004). The paradigm framework reduces the range of possible metacommunity types, and their corresponding model parameterizations, to a smaller representative subset. The four paradigms—neutral, species sorting, mass effects, and patch dynamics—present a simplified view of spatially structured communities and provide a framework for comparing community dynamics and co-occurrence patterns from both theoretical and empirical perspectives (Leibold et al. 2004; Holyoak et al. 2005). The four paradigms are described in

detail in Leibold et al. (2004) and Holyoak et al. (2005) but we describe them briefly here.

In the *neutral paradigm* species are demographically equivalent and all respond to the environment in the same manner (Bell 2000, Hubbell 2001, Leibold et al. 2004). Dynamics of stochastic neutral metacommunities are governed by ecological drift, where communities follow a random walk through time (Vellend 2010). Neutral metacommunity dynamics have been observed empirically in systems ranging in scale from aquatic microbial communities (Ostman et al. 2010) to tropical trees in Panama (Jabot et al. 2008).

In comparison, species sorting, mass effects, and patch dynamics are niche-based paradigms, where species systematically differ from one another. The *species sorting* and *mass effects* paradigms fall along a continuum from low to moderate dispersal rates (Mouquet and Loreau 2003, Loeuille and Leibold 2008). They require patches to be heterogeneous in environmental conditions, and each species is better adapted to a specific patch type, often via higher fecundity or survival (Leibold et al. 2004). In the species sorting paradigm dispersal rates are low and equal among species, leading to high abundance of a species in its optimal patches and low abundance or absence in other patch types. Species sorting has been observed in coral colonies between two commensals, a crab (*Trapezia cymodoce*) and a shrimp (*Palaemonella* sp.) (Caley et al. 2001), as well as explored experimentally, such as in benthic microalgal communities (Matthiessen and Hillebrand 2006). In the mass effects paradigm dispersal rates are higher but still equal, leading to higher abundance of species in sub-optimal habitats and source-sink dynamics within the metacommunity (Mouquet and Loreau 2003, Leibold et al. 2004). Mass effects dynamics likely occur for beetles dispersing between the matrix and habitat fragments in a forest fragmentation experiment in southeast Australia (Davies et al. 2005).

The final metacommunity paradigm, termed *patch dynamics*, stems from Levins's (1969)

metapopulation model extended to multiple species. Patches are homogeneous and undergo patch-level disturbance events (Hastings 1980, Tilman 1994). Patch dynamics relies on a tradeoff between species at the regional and local scale (Leibold et al. 2004, Holyoak et al. 2005). Typically, one species exhibits a dispersal advantage (regional scale), while the other is better adapted at the local (patch) scale, either through competitive ability (Hastings 1980, Nee and May 1992) or fecundity (Yu et al. 2001, Yu and Wilson 2001). Patch dynamics is often studied experimentally, such as with a bacteria, protozoa, and rotifer system (Cadotte 2006). A few observational studies have also found evidence for patch dynamics, such as for pond-breeding mosquitoes (Chase and Shulman 2009).

Key differences between the four paradigms, such as homogeneous versus heterogeneous patches, competition-colonization versus species sorting dynamics, and niche structure versus species equivalency, have so far made it difficult to directly compare paradigms. Different models are used for each paradigm in theoretical studies (but see Amarasekare et al. 2004), and empirical studies focus on identifying the primary paradigm at play in a particular system, although many studies find evidence of multiple paradigms within a single system (e.g. Debout et al. 2009, Logue et al. 2011). Little work has focused on comparing coexistence mechanisms among paradigms within one modeling framework or quantifying the contribution of multiple paradigms to coexistence in more complex metacommunities.

However, spatial coexistence theory provides an avenue to directly compare community dynamics between the four metacommunity paradigms and to extend beyond the paradigm framework (Chesson2000a, Amarasekare 2003, Amarasekare et al. 2004). Stable coexistence occurs if all species in a community have positive low-density growth rate, while competitive exclusion occurs for any species with negative low-density growth rate (Chesson and Valladares

2008). We refer to the low density growth rate as *coexistence strength* and note that it can be measured in both theoretical and empirical systems, thus providing a common currency for examining community dynamics and spatial niche structure (Chesson 2000a, Snyder and Chesson 2003, Snyder et al. 2005, Adler et al. 2013).

We analyze coexistence strength within each metacommunity paradigm by partitioning spatial coexistence into four mutually exclusive and exhaustive mechanistic components: (1) the non-spatial mechanism, (2) the spatial storage effect, (3) fitness–density covariance, and (4) nonlinear competitive variance (Chesson 2000a). Adler et al. (2007) provides an interpretation of Chesson's theory that places particular emphasis on equalizing versus stabilizing mechanisms. Chesson's *non-spatial mechanism* corresponds to equalizing mechanisms and incorporates all mechanisms that do not depend on spatial variation (Chesson 2000a; Chesson and Valladares 2008). Specifically, the non-spatial mechanism quantifies the relative fitness among species if spatial structure was absent. In comparison, the spatial storage effect and fitness–density covariance measure the effect of a species' spatial niche on coexistence strength and correspond to stabilizing mechanisms (Adler et al. 2007; Chesson 2000a). The *spatial storage effect* quantifies the ability of a species to take advantage of high-quality habitat and store individuals within such habitat without losing individuals to poor-quality habitat (Chesson 2000a, Sears and Chesson 2007). Biologically, the spatial storage effect is often the result of different habitat suitability between species, where high-quality habitat for a given species has the added benefit of low competition from other species. This scenario occurs when the high-quality habitat for one species is low-quality habitat for other species, due to niche differentiation. *Fitness–density covariance* measures the correlation between the intrinsic fitness of a species and its population size within patches. The fitness–density covariance mechanism can be viewed as a concentration

effect. For example, a positive fitness–density covariance occurs when the spatial dynamics concentrate a species into areas of high fitness, such as where the environment is more favorable or where individuals experience less competition. Chesson's final mechanism, *nonlinear competitive variance*, occurs when spatial variation in competition causes a net increase or decrease in overall fitness levels (Chesson 2000a; Snyder et al. 2005). However, this mechanism is not considered in the conceptual foundation of the four metacommunity paradigms of Leibold et al. (2004). We mention it here for completeness but do not pursue it further. Further details of each metacommunity paradigm and coexistence mechanism are given in Box 2 of Melbourne et al. (2007).

Here, we compare the relative roles of equalizing and different stabilizing mechanisms in the four metacommunity paradigms. The two stabilizing mechanisms, fitness–density covariance and the storage effect, together quantify the role of a species' spatial niche in structuring the metacommunity (Shea and Chesson 2002). In our approach we first develop a common mathematical model that contains all paradigms, thus removing the constraints and confounding effects of different modeling approaches for different paradigms. We model the four paradigms by varying key parameters: (1) dispersal rates, (2) growth rates, (3) habitat heterogeneity, (4) disturbance, and (5) stochasticity. To analyze the model, we present a hybrid approach of mathematical derivations and simulations, which together precisely quantify the equalizing and stabilizing mechanisms. Furthermore, coexistence analyses allow us to extend metacommunity theory beyond the four paradigms to more complex, and biologically realistic, metacommunity structures and processes. We provide examples of more complex metacommunities in two ways: first by analyzing coexistence potential in scenarios that combine features of multiple paradigms, specifically (a) species sorting combined with mass effects and (b) species sorting combined

with patch dynamics, and second by analyzing the contribution of demographic, dispersal, and disturbance stochasticity to coexistence and niche-based mechanisms (whereas the role of stochasticity is mistakenly often only investigated as part of the neutral paradigm and equalizing mechanisms).

2.2 Methods

2.2.1 Model Description

We began with a deterministic model of within-patch dynamics coupled with dispersal between patches. We then added stochastic local population growth, stochastic dispersal, and stochastic disturbance in various combinations to the deterministic model. In deterministic and stochastic versions of the model with parameter settings for different metacommunity types, we compared coexistence mechanisms for two-species, 500-patch metacommunities (where heterogeneous metacommunities had 50% of each of two patch types), although our model is general to any number of species, patches, and patch types. For selected parameter combinations, we also examined the role of stochasticity in small (2 or 20 patch) metacommunities.

Dispersal connects individual patches within the metacommunity model. Here, we used global dispersal, where individuals disperse with equal propensity between all patches (although the approach presented to calculate stable coexistence generalizes to any dispersal scenario). In the deterministic model, the abundances, N, of all species, $j = 1 \ldots n$, in patch $x = 1 \ldots p$ at time $t+1$ are given by,

$$N_{t+1,jx} = N_{t+h,jx} + d_j\left(\sum_{z \neq x} \frac{N_{t+h,jz}}{p-1} - N_{t+h,jx}\right) \qquad (2.1)$$

where $t+h$ is the period up until just before dispersal (dispersal occurs from $t+h$ to $t+1$), d_j is the dispersal rate of species j, z indexes patches ($z = 1 \ldots p$), and p is the number of patches.

We modeled within-patch dynamics before dispersal using the multispecies form of the classic discrete-time Beverton-Holt (1957) population model:

$$N_{t+h,jx} = R_{jx} N_{t,jx} \frac{1}{1+\sum_k \alpha_k N_{t,kx}} \qquad (2.2)$$

where R_{jx} is the density independent growth rate of species j in patch x and α_k is the competition coefficient for each species $k = 1 \ldots n$. R_{jx} determines the type of patch x and thus variation in R_{jx} among patches represents spatial environmental heterogeneity. As Beverton-Holt growth is the discrete time analogue of logistic growth, it is widely used in theoretical studies and can be interpreted in multiple contexts (e.g. Brännström and Sumpter 2005a).

We extended this deterministic model to include stochasticity. We modeled demographic stochasticity by drawing the number of individuals at a given time from a Poisson distribution such that $N_{t+h,jx} \sim \text{Poisson}(\mu)$, where μ, the mean of the Poisson distribution, equals the right hand side of Eqn. 2. This allows for stochasticity in both births and survival (Melbourne and Hastings 2008). We modeled dispersal stochasticity by first drawing the number of dispersing individuals from a binomial distribution with the number of trials equal to population size in patch x at time $t + h$ and probability equal to dispersal rate d_j. Individuals then randomly dispersed with equal probability to a new patch. This approach is equivalent to modeling dispersal as a multinomial distribution with probabilities of $1 - d_j$ of not dispersing and $d_j/(p-1)$ of dispersing to a patch $z = 1 \ldots p$ such that $z \neq x$. We modeled patch-level disturbance stochasticity in the patch dynamics paradigm by imposing disturbance events that resulted in extinction of all species in the patch. Disturbance events were drawn from an independent Bernoulli distribution for each patch with probability equal to the rate of extinction, e. We also modeled disturbance events deterministically, where extinction occurred in each patch every $1/e$ generations.

To parameterize the above model for each of the metacommunity paradigms and the

more complex communities combining paradigms, we altered R_{jx} , d_j , and e (model parameterizations in Table 2.1). Species sorting and mass effects are mechanistically equivalent models with either low or high dispersal rate, respectively. Thus to change between these paradigms we altered only the dispersal rate (from 0.05 to 0.15). To compare paradigms on the same scale, we parameterized species sorting, mass effects, and the neutral paradigms such that the average landscape level fitness, defined as the average density independent growth rate, $\overline{R_j}$ where the overbar indicates the average across patches, was equal for each species. This is not necessary for coexistence or for the general approach described here, but it allows for a direct comparison between niche-based paradigms and the neutral paradigm while controlling for competitive differences between species. The neutral model had equal fitness of all species in all patches and a dispersal rate of 0.1 (intermediate between the rate used in the species sorting and mass effects models). In the patch dynamics paradigm, we used a density independent growth rate-dispersal rate tradeoff (an instance of the classic competition-colonization tradeoff; Tilman 1994) where species 1 was the better disperser with a higher dispersal rate, d_j, between patches and species 2 was the better competitor with a higher average landscape level fitness, $\overline{R_j}$. Patch disturbance occurred with an extinction rate, e, of 0.05 in the patch dynamics paradigm. We examined the generality and robustness of our results to parameter choices by systematically altering R_{jx}, d_j, and the differences between species in these parameters for all paradigms.

	d_1	d_2	R_1 patch type 1	R_1 patch type 2	R_2 patch type 1	R_2 patch type 2	e	α
Neutral	0.1	0.1	1.45	--	1.45	--	0	1/2000
Species sorting	0.05	0.05	1.6	1.3	1.25	1.65	0	1/2000
Mass effects	0.15	0.15	1.6	1.3	1.25	1.65	0	1/2000
Patch dynamics	0.2	0.05	1.4	--	1.45	--	0.05	1/2000
Species sorting/Mass effects	0.15	0.05	1.7	1.3	1.25	1.65	0	1/2000
Species sorting/Patch dynamics	0.2	0.05	1.6	1.3	1.25	1.75	0.05	1/2000

Table 2.1 Parameter values used in the metacommunity models.

We created the species sorting/mass effects combined scenario with unequal dispersal rates between species 1, the low disperser, and species 2, the high disperser. Species 1 was parameterized according to the species sorting paradigm while species 2 was parameterized according to mass effects. For illustration of coexistence in metacommunities without metacommunity level neutrality, species 1 additionally had a higher metacommunity average intrinsic growth rate. In the species sorting/patch dynamics combined model, patches were heterogeneous, with each species exhibiting a higher intrinsic growth rate in a given patch type. Species 1 was a better disperser and species 2 was, on average, a better competitor (see Table 2.1 for details).

2.2.2 Mutual Invasibility Criterion and Strength of Coexistence

Stable regional coexistence occurs if each species can increase when rare in the landscape (Chesson 2000b, Chesson and Valladares 2008). While multiple processes across both spatial and temporal scales can promote or hinder coexistence, mutual invasibility is a strong test for stable coexistence, regardless of the mechanism (Chesson 2000a, Adler et al. 2007, Chesson and

Valladares 2008). Furthermore, the strength of coexistence can be inferred from the magnitude of the total low-density growth rate, which can be decomposed into contributions from the spatial coexistence mechanisms.

Following Chesson (2000a), to test for and quantify regional coexistence, we defined a given species as the invader, *i*. We removed the invader from the metacommunity, and allowed the community to reach equilibrium (deterministic model) or a stationary distribution (stochastic model) both within and across patches. Then, we introduced species *i* at low-density (0.5% of the total metacommunity carrying capacity), which we refer to as the invader's regional abundance *I*. At each time step, we reset the number of individuals in the invading metapopulation to *I* by dividing the number of invaders in each patch by *I* while allowing for patch-level abundance to change during each time step via birth and dispersal. Thus, the relative abundance of the invading species across patches changed during each iteration, while the regional metacommunity abundance was maintained at abundance *I*. We repeated this process until the number of invaders in each patch reached a spatial equilibrium and remained constant between time steps. To calculate coexistence strength in the deterministic case, we then iterated one more time step to obtain the low-density growth rate of the invader relative to the resident species, which we decomposed into contributions from the different coexistence mechanisms (Chesson 2000a, 2000b, Snyder et al. 2005, Chesson and Valladares 2008). We thus calculated coexistence strength with the invader at low abundance, the resident at equilibrium abundance, and invader and residents at their equilibrium spatial distributions. We repeated this process for each species in the community. If all species were able to invade at low densities (low-density growth rate > 0), we concluded that the metacommunity exhibits regional stable coexistence.

In the stochastic models, we calculated the low-density growth rate as the average of 100

separate time steps, where we reset the regional invader density to *I* for each time step. We also examined between versus within-run stochasticity in coexistence strength using a linear mixed effects model with time-step nested within run using the function lmer in R.

2.2.3 Contributions to Coexistence from Spatial Mechanisms

Here we briefly describe the derivation of coexistence mechanisms (the full derivation is given in Appendix 1). While we focus in the main text on the derivation and results for a two-species system, we also extend this derivation to the *n*-species case in Appendix 1. Coexistence occurs in a metacommunity if, for each species, the low-density growth rate, $\tilde{\lambda}_i$, of the invader is greater than the equilibrium growth rate, $\tilde{\lambda}_r$, of the resident species, i.e. $\tilde{\lambda}_i - \tilde{\lambda}_r$ is greater than 0, where $\tilde{\lambda}_j = \frac{\bar{N}_{t+1,j}}{\bar{N}_{t,j}}$ (Chesson 2000a), *N* is the number of individuals of species *j*, and the overbar indicates the average across patches. The tilde indicates that we are measuring the invasion criterion, i.e. $\tilde{\lambda}_r$ is the growth rate of the resident species at equilibrium abundance in the absence of the invader and $\tilde{\lambda}_i$ is the growth rate of the invader at low-density while the resident is at equilibrium.

For ease of calculation, we subtract 1 from the growth rate such that $\tilde{\lambda}_i - 1 - (\tilde{\lambda}_r - 1) = \frac{\bar{N}_{t+1,i}}{\bar{N}_{t,i}} - 1 - (\frac{\bar{N}_{t+1,r}}{\bar{N}_{t,r}} - 1)$. Subtracting 1 does not alter the relationship, but allows us to solve for the exact form of each spatial coexistence mechanism. Following Chesson, we divide both sides by the natural scaling units for both the resident and invader (Chesson and Valladares 2008). The natural scaling units correct for the sensitivity of different species to the common competitive factor (competition for space, in this case) (Chesson and Valladares 2008) and this correction allows for a direct comparison of the invader and resident by standardizing using

average growth rate (Chesson 2000b, Chesson et al. 2005, Chesson and Valladares 2008). We define the natural scaling units as the average metacommunity growth rate for each species, or $\overline{R_J}$. We therefore use

$$\frac{\tilde{\lambda}_i - 1}{\overline{R_i}} - \frac{\tilde{\lambda}_r - 1}{\overline{R_r}} = \frac{\frac{\bar{N}_{t+1,i}}{\bar{N}_{t,i}} - 1}{\overline{R_i}} - \frac{\frac{\bar{N}_{t+1,r}}{\bar{N}_{t,r}} - 1}{\overline{R_r}} \qquad (2.3)$$

to derive an expression for the spatial coexistence mechanisms.

We next define the competitive term, C_x, for the environment from the competitive term in the Beverton-Holt equation, thus: $C_x = 1 - \frac{1}{1+\sum_j \alpha_j N_{t,jx}}$. This function provides an intuitive choice for the competitive term, where more competition is reflected by a higher numerical value. We define the effect of environment on fitness, E_{jx}, as the fitness for a given patch relative to metacommunity-level fitness: $E_{jx} = \frac{R_{jx}}{\overline{R_J}}$. We use equation 2.3 to derive expressions for the equalizing (e.g. non-spatial fitness) and stabilizing (e.g. the storage effect and fitness–density covariance) spatial coexistence mechanisms and find

$$\frac{\tilde{\lambda}_i - 1}{\overline{R_i}} - \frac{\tilde{\lambda}_r - 1}{\overline{R_r}} = \underbrace{\frac{1}{\overline{R_r}} - \frac{1}{\overline{R_i}}}_{\substack{\text{non-spatial} \\ \text{fitness}}} - \underbrace{\text{Cov}((E_{ix} - E_{rx}), C_x)}_{\substack{\text{storage} \\ \text{effect}}} + \underbrace{\frac{\text{Cov}\left(\lambda_{ix}, v_{t,ix}\right)}{\overline{R_i}} - \frac{\text{Cov}\left(\lambda_{rx}, v_{t,rx}\right)}{\overline{R_r}}}_{\substack{\text{fitness-density} \\ \text{covariance}}} \qquad (2.4) \cdot$$

Here, Cov is the covariance, $v_{jx} = \frac{N_{t,jx}}{\bar{N}_{t,j}}$ is the relative density of species *j* in a patch (the number of individuals in patch *x* divided by the average number of individuals across all patches) and λ_{ix} and λ_{rx} are the growth rates of the invader and resident species respectively in patch *x*. Because both species have the same growth equation, there is no contribution to coexistence from nonlinear competitive variance (Chesson 2000a, 2000b, Chesson and Valladares 2008). Future extensions include modifying the metacommunity paradigm framework such that nonlinear

competitive variance, the final spatial coexistence mechanism of Chesson (2000a), is incorporated. Eqn 4 provides an exact decomposition of the relative contributions of the different coexistence mechanisms (i.e. no approximations were made to derive this expression). Analytical expressions for the covariances on the right hand side of Eqn 4 cannot be obtained in general but the covariances are straightforward to quantify from model simulations. Thus, Eqn 4 together with model simulations provides a hybrid analytical-simulation approach to precisely quantify the contributions of equalizing and stabilizing mechanisms.

2.3 Results

As expected, and by definition, species in the neutral paradigm did not exhibit stable coexistence, but rather co-occurrence (Figure 2.1). The low-density growth rate in the neutral paradigm was zero for both species in the deterministic model. A growth rate above zero indicates long-term stable coexistence, while a growth rate below zero indicates competitive exclusion. Species were unable to recover from low densities, and persisted indefinitely in the deterministic neutral model and on average for 2,180 generations in the stochastic two patch model.

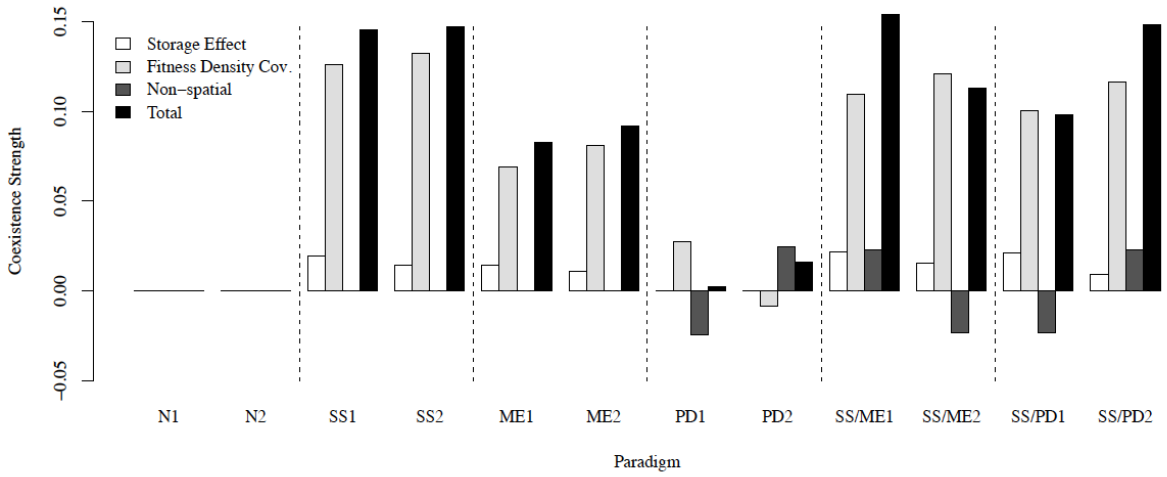

Figure 2.1 Spatial coexistence strength in different metacommunity paradigms (500-patch deterministic models). The total for both species must be positive for coexistence. For species 1 and 2 (indicated by numbers), non-spatial coexistence, the storage effect, fitness–density covariance and total community level coexistence strength is shown for the neutral paradigm (N), species sorting (SS), mass effects (ME), patch dynamics (PD), and two scenarios representing a mixture of paradigms. SS/ME is a mixture of species sorting and mass effects and SS/PD is a mixture of species sorting and patch dynamics paradigms (see methods).

All three niche-based paradigms exhibited stable, long-term coexistence. For our model structure, species sorting had the highest coexistence strength of all paradigms, as measured by the total low-density growth rate for each species (Figure 2.1). The largest contribution to coexistence strength in the species sorting model came from fitness–density covariance, with the storage effect playing a more minor role (Figure 2.1). Since species by design had landscape-level neutrality, the non-spatial mechanism contributed by equalizing species. That is, the non-spatial fitness difference was zero. Stable coexistence thus required only a non-zero contribution from stabilizing mechanisms. For the mass effects model the overall strength of coexistence was lower than species sorting, and the largest contribution was from fitness–density covariance (Figure 2.1).

Patch dynamics had the smallest coexistence strength of the three niche-based paradigms.

It was the only niche-based paradigm without contribution from the spatial storage effect (Figure 2.1). Because patches are homogeneous in the patch dynamics paradigm, and our model of disturbance did not alter the environmental conditions of patches, there was no environmental variability and thus no spatial storage effect. Species 1 (the poorer competitor) had a negative contribution from the non-spatial mechanism, which was counteracted by a positive contribution from fitness–density covariance to give positive coexistence strength. Because species 1 was a poorer competitor, non-spatial fitness was negative. Species 1 therefore depends on fitness–density covariance for coexistence, since the storage effect is absent in homogeneous metacommunities, regardless of model specifics. In contrast, species 2 (the better competitor) had a positive contribution from the non-spatial mechanism, while fitness–density covariance eroded its low–density growth rate. Species 2 still maintained a positive overall coexistence strength. Thus, a hallmark of the patch dynamics paradigm is that the two species show opposing effects of fitness–density covariance, which is an outcome of the spatial pattern formation driven by the competition-colonization tradeoff.

The model combining both species sorting and mass effects had positive contributions from all spatial coexistence mechanisms for species 1, leading to a higher coexistence strength than for species 2 (Figure 2.1). For species 2, the non-spatial mechanism was negative, eroding the strength of coexistence from stabilizing mechanisms. This was offset by a positive storage effect and fitness–density covariance. The low-density growth rate was enhanced for both species in the combined model when compared to their respective individual paradigms (Figure 2.1).

The model combining both species sorting and patch dynamics had a positive contribution from the storage effect (Fig 1). This differs from the pure patch dynamics model,

where the spatial storage effect did not contribute to coexistence. The coexistence strength was slightly lower than species sorting but much greater than for the patch dynamics paradigm.

2.3.1 Generality of Coexistence Strength

A coexistence strength of zero, indicating co-occurrence but not coexistence, occurred in the neutral paradigm, regardless of dispersal rate, growth rate, or carrying capacity (Figure 2.2). This is a general phenomenon, characteristic of species that are ecologically equivalent.

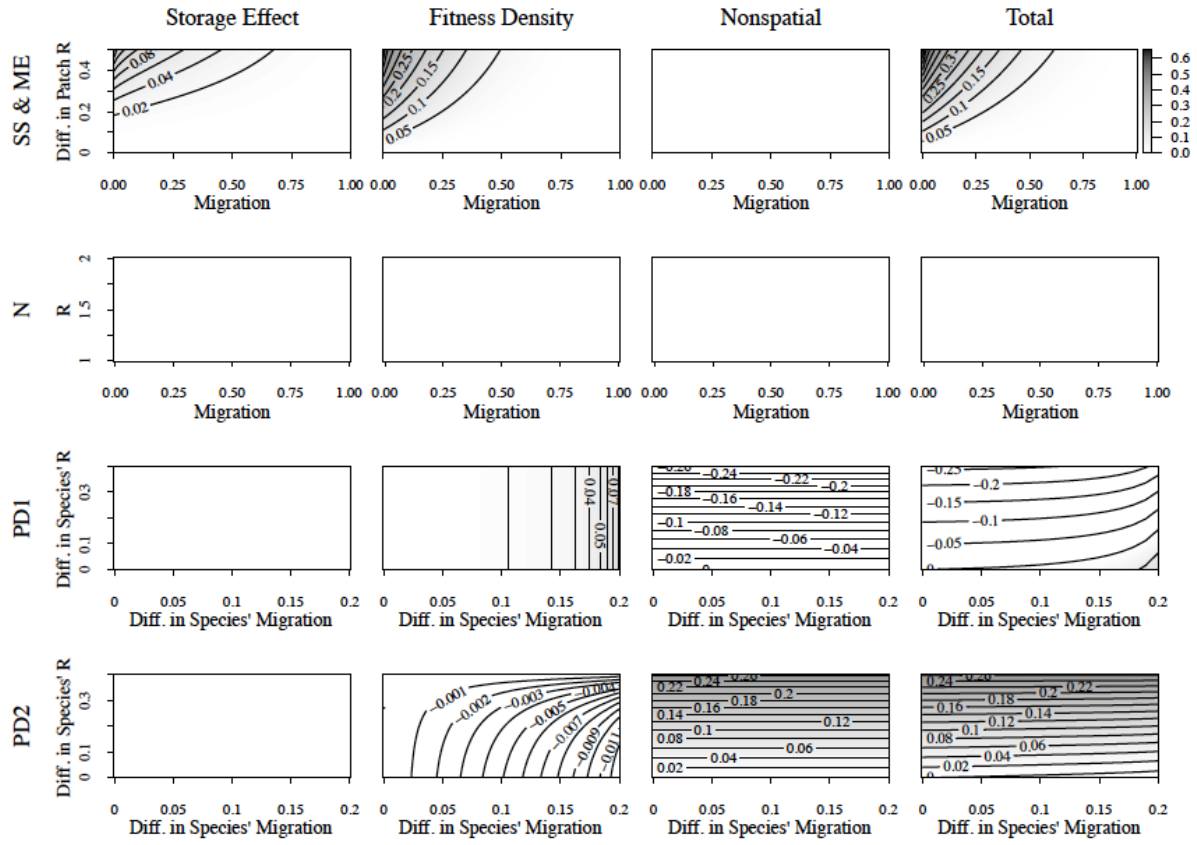

Figure 2.2 Comparison of coexistence mechanism strength across parameter space for species sorting (SS) and mass effects (ME), the neutral paradigm (N), and for both species in patch dynamics (PD1 and PD2). Gray areas show positive low-density growth rate. Low dispersal rates and high niche differentiation yields the highest coexistence strength in species sorting and mass effects. The neutral paradigm always exhibits a coexistence strength of 0, regardless of parameterization. In patch dynamics, species 2 (the better competitor) is able to persist across parameter space. However, only a limited area of parameter space, with relatively low differences in growth rate (R) and high differences in dispersal rate allow for coexistence.

Dispersal and niche differentiation (i.e. differences in growth rates between patch types) both altered the relative contributions of the storage effect and fitness–density covariance along the species sorting to mass effects continuum, where low dispersal rate with high differences in growth rates gave the largest coexistence strength (Figure 2.2). Fitness–density covariance and

the storage effect both decreased with increasing dispersal rate, and fitness–density covariance was greater than the storage effect for low to moderately high dispersal in our model ($d_j < 0.6$).

Patch dynamics generally exhibited lower coexistence strength than the species sorting or mass effects paradigms. The poorer competitor (species 1) had a linear positive response to increases in the difference in dispersal rates between the two species, while the better competitor (species 2) had a negative nonlinear response to increases in dispersal rates (Figure 2.2). A relatively large difference in dispersal rate but a small difference in growth rates was required for coexistence in the patch dynamics model.

2.3.2 Effect of Stochasticity

Metacommunities with fewer patches had more between-run and within-run variation in the strength of coexistence. Using species sorting in a two-patch metacommunity as an example, demographic stochasticity caused runs with negative low-density growth rates in scenarios where the two-patch deterministic model or the 500-patch models (with or without stochasticity) had positive low-density growth. The majority of this variation was from within-run (between time step) variation rather than between-run variation. A maximum of 4% of variation in the storage effect was from between-run variability, while for fitness–density covariance and overall low-density growth rate, a maximum of 12% was from between-run variability. Between-run variation represents non-neutral drift and arises within this niche-based model because of the evolving spatial pattern of abundances between metacommunity patches.

Importantly, in small metacommunities, stochasticity can alter the average strength of spatial coexistence mechanisms. As an example, the stochastic 20 patch species sorting/patch dynamics model had much stronger coexistence on average compared to the 500-patch stochastic model or the deterministic model (Figure 2.3). Species 2 had lower storage effect strength, but markedly higher fitness–density covariance, resulting in higher coexistence strength. Species 1 also had higher coexistence strength, resulting from higher storage effect and fitness–density covariance strengths. This increase occurred only with disturbance stochasticity (where patches experience stochastic local extinctions) rather than demographic or dispersal stochasticity alone (Figure 2.3). In other words, stochastic disturbance promoted coexistence more in small than large metacommunities. Stochastic disturbance also reduced variance in fitness–density covariance and thereby reduced variance in total coexistence strength for our model (Figure 2.3).

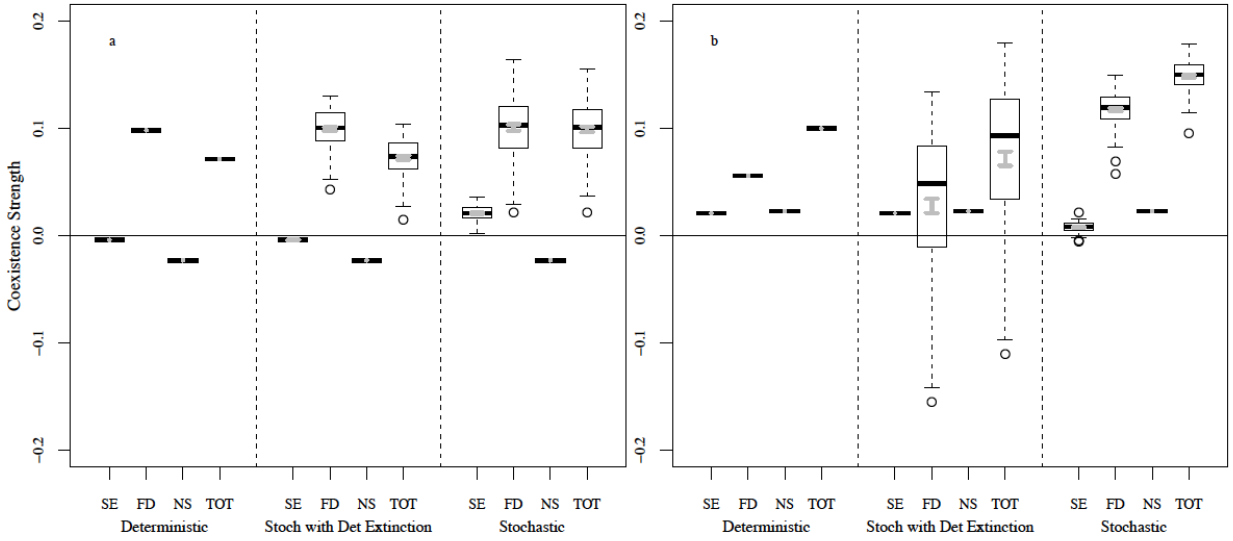

Figure 2.3 Spatial storage effect (SE), fitness–density covariance (FD), non-spatial fitness (NS) and total coexistence strength (TOT) for the species sorting-patch dynamics combined metacommunity model with 20 patches. Relative contributions of each mechanism are compared for both species in the fully deterministic model, a model with stochastic birth and dispersal but deterministic extinction, and the fully stochastic model (100 runs). Overlaid grey bars show plus

and minus one standard error from the simulation means. Stochasticity in disturbance events alters the strength of coexistence compared to models with deterministic disturbance. Tukey boxplots are shown.

2.4 Discussion

While the metacommunity paradigms of Leibold et al. (2004) have a rich history of qualitative comparison both theoretically and empirically, Chesson's (2000a) spatial coexistence theory provides a way to quantitatively compare paradigms and allows for a detailed analysis of metacommunities that do not fit neatly within the paradigm framework. We show that each metacommunity paradigm is characterized by its own signature of spatial coexistence mechanisms and that more complex metacommunities, such as those with multiple paradigms or with stochasticity, can also be compared using Chesson's (2000a) spatial coexistence theory.

2.4.1 Coexistence Signatures of Metacommunity Paradigms

As expected, when examining coexistence mechanisms in the neutral paradigm, we find co-occurrence, rather than stable coexistence because species are equivalent and thus no stabilizing mechanisms are present. Regardless of parameterization, the neutral paradigm yields low-density growth rates of zero for each species, which is insufficient for stable coexistence. Species instead go extinct from population drift through time, where no species outcompetes another. The rate of drift to extinction depends on biological and spatial structure, such as the number of patches or carrying capacities of each patch (Economo and Keitt 2007).

In comparison, all niche-based metacommunity paradigms exhibit stable coexistence rather than co-occurrence, meaning that niche based coexistence mechanisms allow for species to recover from low-density. Stable coexistence occurs with three distinct signatures in our model of the niche-based paradigms: (1) in species sorting the storage effect and fitness–density

covariance work in unison leading to the highest coexistence strength of all paradigms, as species segregate into their preferred habitat types, (2) in mass effects the storage effect and fitness–density covariance also work in unison but the increased dispersal rate erodes the effect of both mechanisms compared to species sorting, and (3) in patch dynamics there is no storage effect but trait tradeoffs lead first to the formation of spatial structure that in turn leads to opposing effects of fitness–density covariance between species that, when properly balanced, allow for coexistence.

In our model, both species sorting and mass effects rely to a much greater degree on fitness–density covariance than on the storage effect for coexistence in metacommunities. Fitness–density covariance is stronger than the storage effect in all cases that have the low to moderate dispersal characteristic of metacommunities ($d_j<0.6$) (Figure 2.2). A lower dispersal rate in species sorting allows a higher proportion of individuals to remain in their optimal habitat, thus maximizing both the spatial storage effect and fitness–density covariance. In comparison, as dispersal becomes high and the community well-mixed, fitness–density covariance tends toward zero because density is homogenized across the metacommunity. By exploring parameter space we show that the dominance of fitness–density covariance over the storage effect is robust to different dispersal rates and habitat contrasts along the species sorting to mass effects continuum (Figure 2.2, row 1) and is the only spatial coexistence mechanism in the patch dynamics paradigm. While empirical studies have so far focused on the spatial storage effect (Sears and Chesson 2007, Caballero et al. 2007), our results suggest that increased attention to fitness–density covariance would also be fruitful. Since our model captures the essential features of the metacommunity paradigms, we expect the dominance of fitness–density covariance to be quite general, at least for competitive communities. However future work is needed to see if a greater

contribution from fitness–density covariance is found in natural systems and different mathematical models of the metacommunity paradigms.

The patch dynamics paradigm is the only niche-based paradigm without the storage effect. This is because patch environmental conditions are homogeneous, whereas the storage effect requires environmental heterogeneity. Instead, the effect of dispersal on spatial pattern formation is key to coexistence in patch dynamics, where the negative effect of a lower non-spatial fitness needs to be balanced by a positive effect of fitness–density covariance for the worse competitor. Without disturbance or other events that reduce the abundance of competitors, the better competitor would exclude the poorer competitor through its superior non-spatial fitness (Roxburgh et al. 2004). However, the poorer competitor—who is the better disperser—can take advantage of recent disturbance events. On average, the better disperser migrates to disturbed patches sooner and in higher densities, and thus can increase in population size because of the lack of interspecific competition (Nee and May 1992, Yu and Wilson 2001). The more general explanation provided here is that the combination of dispersal and disturbance creates spatial structure, captured by a unique signature of spatial coexistence mechanisms. The better disperser is given a boost through fitness–density covariance, compensating for its relative deficit in non-spatial fitness. In comparison, the better competitor persists from non-spatial fitness greater than the negative effect of fitness–density covariance.

2.4.2 Complex Metacommunities and Effect of Stochasticity

By focusing on spatial coexistence mechanisms, we can examine more complex metacommunities than encompassed by the four paradigm framework. We illustrate this in two ways. In the first, we explore complex metacommunity dynamics, exemplified by the combined

species sorting/mass effects and species sorting/patch dynamics scenarios. In the species sorting/patch dynamics scenario, trait tradeoffs still lead to opposing effects of coexistence mechanisms. However, in this scenario and in some cases with more complex disturbance regimes (e.g. Miller et al. 2011a), patch heterogeneity allows the storage effect to also contribute to coexistence. In metacommunity models that deviate from the patch dynamics paradigm such that disturbance alters the abiotic conditions within a patch and creates environmental heterogeneity (Miller et al. 2011a, 2011b), we would also expect to see a spatial storage effect along with potentially a lesser effect of fitness–density covariance.

Stochasticity within metacommunities not only causes variability in coexistence strength, but also can alter mean coexistence strength. Spatial coexistence mechanisms rely on spatial variation in environmental quality and competition; metacommunities with environmental stochasticity tend to experience more variability than deterministic systems, which can increase coexistence strength in the metacommunity. This effect is exemplified in the species sorting/patch dynamics model, where stochasticity in disturbance events increases coexistence strength compared to deterministic disturbance, especially in the smallest metacommunities. Because the better disperser has an advantage only after disturbance, variability in the timing of disturbance among patches increases coexistence via the storage effect and fitness–density covariance. This in turn, actually decreases variance in coexistence strength in our model, contrary to the common intuition that increasing stochasticity increases variability or instability in communities. In this case, stochasticity plays a larger role than just contributing to neutral drift (Vellend 2010). Instead, stochasticity contributes to niche based metacommunity coexistence by altering the spatial structure between patches, thus reinforcing the distinction between the effects of stochasticity and the effects of neutrality.

2.5 Conclusion

Empirical metacommunity studies often focus on disentangling the paradigms within a given system to determine the primary metacommunity paradigm at play (Ellis et al. 2006, Calcagno et al. 2006). Not surprisingly, the majority of studies find that the four paradigm framework is too restrictive and non-theoretical systems often do not conform to a single paradigm, but rather exhibit features described by multiple paradigms (Cottenie 2005, Ellis et al. 2006, Cadotte 2007, Logue et al. 2011). The approach of Chesson (2000a) using spatial coexistence mechanisms can be applied to the traditional paradigms but also, as we have shown, to more complex, biologically realistic metacommunities that mix paradigms, such as patch dynamics with spatial heterogeneity or metacommunities with varying dispersal abilities between species. This framework can also be extended to species rich metacommunities (Appendix 1), allowing for comparing complex multi-species metacommunities. We have shown that examining coexistence mechanisms in metacommunities provides a flexible framework for comparing metacommunities because systems that do not easily fit within one of the four paradigms can still be analyzed using a single, unifying framework.

2.6 Acknowledgements

LGS was supported during this work by NSF GRFP-1144083 and IGERT-1144807. BAM was supported by NSF DEB 1258160. We thank Peter Chesson for valuable insights with the derivation of the coexistence mechanisms. We thank S. Roxburgh and two anonymous reviewers for their comments which greatly improved the quality of the manuscript.

Chapter 3

Differentiating between niche and neutral assembly in metacommunities using null models of beta-diversity

Lauren G. Shoemaker, Caroline M. Tucker, Kendi F. Davies, Diana Nemergut, and Brett A. Melbourne

Published as: Tucker*, C. M., Shoemaker*, L. G., Davies, K. F., Nemergut, D. R. and Melbourne, B. A. (2016), Differentiating between niche and neutral assembly in metacommunities using null models of β-diversity. Oikos, 125: 778–789. doi: 10.1111/oik.02803.

* denotes equal contribution. Lauren Shoemaker created and analyzed the simulation model and coexistence strength under all scenarios. Caroline Tucker analyzed simulation model outputs using the presence/absence and abundance β-null deviation measure. Both first-authors contributed equally to writing and editing.

The β-null deviation measure, developed as a null model for β-diversity, is increasingly used in empirical studies to detect the underlying structuring mechanisms in communities (e.g. niche vs. neutral and stochastic vs. deterministic). Despite growing use, the ecological interpretation of the presence/absence and abundance-based versions of the β-null diversity measure have not been tested against communities with known assembly mechanisms, and thus have not been validated as an appropriate tool for inferring assembly mechanisms. Using a mechanistic model with known assembly mechanisms, we simulated replicate metacommunities

and examined β-null deviation values (1) across a gradient of niche (species-sorting) to neutrally structured metacommunities, (2) through time, and (3) we compared the effect of changes in assembly mechanism on the performance of the β-null deviation measures. The impact of stochasticity on assembly outcomes was also considered. β-null deviation measures proved to be interpretable as a measure of niche or neutral assembly. However, the presence/absence version of the β-null deviation measure could not differentiate between niche and neutral metacommunities if demographic stochasticity were present. The abundance-based β-null deviation measure was successful in distinguishing between niche and neutral metacommunities and was robust to the presence of stochasticity, changes through time, and changing assembly mechanisms. However, we suggest that it is not robust to changing abundance evenness distributions or sampling of communities, and so its interpretation still requires some care. We encourage the testing of the assumptions behind null models for ecology and care in their application.

3.1 Introduction

There are two traditionally separate approaches to understanding ecological community structure. Theoretical approaches rely on mathematical models of species interactions to predict the resulting dynamics, including species coexistence, community diversity, stability, and evenness. Alternately, empirical approaches (both experimental and observational) rely on sampling existing or constructed ecological communities and collecting data on species' identities or abundances, and then analyzing observed presence/absence or abundance patterns using statistical models. Merging theoretical and empirical approaches is often problematic, as it is difficult to connect observed patterns with models of community processes: a single

mechanism may produce multiple patterns depending on parameter values, while multiple mechanisms may lead to convergent patterns (e.g. Mackey and Currie, D. J. 2001, Mayfield and Levine 2010).

Null models, which compare observed statistical patterns to those expected in the absence of a particular assembly mechanism (Colwell and Winkler 1984, Gotelli and Graves 1996, Ulrich and Gotelli 2007), represent one common approach for connecting statistical patterns to assembly mechanisms. Null models randomly sample ecological data to generate patterns representative of random or 'null' processes; empirical data are then compared to the generated null distribution and differences from null are often used to infer the specific processes, which are (or are not) structuring the community. Null models in a variety of formulations have been used to explore community co-occurrence patterns (Connor and Simberloff 1979), community phylogenetic patterns (Kembel 2009), assembly rules (Weiher and Keddy 1999), and macroecology (Colwell and Winkler 1984) and are a fundamental component of modern ecological analysis.

Local and regional diversity, and the ecological processes creating observed diversity patterns, are often the focus of empirical studies: such studies may consider the multiple components of diversity, including local species richness or α-diversity; compositional variance between communities or β-diversity; and regional richness or γ-diversity. α-, β-, and γ-diversity are interrelated (Jost 2007), and thus when local richness is low, small changes in composition can have disproportionate effects on β-diversity, making it difficult to differentiate meaningful (process-driven) changes in β-diversity from those resulting from random variability in species identity and low local richness. To control for this, Chase and colleagues (2011) emphasized the use of β-null deviation: a null model to account for such changes in β-diversity while controlling

for stochastic variation and associated changes in α-diversity (i.e. local species richness) (see also Crist et al. 2003). β-null deviation methods have also been used to correct for the interrelation between α-diversity and β-diversity (e.g. Grman and Brudvig 2014). It logically follows that if observed communities are more or less similar than expected compared to null communities, this could provide evidence for certain community assembly mechanisms and, therefore, that β-null deviation values could also be used as indices of community structure (Chase 2010)

The β-null deviation method as introduced in Chase et al. (2011) relies on occurrence (presence/absence) data and uses a null model to generate a distribution of β-diversity values expected when artificial communities, equal in α-diversity to the observed communities, are randomly assembled from the regional species pool. The observed β-diversity is then compared to this null distribution, e.g. $\beta_{obs} - E(\beta_{null})$, where $E(\beta_{null})$ is the expected value of the β_{null} distribution. The resulting value represents β-diversity that is independent of α-diversity. As such, null deviation values may represent communities that are more similar than expected by chance (a negative null deviation value), less similar than expected by chance (a positive null deviation value), or close to the chance expectation (values near zero). Large deviations from the random expectation have been interpreted as reflecting communities structured by non-neutral assembly mechanisms, such as shared environmental filtering (negative values; communities more similar than expected by chance) or competitive interactions (positive values; communities less similar than expected by chance) (Chase 2010, Chase and Myers 2011). Of course, other processes (or combinations of processes) may produce negative or positive β-null deviation values but these interpretations of β-null deviation measure dominate applications of the measure.

Additional formulations of β-null deviation incorporate local densities to more finely understand how community structure might diverge from random expectations: the null model in such approaches removes spatial aggregation within and among species and possible effects of random sampling (Kraft et al. 2011, Stegen et al. 2013). In these, the random communities are constructed by shuffling individuals of each species among sites, while maintaining each species' total abundance in the metacommunity. Abundance-based measures may be more robust to minor variation in community composition, such as occurs when a species' local population is maintained by dispersal from source populations.

The usage of β-null deviation measures in this capacity – to hint at underlying assembly mechanisms – has increased rapidly across multiple sub-disciplines (e.g. Azeria et al. 2011, Ferrenberg et al. 2013, Germain et al. 2013, Guo et al. 2013, Mori et al. 2015, Püttker et al. 2014, Rocha-Ortega and Favila 2013, Segre et al. 2014, Siepielski and McPeek 2012, Stegen et al. 2012, Tanentzap et al. 2013). Most papers citing the Chase et al. (2011) methods paper include the term "assembly" in the title or abstract, reflecting the trend for the increasing usage of β-null deviation as an index of assembly processes, rather than simply as a null model for β-diversity that controls for differences in α-diversity. Despite the growing popularity of this approach to disentangle ecological processes in observational data, there are a number of issues that currently remain unaddressed. First, the papers that originated the method and those that have applied it are inconsistent in their interpretation of the β-null deviation values. While deviation from zero is consistently interpreted as reflecting some ecological structuring process, exactly what process drives changes in the value of the β-null deviation is unknown and interpreted in multiple ways. Initial usage (Chase 2010, Chase et al. 2011) suggested that deviations from zero in β-null deviation values might reflect deterministic assembly. Values near to zero were interpreted as

showing increasingly stochastic assembly of communities (since stochasticity in assembly should result in greater randomness in community composition, implying that such communities would appear similar to those assembled by randomizing the empirical data) while values much greater or much less than zero were suggestive of deterministic processes driving community assembly. More recently the measure has been interpreted as differentiating between niche versus neutral processes (Ferrenberg et al. 2013, Püttker et al. 2014). Values closer to zero were interpreted as neutral communities, where species are ecologically equivalent to one another. Deviations from zero were interpreted as niche structured communities, where increasing ecological differences among species in heterogeneous environments cause greater deviations from zero. Other interpretations suggest that β-null deviations could capture dispersal limitation or homogenizing dispersal versus drift (Stegen et al. 2012). Which, if any, of these interpretations best reflects the meaning of the β-null deviation measure is unexplored.

One outcome of the popularity of this measure for empirical studies is that mechanistic interpretations have not kept pace – for example, null deviation values of zero have been interpreted as representing both *stochastic* and *neutral* assembly; differences from zero have been interpreted as representing both *niche* and *deterministic*. These terms are not interchangeable (Leibold and McPeek 2006, Vellend et al. 2014), and clarifying the precise interpretation of β-null deviation values would greatly benefit our understanding of processes in natural systems. Demographic rates such as birth, death, and dispersal are key. An interpretation of *neutrality* reflects that species are ecologically equivalent and so share identical demographic rates (Hubbell 2001), while *stochasticity* implies that there is random variation in demographic rates (i.e. they are probabilistic) without implying anything about the mean values of those demographic rates (Table 3.1). Similarly, *niche* processes imply differentiation in mean

demographic rates between species (Carroll et al. 2011), while *determinism* indicates an absence of random variation in species' demographic rates. Though simplistic, one can interpret the niche-neutral axis as reflecting differences in mean demographic rates or lack of differences, while the stochastic-deterministic axis reflects the presence or absence of probabilistic variation about those mean demographic rates. Vellend *et al.* (2014) reduce these two axes/dimensions to a single dimension with a continuum from drift (neutral stochasticity) to selection, but our categorization is useful for exploring the full range of models and contains their broader conceptualization as a special case. For example, a system may be both neutral (mean demographic rates constant across species) and deterministic (no variation about these demographic rates), and as a result dynamics in such a system would differ from those expected from a neutral and stochastic (variation about demographic rates) system (Adler et al. 2007). Natural communities of course are unlikely to exist at the extremes of these two axes, and instead will be structured by multiple levels of these processes, e.g. demographic stochasticity and niche differentiation (Adler et al. 2007, 2014). In the case of multiple structuring processes, the interpretation of β-null deviation values is altogether unexplored.

Term	Definition	Model	Term
Niche	Ecological differentiation between species in a community.	Each species has an optimal patch where its growth rate is maximum, with lower growth in the sub-optimal patches.	$R_{otimal} > R_{sub-optimal}$
Neutral	Ecological equivalence of species in a community.	All species have identical intrinsic growth rates to one another in all patches.	$R_{otimal} = R_{sub-optimal}$
Deterministic	Processes are non-probabilistic, invariant outcomes of the systems inputs.	Growth and dispersal rates are fixed.	*R_{ix} is fixed according to values in Table 3.2 and m=0.05*
Stochastic	Processes are probabilistic and affected by randomness in the system, such as through demographic variability in birth, death, and dispersal rates.	Growth and dispersal rates are drawn from distributions (Poisson and binomial, respectively), where the mean is equivalent to the deterministic rate.	$R_{ix}N_{t,ix} \sim Pois(\mu_{ix}N_{t,ix})$ $\mu_{ix} = R_{ix}\frac{1}{1+\alpha\sum_j N_{t,jx}}$ $m_{ix}R_{ix}N_{t,ix} \sim Binom(R_{ix}N_{t,ix}, m)$

Table 3.1 Definition of the focal four processes affecting community assembly—as modelled in this study—including details on how they are incorporated into the model described in Equation 3.1.

The meaning of β-null deviation values cannot be determined using observational data alone, but rather requires that the β-null deviation measure be applied to communities assembling with known processes (whether neutral, niche, deterministic or stochastic). This will help clarify the interpretation of the null deviation measure and its robustness to differences in assembly processes and in communities with multiple processes at play. Like a statistical null hypothesis (H_o), the null model for β-null deviation values may find, for a given community, that data differ from a random distribution of species. Without testing against simulated communities with known assembly processes, we cannot infer which particular ecological process may create

this significant difference, as the β-null deviation measure is currently used to do. The connection between a statistical null model and the ecological 'null' process it is supposed to represent must be justified. The null model at the heart of the β-null deviation measure could differ substantially in community structure from a neutral community model—the mechanistic ecological 'null' model. Appropriate tests of the β-null deviation measure for communities with known assembly processes (whether neutral, niche, deterministic or stochastic) are lacking, and its robustness to changes in ecological parameters and assembly processes remains unknown.

In this paper, we use simulated metacommunities to explore how both stochastic and deterministic formulations of metacommunity models with varying strengths of niche structure alter the value (and interpretation) of the presence/absence and abundance β-null deviation measures, and thus the appropriate use of the measure for inferring assembly mechanisms. We show that β-null deviation values near zero occur when assembly dynamics are neutral, and the absolute value of the measure diverges from zero when assembly dynamics are niche-based. However, this is only true in specific cases. We show that (1) stochasticity, (2) changes in assembly mechanism thru time, and (3) population drift through time alter the value of the presence/absence β-null deviation in unexpected ways, but that the abundance β-null deviation measure is robust to these processes. Finally, we provide a discussion of the conditions for which null deviation measures may be appropriate for inferring community assembly processes.

3.2 Methods

We generated replicated artificial data using a metacommunity model: β-diversity and β-null deviation values were then calculated using these data. Further, we varied parameters of the

model to generate metacommunities along a gradient from niche to neutral structure. We also generated both deterministic and stochastic versions of metacommunities.

3.2.1 Mathematical formulation of metacommunity model

We created a discrete time mechanistic metacommunity model of 25 species and 25 patches (e.g. a habitat patch that can contain a local community). The model includes birth and death of individuals, inter- and intra-specific competition for space within patches, and migration between patches. The model with global migration between patches is a patch model and not spatially explicit (Mouquet and Loreau 2003) (although it could be made spatially explicit). Dynamics within patches were modeled using the classic competition form of the Beverton-Holt model (Beverton and Holt 1957, Leslie and Gower 1960):

$$N_{t+h,ix} = R_{ix}N_{t,ix}\frac{1}{1+\alpha\sum_j N_{t,jx}} \quad \mathrm{N_{t+h,ix}} = \mathrm{R_{ix}N_{t,ix}}\frac{1}{1+\sum_j \alpha_j \mathrm{N_{t,jx}}} \quad (3.1).$$

N represents the population of a given species *i* in patch *x* at time *t*, and $t + h$ is the time up until just before migration. R_{ix} is the density-independent growth rate of species *i* in patch *x*, which depends on the niche-structure in the simulation (see Table 3.2 for parameter values). The term $1 + \alpha \sum_j N_{t,jx}$ is the competition experienced by species *i* (Chesson 2000b), where α is the competition coefficient (α = 1/600 for all simulations). Migration occurred after within-patch dynamics. For global dispersal, metacommunity dynamics were given by

$$N_{t+1,ix} = N_{t+h,ix} + m_i(\sum_{z\neq x}\frac{N_{t+h,iz}}{p-1} - N_{t+h,ix}) \quad (3.2)$$

where m_i is the migration rate of species *i*, *z* indexes patches, and *p* is the total number of patches (25 for all analyses). To model local dispersal, we modified the above global dispersal model (Eq. 2) into a coupled map lattice (Brännström and Sumpter 2005b). For local dispersal, an individual could only migrate to a patch directly adjacent in one of the four cardinal directions (5

x 5 lattice). We present results from global and local dispersal with $m = 0.05$. Lower values of m did not lead to results qualitatively different from those presented here; higher values of m produced metacommunities with β-null deviation values closer to zero. We started all simulations with 150 individuals of each species in each patch.

	Regional neutrality	**Community type**	**Intrinsic growth rate, optimal patch ($R_{optimal}$)**	**Intrinsic growth rate, sub-optimal patch ($R_{sub\text{-}optimal}$)**
Niche ↓ ***Neutral***	Yes	1	1.45	1.095833
	Yes	2	1.35	1.1
	Yes	3	1.25	1.104167
	Yes	4	1.15	1.108333
	Yes	5	1.11	1.11
Niche ↓ ***Neutral***	No	1	unif(1.55, 2.1)	unif(1.0, 1.22)
	No	2	unif(1.45, 1.9)	unif(1.0, 1.22)
	No	3	unif(1.35, 1.7)	unif(1.0, 1.22)
	No	4	unif(1.25, 1.4)	unif(1.0, 1.22)
	No	5	1.11	1.11

Table 3.2 Species' density-independent growth rates for their optimal (niche) and sub-optimal patches in the metacommunity, for each of the five metacommunity types. Parameter values are listed for cases with regional neutrality, and without regional neutrality.

Because the deterministic model has abundance on a continuous scale (i.e. there can be less than one individual), by definition no species ever goes extinct in a patch. For deterministic models, we therefore applied a detection threshold of 2 individuals per species to determine presence/absence – this is a conservative choice representing the minimum requirement for reproduction in a sexual population.

3.2.1a Stochastic and deterministic versions of the model

The above deterministic model is the mean field counterpart to its stochastic version (Hiebeler 1997), in which we include demographic stochasticity for births and dispersal (Table 3.1). We incorporated demographic stochasticity by drawing the number of individuals at a given time from a Poisson distribution, where the mean of the distribution equaled N_{t+h}/N_t from Eqn. 1. This allows for stochasticity in both births and survival (Melbourne and Hastings 2008). Stochasticity in dispersal was included by using a multinomial distribution with probability $m/(p-1)$ of dispersing to patch $z=1, 2, \ldots 25$ such that $z \neq x$.

3.2.2 Establishing metacommunities along a niche to neutral gradient

To create a gradient from niche to neutral, we varied density-independent growth rates, R_{ix}, among patches between the five scenarios (Table 3.2 shows parameter values). Differences in R_{ix} can be interpreted as representing differences in the species' responses to the abiotic environments of the patches. The metacommunity with the greatest niche structure (type 1 in Figure 3.1) had the largest difference in growth rate between the optimal patch (e.g. niche) for each species compared to all other patches. In this scenario, competitive exclusion of all species not in their optimal patches occurred, creating a species-sorting metacommunity (Leibold et al. 2004). At the other extreme, the metacommunity was neutral, where all species had identical density-independent growth rates in all patches (type 5 in Figure 3.1). Metacommunities of types 2, 3, and 4 were intermediate between species sorting and neutrality. For all metacommunity types, we held average fitness equal among all species at the metacommunity level, thus removing any effect of variation in average fitness among metacommunities and among scenarios. Thus, although species had niches or different growth rates in patches within the

metacommunity, their average fitness across the metacommunity was identical ("regional similarity", Mouquet et al. 2003). This assumption of regional similarity controls for the effect of fitness difference variation on the β-null deviation measure, allowing us to explore the effects of changes in local structuring processes while controlling for regional level contributions to local coexistence.

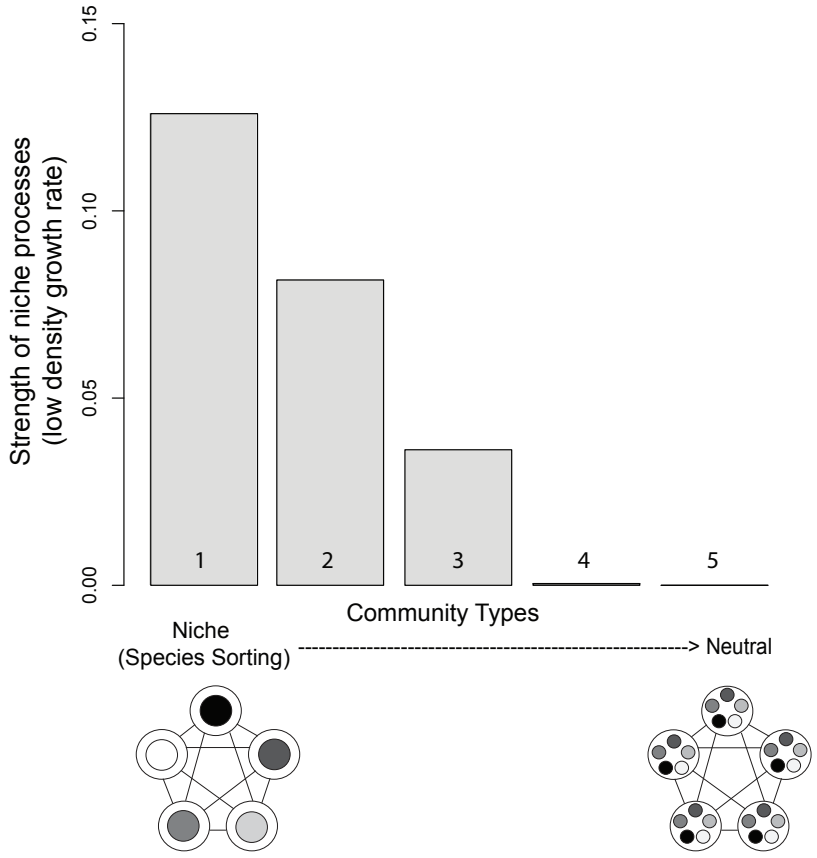

Figure 3.1 Strength of niche processes as measured by the magnitude of stabilizing coexistence mechanisms for the five possible models of metacommunity assembly, ranging from niche-structured (type 1, species sorting), to neutral (type 5) in which species co-occur in all patches. Model parameter values are listed in the Methods and Table 3.2.

3.2.3 Quantifying the strength of stabilizing coexistence mechanisms

We quantified the relative strength of niche-partitioning within each community type using the spatial coexistence mechanisms defined in Chesson (2000a). We measured the strength of stable coexistence as the tendency of a focal species to recover from low density (the long term low-density growth rate) while the rest of the community was at equilibrium for deterministic models or stationarity for stochastic models (Armstrong and McGehee 1980, Chesson 2000a, Turelli 1981). Because the average, metacommunity level fitness was equal for all species, low-density growth rate reflected contributions to coexistence exclusively from two stable coexistence mechanisms: fitness-density covariance and the spatial storage effect, which together define the spatial niche of a species (Chesson 2000a, Chesson 2008). Thus, the magnitude of the low-density growth rate is the sum of the contribution of these stabilizing mechanisms along the gradient from niche separation (species-sorting) to neutrality. In the neutral case, the low-density growth rate is zero, indicating a lack of stabilizing mechanisms and a metacommunity structured exclusively by equalizing mechanisms (Adler et al. 2007).

3.2.4 Removing regional similarity of species

To explore whether the absence of regional similarity alters our findings, we also constructed stochastic metacommunities in which species do not exhibit metacommunity-level neutrality. Following Melbourne et al. (2007), we did this by randomly drawing growth rates for each species in each patch from uniform distributions (Table 3.2). If that species coexisted with all other species thus far drawn (i.e. had a positive low-density growth rate), we kept that species for the simulation. If the species was unable to coexist, it was removed. We repeated this process until a metacommunity with 25 coexisting species was obtained: we used this process to produce

50 replicates of each metacommunity type.

3.2.5 Beta-null deviation calculation

β-null deviation values indicate the magnitude of deviation between the observed β-diversity (β_{obs}) and the expectation for β-diversity, $E(\beta_{null})$, from a randomly assembled pair of patches. We follow the method described in Chase et al. (2011) for the presence/absence β-null deviation measure. β_{obs} represents the pairwise Jaccard dissimilarity between two patches. To determine the null expectation $E(\beta_{null})$ for this pair of patches, 1000 pairs of patches—with α-diversity matched to the observed two patches—were then assembled by randomly selecting species weighted by their observed frequency in the metacommunity. Pairwise β-diversity between the 1000 randomly assembled pairs of patches was then calculated to produce a distribution of null β-diversity values: the null deviation value represents the difference between the observed pairwise β-diversity and the mean of the null distribution of β-diversity values (that is, $\beta_{obs} - E(\beta_{null})$). For a metacommunity, the overall β-null deviation was the mean deviation across all patch pairs.

Abundance-based β-null deviation values used the same procedure but with a different dissimilarity metric and null model. We used the Bray-Curtis dissimilarity metric, which takes account of species' relative abundances (Tuomisto 2010).The null model was created by randomly placing each observed individual into a patch until every individual had been placed into a patch in the metacommunity (Kraft et al. 2011, Stegen et al. 2013). This maintains the observed metacommunity-level abundance distribution but randomizes the location of individuals.

3.2.6 Analyses

We calculated both presence/absence and abundance-based β-null deviation measures for four distinct scenarios. In ***scenario 1***, we examined how β-null deviation values changed for metacommunities along the gradient from niche to neutral assembly (types 1-5), for both deterministic and stochastic formulations of the model. We allowed dynamics to continue for 150 generations to ensure that analyses captured the equilibrium state (deterministic) or stationary distribution (stochastic) rather than transient dynamics, and then calculated β-null deviation measures. In ***scenario 2***, we explored how the β-null deviation measure captures transient dynamics in stochastic models for niche (type 1) and neutral (type 5) communities. We measured β-null deviation for 750 generations (measuring values at 10, 50, 100, 150, 250, 500, 750 generations) while holding all parameters constant. In ***scenario 3*** we considered the effect of changes in assembly mechanism through time, such as is typical in manipulative experiments. After the metacommunity reached its equilibrium (deterministic) or stationary distribution (stochastic), we applied a simulated experimental treatment that caused either (1) a niche structured metacommunity to become neutrally structured (parameter values changed from type 1 to type 5) or (2) a neutral metacommunity to become niche structured (parameter values change from type 5 to type 1). We then compared the β-null deviation values before treatment to a 150-generation time-series after the treatment for both stochastic and deterministic versions of the model. In ***scenario 4***, we examined how β-null deviation values changed along a gradient from niche to neutral assembly (types 1 through 5), but this time removing the constraint of regional similarity. In all analyses of stochastic models, we simulated 50 metacommunities for each model type and calculated the β-null deviation measure for each metacommunity.

3.2.7 Effect of degree of regional species pool sampling on beta-null deviation

Thus far we have assumed a complete census of the regional species pool. However, observational data are typically from a sample and involve uncertainty about the true abundances of species in a region. To examine the effect of this uncertainty, we sampled less than the true number of patches in the 25 species metacommunity, including only 5, 10, 15, or 20 local patches from the 25-patch metacommunity to calculate the null deviation measure. We repeated the sampling 250 times for each level to determine whether the accuracy of the abundance-based measure varied with the proportion of sites sampled from the metacommunity. Results for samples of 10, 15, and 20 patches fell predictably between those of 5 patches and all 25 patches, so we present results from the most extreme case (only 5 patches or 20% of the metacommunity).

3.3 Results

3.3.1 Niche to neutral gradient

We confirmed that the species-sorting (type 1) to neutral (type 5) metacommunity gradient represented a gradient of niche strength. Along the niche to neutral gradient, metacommunities of type 1 (species-sorting) had the highest low-density growth rate (Figure 3.1), which declined in each metacommunity type to a value of 0 for neutral communities. This means that in neutral metacommunities, while species did not drive others towards extinction, they did not have a tendency to recover from low-density. Thus, stabilizing coexistence mechanisms (or niches) were strongest in type 1 metacommunities and absent from type 5 metacommunities, which were structured exclusively by equalizing mechanisms.

3.3.2 Scenario 1

Jaccard dissimilarity β-diversity values for the deterministic metacommunities varied from 1 (patches differ completely in their composition) to 0 (patches have identical compositions), respectively, along the gradient from niche-structured to neutral metacommunities. Values of the presence/absence β-null deviation measure reflected the changing structure along this gradient. They distinguished between neutral or near-neutral metacommunities (types 4-5), which had β-null deviation values of zero—indicating an absence of niche processes—and niche metacommunities (1-3), which had values larger than zero (Figure 3.2a)—indicating niche processes were causing patches in a metacommunity to be more dissimilar than expected. The abundance β-null deviation measure also varied for metacommunities along this gradient: from mean values of 0.793 for niche structured metacommunities (type 1) to -0.341 for neutral metacommunities (type 2). Negative β-null deviation values suggest that species composition is more similar between patches than expected under the null model of random assembly. This makes sense because, in contrast to the null model, deterministic neutral communities are not randomly assembled thus removing a source of dissimilarity. The abrupt jump in β-null deviation values between metacommunities of type 3 and 4 in the deterministic case reflects the detection threshold.

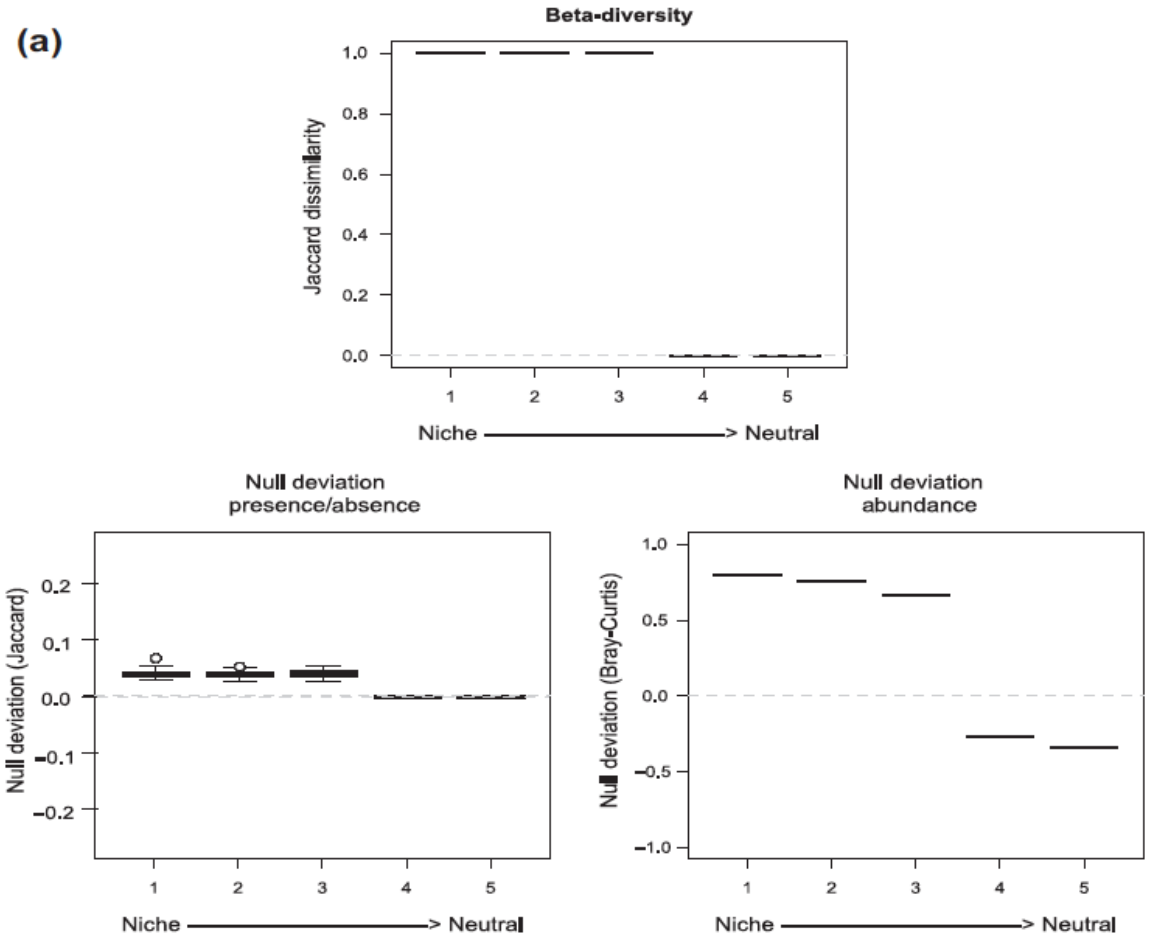
(a)
Beta-diversity
Jaccard dissimilarity
1.0
0.8
0.6
0.4
0.2
0.0
1
2
3
4
5
Niche ——> Neutral
Null deviation
presence/absence
Null deviation (Jaccard)
0.2
0.1
0.0
−0.1
−0.2
1
2
3
4
5
Niche ——> Neutral
Null deviation
abundance
Null deviation (Bray-Curtis)
1.0
0.5
0.0
−0.5
−1.0
1
2
3
4
5
Niche ——> Neutral

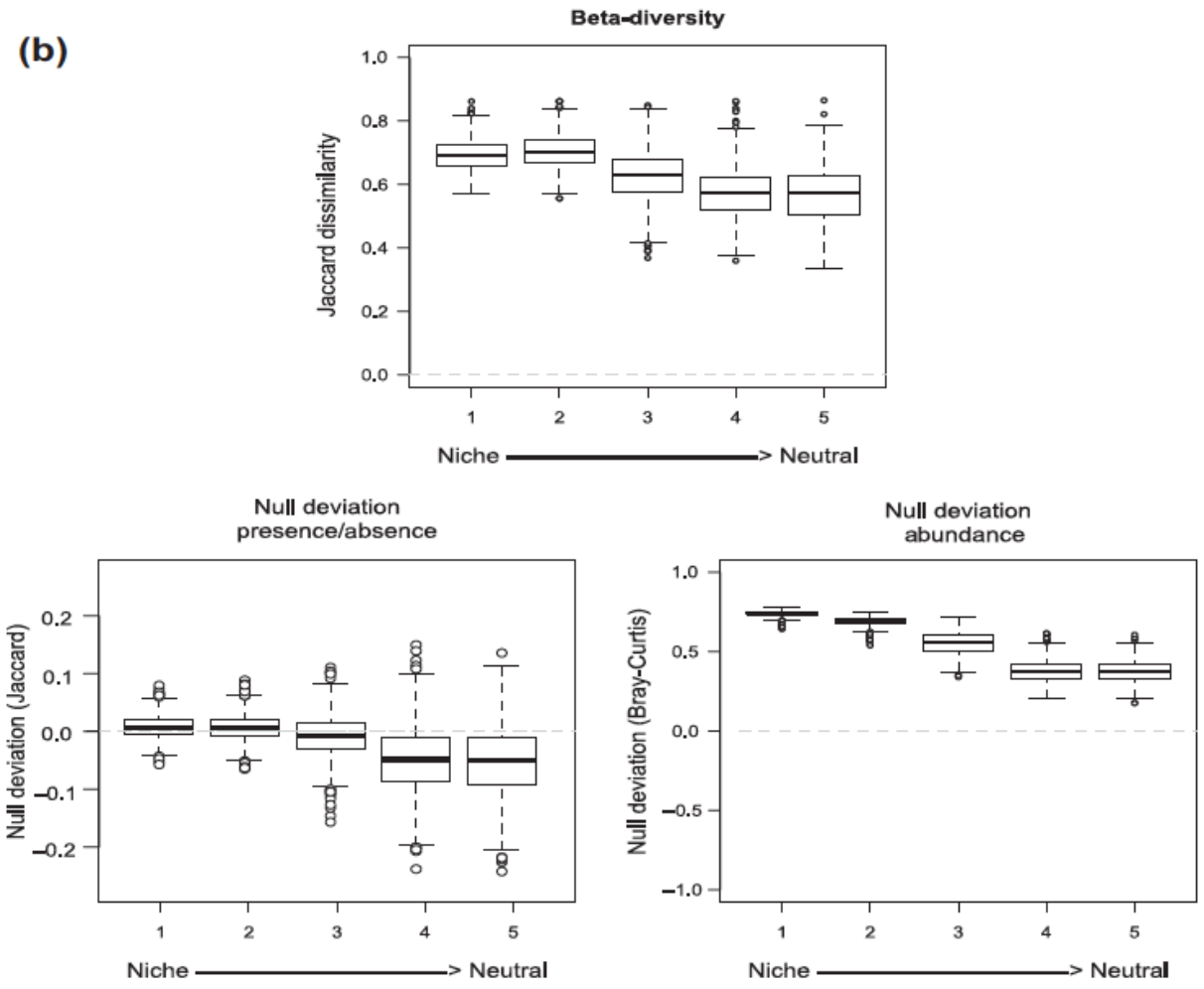

Figure 3.2 β-null deviation values from simulated metacommunity models, for five assembly types representing a gradient from niche to neutral. Subplots show beta-diversity (Jaccard), presence/absence β-null deviation values, and abundance β-null deviation values for (a) deterministic metacommunity models and (b) stochastic metacommunity models. Each bar represents 50 replicate metacommunities (see Methods): dark lines show the mean value, whiskers capture the interquartile range, and points show extreme values. Note that y-axes differ for presence/absence and abundance b-null deviation results.

We considered the same gradient of assembly for stochastic metacommunity models. Compared to deterministic metacommunities, which had little variability in β-null deviation values, stochastic metacommunities had more variability in β-null deviation values, indicated by the greater interquartile range (Figure 3.2b). Variability in β-null deviation in deterministic

metacommunities is due exclusively to Monte Carlo error induced by the null model, whereas variability in β-null deviation in stochastic models reflects variability in metacommunity structure. Monte Carlo error is the error in the null deviation that arises because its estimate relies on a stochastic simulation of the null model (Hammersley and Handscomb 1964, Koehler et al. 2009). Mean β-diversity values ranged between approximately 0.5 and 0.7, indicating patch level composition, on average, was quite dissimilar. The presence/absence β-null deviation values ranged between 0.016 (± 0.190) to -0.05 (± 0.062) for niche and neutral metacommunities (here and elsewhere, we report mean ± standard deviation). The trend toward more negative values of β-null deviation for neutral metacommunities suggests that species composition of patches in the metacommunity is more similar than expected under the null model of random assembly. This shows that the null model does not correctly capture beta diversity for the neutral metacommunities. β-null deviation values for the abundance version of the measure varied between 0.739 (± 0.018) to 0.367 (± 0.064) for niche through neutral metacommunities, declining consistently toward zero along the niche-neutral gradient. Positive values of the β-null deviation measure for neutral metacommunities suggest that species composition was less similar between patches compared to the random expectation.

Deterministic and stochastic model results did not depend on dispersal type, suggesting they are robust to variation in dispersal rates and dispersal strategies, ranging from restricted local movement to global dispersal (Appendix 2 Figure S1 and S2).

3.3.3 Scenario 2

For stochastic niche structured metacommunities, the presence/absence β-null deviation measure did not vary greatly over 750 generations (measured at generations 10, 50, 100, 150,

250, 500 and 750 generations), μ±σ: -0.001±0.011, 0.003±0.016, 0.002±0.016, 0.001±0.017, 0.002±0.015, 0.002±0.015, 0.002±0.016). All values were close to zero, the expectation for neutral rather than niche metacommunities. Values for abundance β-null deviations initially rose, in response to the non-equilibrium starting conditions, and then remained constant with positive values over the 750 generations (measured at generations 10, 50, 100, 150, 250, 500 and 750 generations): 0.350±0.039, 0.750±0.015, 0.750±0.015, 0.750±0.016, 0.750±0.016, 0.750±0.015, 0.750±0.015) (Figure 3.3).

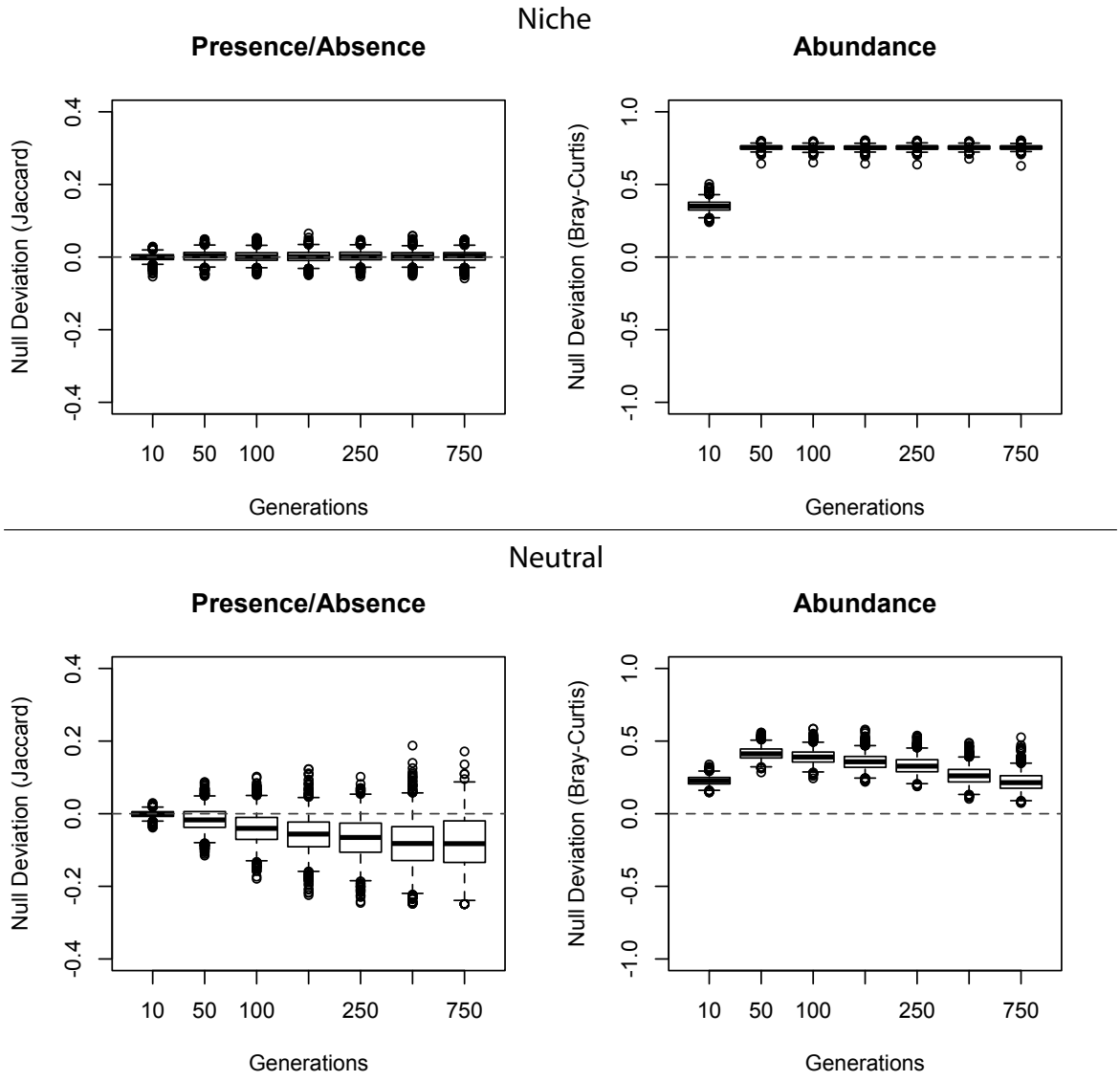

Figure 3.3 Changes in β-null deviation values over time. β-null deviation results are shown for niche-structured metacommunities (type 1) and neutrally-structured metacommunities (type 5) for stochastic models, where dynamics were allowed to continue for 750 generations. Both presence/absence and abundance β-null deviation measures were calculated. Each bar represents 50 replicate metacommunities. Note the x-axis is categorical, not a continuous scale.

For stochastic neutral metacommunities, presence/absence β-null deviation values initially centered at zero (as expected), but became more negative with time and increased in variance (for time points 10-750: -0.001±0.010, -0.016±0.034, -0.040±0.044, -0.057±0.052, -

0.066±0.057, -0.082±0.070, -0.084±0.072). The abundance-based β-null deviation values for stochastic neutrally structured metacommunities rose slightly and then declined through time, although values remained positive (for time points 10-750: 0.228±0.032, 0.415±0.044, 0.391±0.044, 0.359±0.051, 0.332±0.057, 0.265±0.061, 0.222±0.066).

3.3.4 Scenario 3

In both scenarios (a change from niche to neutral assembly, and a change from neutral to niche assembly), although the value of the presence/absence measure changed, it did not change in the way expected to correctly detect the structuring mechanism (i.e. the experimental treatment) (Figure 3.4). In the niche to neutral scenario presence/absence β-null deviation values became increasingly negative, falsely indicating an increase in community structure compared to randomly assembled communities: at the start of the experiment, the mean β-null deviation value was 0.007 (±0.020) and after 150 generations it was -0.052 (±0.061). Variance in β-null deviation also increased over time. Conversely, in the neutral to niche scenario, presence/absence β-null deviation values were initially negative (-0.045±0.058) but after the simulated experimental treatment, the β-null deviation values increased to near zero (-0.001±0.02), falsely suggesting a neutral metacommunity rather than a niche-structured metacommunity.

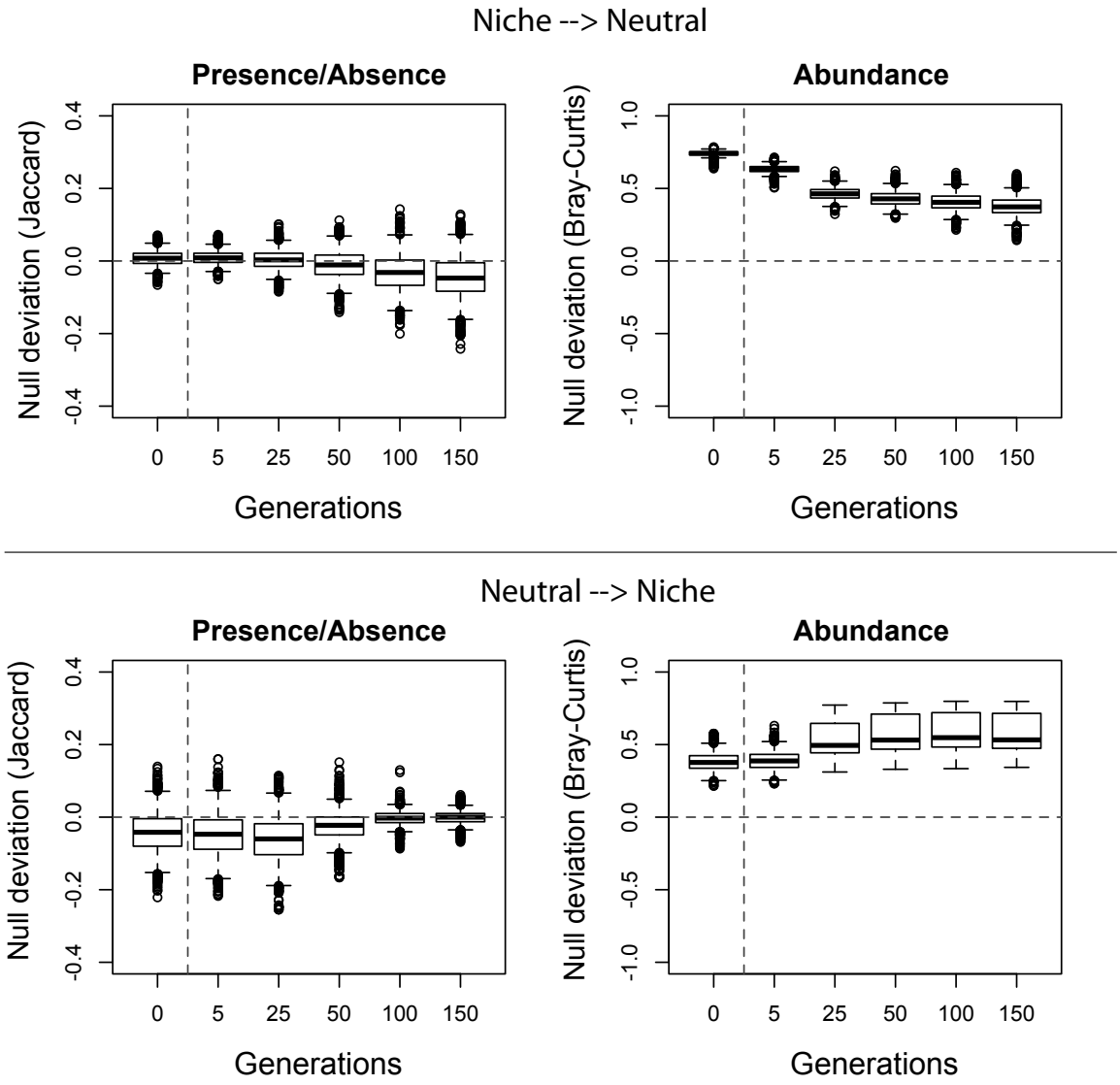

Figure 3.4 The effect of changes in assembly processes on β-null deviation values. Figure shows the effect of changes from niche to neutral assembly (top) and from neutral to niche assembly (bottom) over time, for stochastic metacommunity models. Both presence/absence and abundance β-null deviation measures were calculated. Each bar represents 50 replicate metacommunities. Note the x-axis is categorical, not a continuous scale.

The abundance based β-null deviation measure performed better, declining towards zero after a change to neutral assembly (from 0.740±0.067 at t=0 to 0.377±0.067 at t=150), and becoming increasingly positive after a change to niche assembly processes (from 0.383±0.125 at t=0 to 0.587±0.125 at t=150). Variance in β-null deviation between realizations in the stochastic

neutral to niche models was largely a result of variation in the state of neutral metacommunities (resulting from stochasticity) just before the switch to niche processes.

3.3.5 Scenario 4

Removing the regional similarity constraint did not alter the distribution of β-null deviation values along the niche-neutral gradient (Figure 3.5). Results were qualitatively similar to those from the stochastic metacommunity with regional similarity (Figure 3.2b).

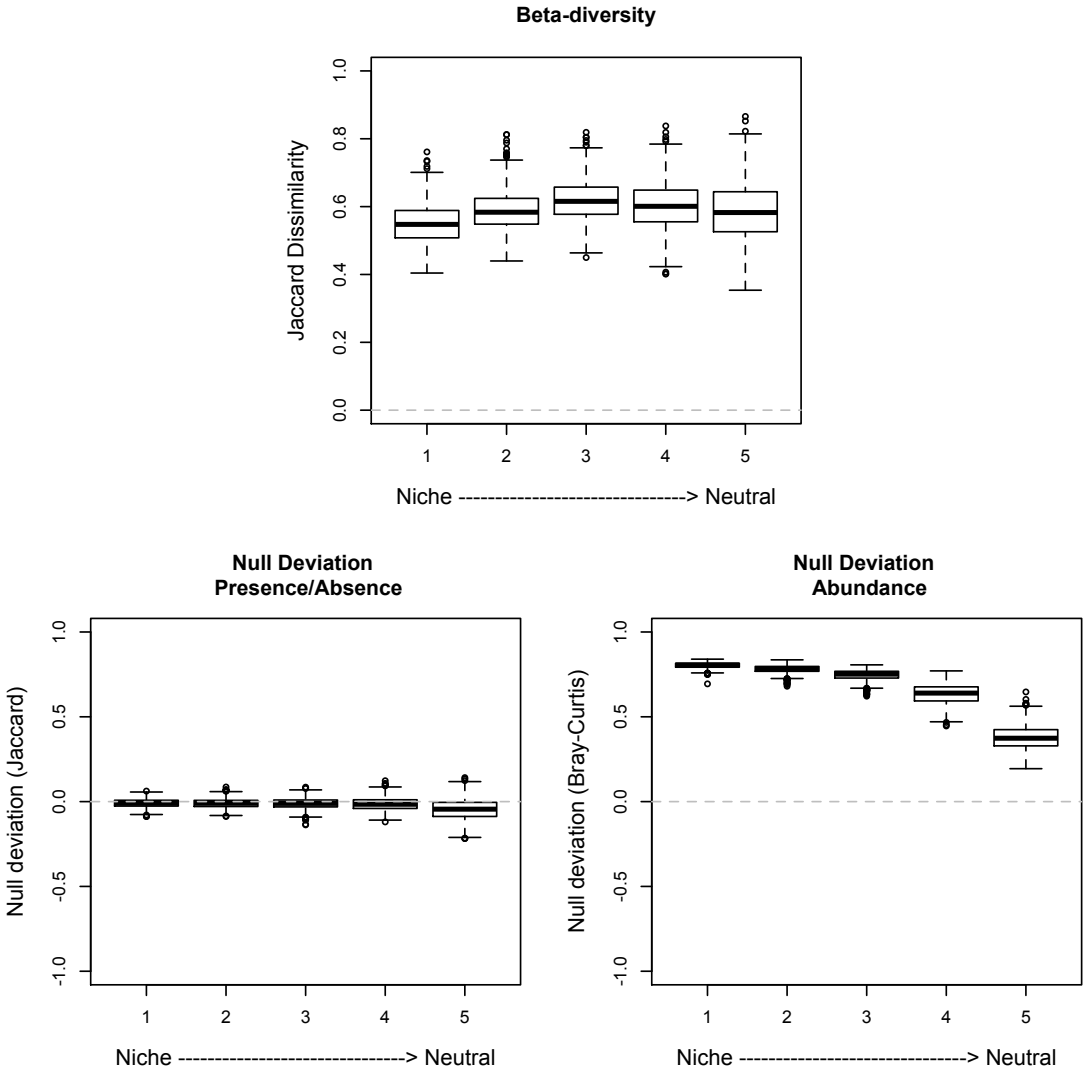

Figure 3.5 β-null deviation values from simulations of stochastic metacommunities when species do not have equal fitness at the metacommunity scale (i.e. in the absence of regional similarity). See Methods for the five assembly types.

3.3.6 Effect of degree of regional species pool sampling on beta-null deviation estimates

Sampling the metacommunity resulted in higher null deviation values than those from a complete census of the metacommunity (Figure 3.6). There was a significant interaction between sample size and metacommunity type: niche metacommunity β-null deviation values were more

biased when under-sampled while neutral metacommunities were more uncertain.

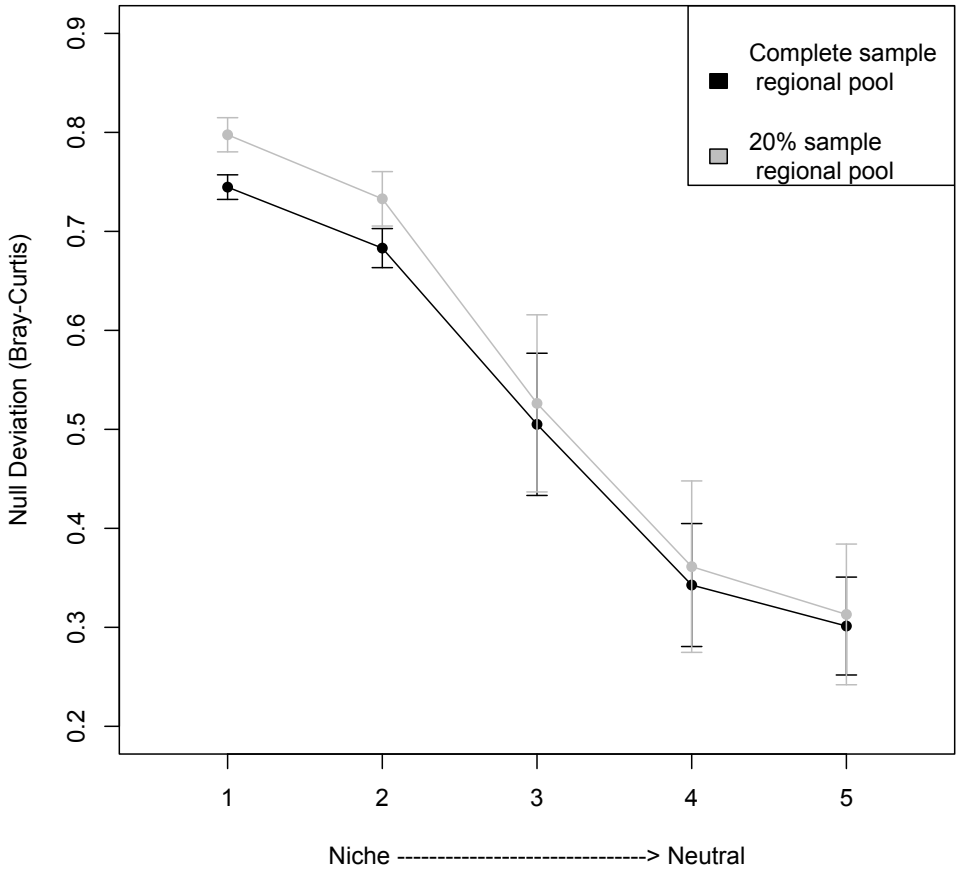

Figure 3.6 Effect of incomplete sampling of the regional species pool for abundance-based null deviation metric values. Error bars represent standard deviations for 50 replicates of the sampling procedure (see Methods).

3.4 Discussion

The β-null deviation measure, initially developed as a null model for β-diversity, has increasingly been used as an index of community assembly mechanisms and applied to empirical data. This analysis compared β-null deviation for simulated communities with known assembly mechanisms to determine how values of the β-null deviation measure should be interpreted and how effectively it performs in this role. Our results help to clarify the correct interpretation of the

β-null deviation measure: we found that its values differentiate between niche (values further from zero) and neutrally structured metacommunities (values nearer to zero). This is in contrast to the interpretation of deterministic versus stochastic processes (e.g. Chase and Myers 2011, Stegen et al. 2013). The presence/absence β-null deviation measure was not robust to the effect of demographic stochasticity on assembly, so we cannot recommend it. In contrast, the abundance based measure changed consistently along the niche-neutral gradient and to changes in assembly, although its utility is primarily as a comparative (focusing on changes in value), rather than absolute measure.

3.4.1 How should beta-null deviation values be interpreted?

In the absence of any stochasticity, presence absence β-null deviation values relate—as originally assumed—to the structuring processes assembling a community. Values of zero differentiate neutral communities from those that are niche structured (absolute values much greater than zero). This differs from the original interpretation of β-null deviation values (Chase 2010, Chase et al. 2011), which suggested that values near zero reflect stochastic assembly processes and those different from zero reflect deterministic processes. Instead, we show that, for the presence/absence measure, the null expectation for β-diversity between random samples of species from the regional species pool converges on the expectation for a neutral community, i.e. all species are similarly likely to be present in a patch. Thus the statistical null model reflects our neutral model of assembly.

3.4.2 Performance of different versions of the β-null deviation measure

We found that β-null deviation measures varied in their properties depending on whether

they were calculated using presence/absence or abundance data. In particular, the presence/absence measure was not robust to (1) stochasticity in assembly, (2) the number of generations from assembly to sampling (due to variation from stochasticity in population dynamics), and (3) changes in assembly mechanisms through time. Demographic stochasticity in particular affects the β-null deviation measure, because it decreases the relative differences in β-null deviation between niche and neutral communities while increasing variance, making it difficult to correctly distinguish between these mechanisms. This difficulty is enhanced when assembly mechanisms change through time. For example, historical contingency can alter community structure far from the expectation for niche or neutral assembly, and the presence/absence measure is not robust to such contingency. The presence/absence β-null deviation measure (and many presence/absence based null models) relies on variation in species identity between local communities to distinguish between structuring processes: except in highly diverse metacommunities, there is often not enough variation in species' composition to provide strong evidence for a particular assembly process.

The abundance-weighted β-null deviation measure was developed in part because of such limitations, and is used to control for the effects of spatial aggregation of individuals in samples (e.g. Stegen et al. 2012). Performance of this measure was markedly better than that of the presence/absence version: the absolute value of the abundance-weighted β-null deviation measure increased in response to niche processes and declined in response to neutral processes. The abundance-weighted β-null deviation measure was effective in identifying increases or decreases in niche or neutral structure in communities through space and/or time. Further, it behaved reasonably consistently in the presence of stochasticity, through time, and for communities lacking regional similarity, all of which suggests that it is better suited to use with

empirical data. However, a number of issues must still be considered. First, similar values of the abundance β-null deviation measure may still reflect different assembly processes, as in Myers *et al.* (2013), in which the authors showed that β-null deviation values for tropical and temperate forests were similar, but different mechanisms (environmental filtering vs. dispersal limitation) produced these similar values. Results of similar magnitudes are not necessarily comparable across different metacommunities: a metacommunity in one system should not be said to be "more niche structured" because it has a larger β-null deviation value than that measured in a different system. The β-null deviation is not robust to comparisons across systems or habitats, and likely should be restricted to geographically similar analyses, such as within metacommunities or regions, or across time or experimental treatments for a single locale.

In addition, absolute values of the abundance β-null deviation measure did not correspond with the expectation for niche or neutral communities. The abundance β-null deviation measure reflects changes in aggregations of individuals, but it is also sensitive to changes in abundance evenness distributions. Non-random abundance evenness distributions, such as may result from neutral assembly of patches, can cause null deviation values to diverge from zero, simply because the null model has random uneven) abundances. This may result in negative values of the β-null deviation metric (e.g. deterministic model, Figure 3.2a, where abundances are more even than random), or positive values (e.g. stochastic model, Figure 3.2b, where abundances are less even than the random expectation due to stochasticity). The inability to disentangle whether the abundance-weighted β-null deviation measure changes as a result of changing aggregations of individuals, or changing evenness in composition, also limits its utility.

The β-null deviation measure relies on knowing the true abundance distribution of the regional species pool. One important limitation occurs when the true abundance distribution of a

regional species pool is unknown, such as due to undersampling of sites or difficulties in delimiting the "regional pool". We found that where only 20% of the true metacommunity patches were sampled (e.g. 5 patches), the decline in the β-null deviation values across the niche-neutral gradient was significantly different from that of the complete sample, though the realized effect size was small (~7%). Because species sorting in our niche-structured metacommunities implies that each patch should have unique species abundances, values of the measure are biased for niche structured metacommunities when there is under sampling of patches in the region. Alternately, a scheme that subsamples individuals in each patch, such as through use of transects or point counts, would tend to be less accurate for stochastic neutral communities (since at each patch many species co-occur and so site abundances are lower if carrying capacity is constant, and undersampling would increase variation). The issue of accuracy in sampling and defining the abundance-weighted regional species pool is an important one for observational data, where uncertainty is expected. β-diversity measures are sensitive to undersampling (particularly those based on presence-absence data) (Beck et al. 2013); compounding this, the reliance of the null deviation measure on the observed abundance or range size distribution provides an additional source of bias when species' abundances or presences are not well reflected by the data. Future work should consider the implications of undersampling for null models such as this one.

We considered five different strengths of stabilizing coexistence mechanisms, from strong niche differences between species to neutrality, covering three of the four metacommunity paradigms: species sorting, neutrality, and mass effects. Our model produced strong gradients in beta-diversity (values from 0-1) as a result of differences in species' innate growth rates in patches, making it a valuable first approach to testing the β-null deviation measure. However, these are likely not the only factors influencing β-diversity in natural systems. Other drivers of β-

diversity, such as speciation, dispersal barriers or limitations, and extinctions, as well as more realistic assumptions (such as larger species pools) should be considered as well. While spatial aggregation may additionally influence the ability of the β-null deviation measure to detect underlying community assembly processes, lowering dispersal rate or using limited local dispersal did not alter our conclusions. However, in well-mixed communities (e.g. a dispersal rate of 50%), increased dispersal causes communities to appear increasingly similar and so measures of β-diversity and community assembly are no longer meaningful (e.g. Appendix 2).

3.5 Conclusion

Though originally developed as a null model for β-diversity, β-null deviation measures are increasingly used as an indicator of the processes structuring communities. They speak to a fundamental issue in ecology – the need to reconcile empirical data, statistical models, and theoretical explanations. However, as with most measures meant to bridge observational and theoretical analyses, many assumptions are needed. This work clarifies for the first time the appropriate interpretation of the β-null deviation measures: to differentiate between niche and neutral communities, rather than between deterministic and stochastic communities. Our results suggest, however, that presence/absence based β-null deviation measures lack the resolution to differentiate between niche and neutral communities, particularly when stochasticity or changes in assembly though time are present, but that the abundance based β-null deviation measure performs adequately under these conditions. However, null models that precisely and robustly disentangle the different processes structuring communities remain elusive.

3.6 Acknowledgements

Thanks to G. Legault for thoughtful comments. CMT, DN, and BAM were supported by DEB 1258160; LGS was supported by the National Science Foundation (GRFP-1144083 and IGERT-1144807); KFD was supported by the National Science Foundation (DEB 0841892); CMT was supported by an NSERC PDF.

Chapter 4

Body Mass Evolution and Diversification within Horses (family *Equidae*)

Lauren G. Shoemaker and Aaron Clauset

Published as: Shoemaker, L., and Clauset, A. (2014). Body mass evolution and diversification within horses (family Equidae). Ecology Letters, 17: 211-220.

Horses (family Equidae) are a classic example of adaptive radiation, exhibiting a nearly 60-fold increase in maximum body mass and a peak taxonomic diversity of nearly 100 species across four continents. Such patterns are commonly attributed to niche competition, in which increased taxonomic diversity drives increased size disparity. However, neutral processes, such as macroevolutionary ``diffusion," can produce similar increases in disparity without increased diversity. Using a comprehensive database of Equidae species size estimates and a common mathematical framework, we measure the contributions of diversity-driven and diffusion-driven mechanisms for increased disparity during the Equidae radiation. We find that more than 90\% of changes in size disparity are attributable to diffusion alone. These results clarify the role of species competition in body size evolution, indicate that morphological disparity and species diversity may be only weakly coupled in general, and demonstrate that large species may evolve from neutral macroevolutionary diffusion processes alone.

4.1 Introduction

Horses (family Equidae) are a classic example of adaptive radiation. First appearing 56 million years ago (Ma) in Holarctica, horses underwent a dramatic diversification in the late

Oligocene and early-to-mid Miocene. By the end of this period, Equidae included nearly 100 contemporaneous species, spread across four continents, in sizes ranging from approximately 10–1200kg (Hulbert 1993, Eisenmann, 2003). Although the biological mechanism driving this dramatic size disparity remains unclear, insights would inform both the evolutionary and ecological history of horses (MacFadden 1992, Janis, 2007) and shed light on the general processes that shape morphological, taxonomic, and ecological diversity in mammals (Stanley 1973, Brown, 1995).

Many characteristics of horses changed during their radiation including body size, hoof shape, diet, and molar characteristics (MacFadden 1992, Janis 2007). Here, we focus on species body mass or size, a fundamental biological variable that correlates strongly with ecological traits, including habitat preference, diet, range, life span, gestation period, metabolic rate, and population size (Brown 1995, West et al. 2002, Cardillo et al. 2005, Smith et al., 2002), as well as trophic level and niche position in food webs (Williams et al. 2010). For these reasons, size is an easy-to-measure proxy (Lucas et al. 2008) for studying and modeling species characteristics, ecosystem structure, and ecological niches, even across evolutionary time (Gittleman 1985). Moreover, the distribution of species sizes within a taxonomic group is an effective summary of species characteristics.

Among major animal lineages, including mammals, birds, fish, and insects, this distribution often exhibits a canonical right-skewed pattern (McShea 1994, Kozlowski and Gawelczyk 2002, Clauset et al. 2009, Smith and Lyons 2011). For example, the most common size of a terrestrial mammal is roughly 40 g (like the common Pacific Rat, *Rattus exulans*), while both larger and smaller species are less common, but asymmetrically so: the largest, like the

African Elephant (*Loxodonta africana*, 4 × 106 g), are orders of magnitude larger, while the smallest, like Remy's Pygmy Shrew (*Suncus remyi*, 2 g), are only slightly smaller.

The origin of this ubiquitous pattern is commonly attributed to one of two biological mechanisms: asymmetric dispersion, produced by macroecological competition for niches, around a preferred or optimal body size (Maurer et al. 1992, Smith et al. 2010), or constrained macroevolutionary "diffusion" (Table 4.1) in the presence of a hard limit at the lower end, due to physiological constraints, and a soft limit at the upper end, caused by extinction rates that gently increase with body size (Stanley 1973, Clauset and Erwin 2008). Traditionally, the evidence for these two mechanisms has been documented separately, and relatively little work has compared them directly using data. Crucially, these explanations make distinct predictions about the relationship between diversity and disparity during the expansion of a taxonomic group: the macroecology explanation predicts that increases in size disparity are driven directly by increases in species diversity or number, while the macroevolution explanation predicts that disparity can increase without a concurrent increase in diversity.

Term	Definition
Body size distribution	Relative frequencies of species body masses within a taxonomic group
Diversity	Number of species in a taxonomic group
Size disparity	Difference in body mass between the largest and smallest species in a group
Diffusion	Aggregate result of many individuals following, possibly constrained, random-walk-like trajectories through a fixed or evolving space
CESR model	Mathematical model of a species size distribution, in which individual species sizes follow a constrained, branching (cladogenetic) multiplicative random walk
Diversity-driven disparity	Mechanism for increased size disparity, in which interspecific competition drives new species into larger bodied, unoccupied niches
Diffusion-driven disparity	Mechanism for increased size disparity, in which species sizes vary independently of nearby niche occupation, as in diffusion
Cope's Rule	Average multiplicative change between an ancestor A's and descendant species D's mass, $\langle ln\lambda \rangle = \langle \ln (\frac{M_D}{M_A}) \rangle$ (While there are two common definitions of Cope's Rule, we use Alroy's, which lends itself to quantitative analysis.) (Alroy, 1998)

Table 4.1 Terminology for body size evolution model

The Equidae family is well suited for investigating this question: it is an ecologically important monophyletic family and has a well resolved fossil record with reliable size estimates for hundreds of species over its duration. Furthermore, horses exhibit many of the patterns associated with adaptive radiations (Gavrilets and Losos 2009): over the past 56 millions of years (My) but particularly from 24–20 Ma, both size disparity and the number of species increased dramatically, horse morphology diversified considerably, with many lineages switching from grazing to browsing and increasing their geographical ranges (MacFadden and Hulbert 1988), new species arose from nonallopatric speciation, and mostly small phenotypic changes occurred after the main diversification period. The concurrent increases in diversity and disparity presents

a simple but fundamental question: was the increase in disparity driven by increased diversity or not?

We investigate this question using a clade-level mathematical model that captures the distinct predictions of the two explanations for species body size distributions. Although still other explanations are possible, we focus on these two general hypotheses. Both hypotheses have extensive associated literatures and examine factors within a given clade that are hypothesized to contribute to expansion of body size.

By using the same mathematical model to capture both mechanisms, we control the impact of auxiliary assumptions and place the hypotheses on equal footing, allowing for a self-contained pairwise comparison. We then use this model to measure the relative importance of each mechanism for explaining the observed increase in Equidae maximum size.

The first mechanism, which we call the diversity-driven model (Foote 1993, Erwin 2003), assumes a fixed set of available niches that are unequal in their attractiveness to species, e.g., due to different associated reproductive rates (Maurer et al. 1992, Brown 1995). When the number of niches at a particular size is small, increasing diversity implies the occupation of progressively less attractive niches, via inter-specific competition. When competition is strong, a fixed number of n species will occupy the n niches closest to the optimal or most attractive size, and as new species are added, niches are occupied in decreasing order of their attractiveness. The result is that most or every available niche at a given size will be filled before many niches at more extreme sizes are filled (Maurer et al. 1992, Foote 1993, Erwin 2003), and when no more niches are available, a saturating maximum body size is observed (Smith et al. 2010). Thus, under this hypothesis, disparity increases only from increasing diversity.

The second mechanism, which we call the diffusion-driven model, assumes that ecological pressures or selective effects on species body size are not dependent on the occupation status of nearby niches, and instead vary randomly both in direction and magnitude over evolutionary time, across a taxonomic group (Stanley 1973, McShea 1994, Clauset and Erwin 2008). The aggregate result of such pressures is a macroevolutionary diffusion process (Raup 1977, Hunt, 2007) in which species body size varies like a random walk from ancestor to descendant. For a fixed number of species, individual lineages are occasionally pushed into larger-bodied niches as the result of these uncorrelated selective pressures, causing size disparity to increase over time without the addition of new species. Heterogenous ecological variables like interspecific competition, life history, and habitat play secondary roles in this type of mechanism, being aggregated across large spatial and temporal scales. Instead, the governing variables are those specifying the distribution of size changes at each step of the random walk and any constraints on the range of possible sizes (Clauset and Erwin 2008). Under this mechanism, niche space remains sparsely occupied (in contrast to the diversity-driven model), species sizes may change independently of the occupation of niches at smaller sizes, and disparity can increase without increased diversity.

We first construct a comprehensive database of size data for Equidae over the past 56 My and then formalize the two hypotheses within a single quantitative framework. The mathematical form of this framework makes precise statements about both the theoretical structure of the one-dimensional body size morphospace as well as its species occupation number, without needing to model individuals or population dynamics. Using this model, we can predict both body size distribution and the increase in disparity through time. We apply this framework to our horse

data to measure the relative importance of the two mechanisms for explaining Equidae's nearly 60-fold increase in maximum size.

4.2 Materials and Methods

4.2.1 Family Equidae

Horses (family Equidae) consist of 246 known fossil species from 43 genera, which are found in North America, Europe, Asia, and South America (Janis 2007). The family originated in Europe 56 Ma (MacFadden 1992), and is a subclade of order Perissodactyla, or odd-toed ungulates (Janis 2007). Over the course of Equidae evolution, horses have ranged in size from roughly 10 kg to over 1200 kg. The horse family is well-represented in the paleontological and paleobiological literatures, making it an ideal group for the study of body size evolution within mammalian taxonomic subgroups. In general, estimates of fossil horse species size are made from molar measurements, using standard techniques (MacFadden 1986).

The earliest horses belonged to *Hyracotherium* (56 Ma), which had small hooves, a footpad, and molars with low crowns for crushing leaves, berries, and other fibrous vegetation (Janis 2007). The subsequent expansion of the Equidae family is divided into three subfamilies, the Hyracotheriinae (Eocene), the Anchitheriinae (Eocene to Miocene), and the Equinae (Miocene to present) (Janis 2007). The first subfamily, the Hyracotheriinae, found in North America and Europe, were relatively small, forest-dwelling horses with a fibrous diet that emphasized leaves (Janis 2007). In comparison, the second subfamily, the Anchitheriinae, developed more specialized hooves and molars, and exhibited three-toes and longer limbs that were more efficient for locomotion (Janis 2007). Their teeth shape and microwear indicates a specialized diet of leaves, now from a temperate rather than tropical forest. From 24 to 20 Ma,

Equidae exhibited enormous taxonomic diversification, increasing from less than 20 to nearly 100 known species, forming three distinct Equidae lineages (Figure 4.1), exhibiting a broad range of body masses (Figure 4.2).

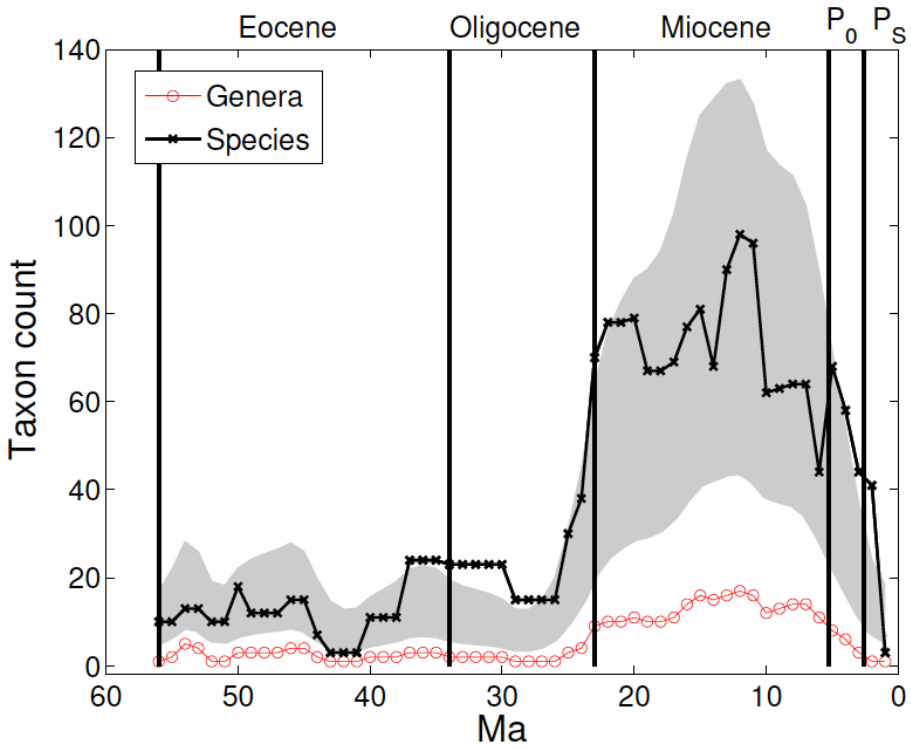

Figure 4.1 Equidae diversity over time, showing species- and genera-level counts from our database of 246 species and the estimated diversity range (shaded region) based on extrapolating high and low species counts from genera diversity. P_O, Pliocene epoch; P_S, Pleistocene.

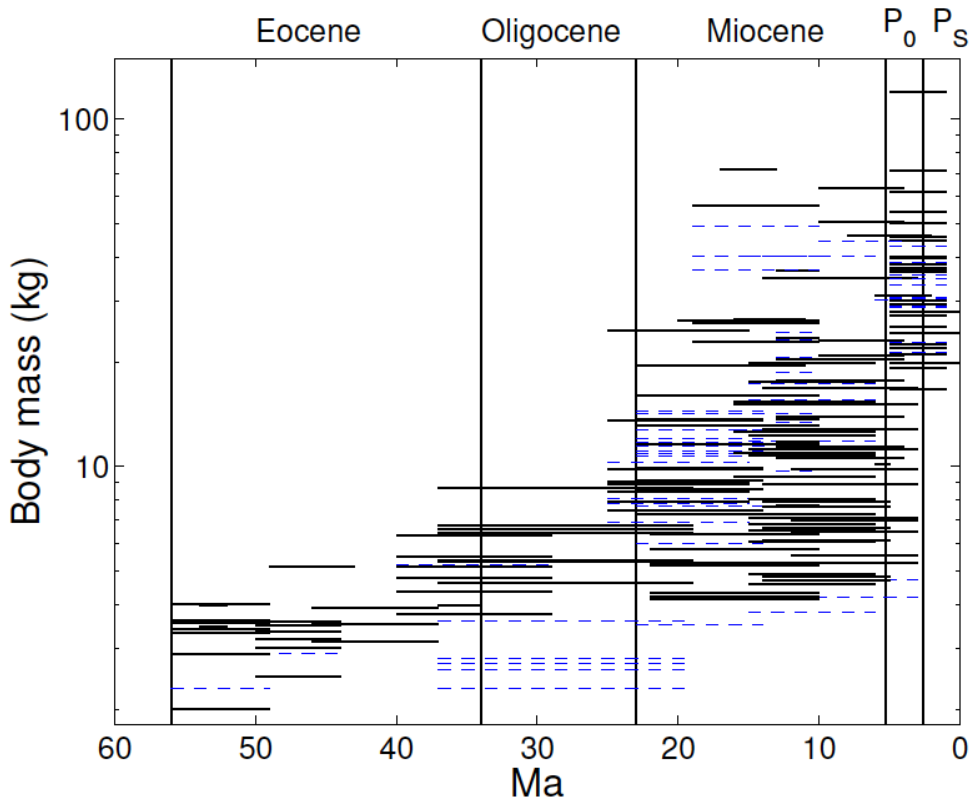

Figure 4.2 Equidae body masses over time for 225 species. Each line gives the estimated body mass of a single species and spans that species' known duration. Solid lines indicate estimates from molar or length measurements; dashed lines indicate estimates from genera-level ranges.

The third subfamily, the Equinae, shifted to a relatively fibrous or grassy diet, just as grasslands expanded at the expense of tropical broadleaf forests, and included the first "grazing horse," *Merychippus*, in North America. Corresponding skeletal evolution includes an elongation of the face and a deepening of the lower jaw. Equinae lost footpads and late Equinae members exhibit the single toe characteristics of modern horses (Janis 2007).

4.2.2 Equiade species mass data

We constructed a database of species body mass estimates that covers 225 (91%) of the 246 known Equidae species, which is nearly four times larger than previous databases

(MacFadden 1986). Only plausibly independent, scientifically derived estimates were included (Hay 1917, Sachs 1967, Radinsky 1978, Janis 1982, Hulbert 1985, MacFadden 1986, Legendre and Roth 1988, Damuth and MacFadden 1990, Gingerich 1991, MacFadden 1992, Hulbert 1993, Storer and Bryant 1993, Janis et al. 1994, MacFadden and Ceding 1994, Alberdi et al. 1995, Silva and Downing 1995, Azzaroli 1998, Blondel 1998, MacFadden 1998, Eisenmann and Sondaar 1998, MacFadden et al. 1999, MacFadden 2001, Forsten 2002, Mustoe 2002, Eisenmann 2003, Ting et al. 2003, Gould and MacFadden 2004, Scott and Maga 2005, Mendoza 2006, Lambert 2006, Pesquero et al. 2006, Janis 2007, Paleobiology Database 2012).

Species body masses were estimated using one of four methods, depending on the data available for a species (see Appendix 3). In the first case, a species' body mass estimate was previously published in the literature; these estimates were included without modification.

Following MacFadden's approach (MacFadden 1986) for the second method, we convert upper first molar measurements, found in the literature, into head-body length estimates, using MacFadden's linear model. We then convert head-body length measurements into species body mass estimates using MacFadden's exponential model (MacFadden 1986) (Appendix 3). Although this method slightly overestimates the sizes of smaller, earlier Equidae species, it is widely used and well accepted. We employ it here to maintain consistency with other studies. Furthermore, overestimating small sizes decreases size disparity for our study, providing a conservative framework for our analysis.

Modifying the above approach (MacFadden 1986) for the third method, we converted lower first molar measurements into head-body length estimates, again using a linear model (Appendix 3). This model was estimated using a dataset of lower molar measurements and body size estimates from methods one or two (see Appendix 3). Subsequently, this model was used to

estimate body sizes when lower first molar measurements were available but no body mass data was found in the literature. Estimates of body mass from head-body length used the exponential model described for method 2 (MacFadden 1986).

If a body mass estimate could be derived using several of the methods, the different results were averaged. Estimates produced by these methods cover 152 (62%) of 246 Equidae species listed in the Paleobiology Database by December 2011.

Finally, for an additional 73 species (30%), only a genus-level size range was known. Here, we estimated a species mass by aligning a Normal distribution's 5 and 95% quantiles with the reported upper and lower values, and then drawing an estimated size from this distribution (a method similar to the convention in paleontology of taking the mid-point of the range). These species included none of the maximum sizes in any part of our study period, but included many of the smaller species, close to the lower-end of the Equidae size distribution.

4.2.3 Modeling species mass distributions

Our mathematical model for the species body mass distribution takes two forms, one for the diversity-driven hypothesis and one for the diffusion-driven hypothesis. For mathematical consistency, we require that the long-term behavior of both forms converge on the same final species mass distribution.

Relatively few mathematical models provide stationary and dynamical models of these distributions that are a good fit to the observed data. Here, we use the model developed by Clauset, Erwin, Schwab, and Redner (CESR model) (Clauset and Erwin 2008; Clauset et al. 2009, Clauset and Redner 2009), which satisfies these requirements and can be fitted to our data on horse body sizes.

Under the diversity-driven model, the allowed distribution of species masses is fixed, representing a stable set of body-mass niches. The number of species is then increased over time, following the empirical diversity data. As new species are added, niches become occupied in proportion to their relative frequencies within the background distribution, which represents a weak assumption on the strength of inter-specific competition for more attractive niches. As species are added, niches closer to the modal or most preferred size in the background distribution tend to be filled before niches farther away, and the maximum size increases steadily until no more niches are available. Under this formalization, disparity increases faster than if all niches at some size were filled before any at more extremal sizes, either larger or smaller—as in the case of strong inter-specific competition. Thus, this approach provides a conservative upper-bound on the rate of disparity increase across a range of strengths for inter-specific competition.

Under the diffusion-driven model, niches are occupied without regard to the occupation status of other niches, and the distribution's evolution is driven instead by stochastic selective pressures on species sizes. The specification for this model is mathematically more complicated as it defines precisely how the species body mass distribution itself changes over time, even while the number of species remains fixed.

A detailed mathematical derivation of the CESR model may be found in the existing literature (Clauset et al. 2009, Clauset and Redner 2009). Here, we summarize the model's basic assumptions and sketch the derivation of the equations that specify the background distributions used in the diversity- and diffusion-driven models. The CESR model assumes only macroevolutionary "neutral" processes (Hubbell 2001): speciation, extinction, size variation, a minimum viable size, all species in the taxonomic group obey a common set of governing

equations and constraints, and individualizing variables, e.g., predation relationships, life history, habitat, and geography, are omitted.

In the CESR model, a species of mass M produces descendant species with masses λM, where λ is a random variable drawn from a fixed distribution that represents the net pressures with different magnitudes and directions. The value of a particular λ summarizes all selective pressures on this species' size at the time of speciation (Figure 4.3), e.g., environmental gradients, interspecific competition and resource constraints. Anagenetic variation, or changes in size between speciation events, need not be modeled separately as their impact is implicitly captured by the λ associated with each speciation event.

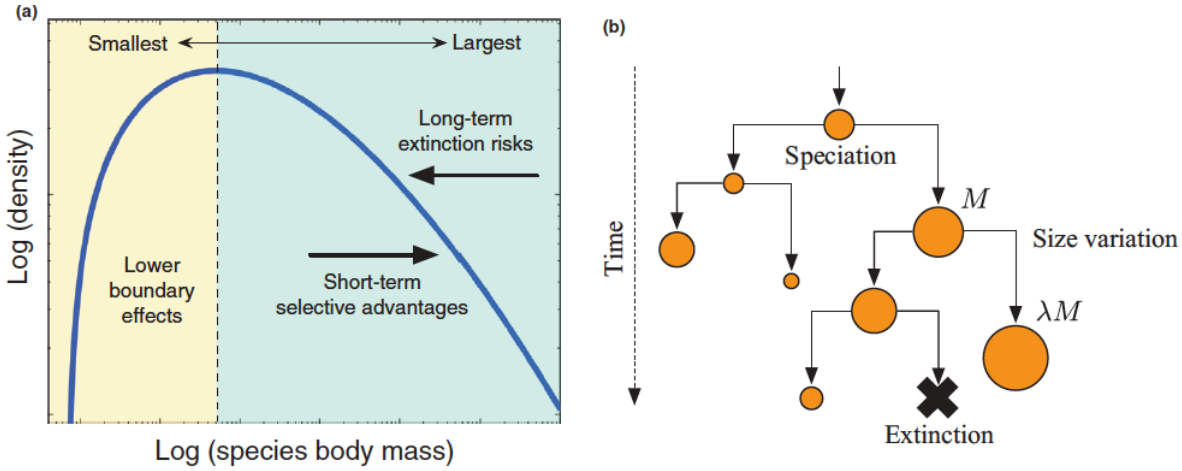

Figure 4.3 Schematic of body mass distribution model. Depicted in (a) are the three factors affecting body mass distribution through time, a lower boundary effect, short-term selective advantages, and long-term risk of extinction; (b) shows the cladogenetic model depiction of species body mass evolution, in which an ancestor species of mass *M* gives rise to descendant species of mass λ*M*, where λ is a random variable. Species masses are constrained to be at least some minimum viable size M_{min} and species extinction increases with larger mass.

The resulting multiplicative random walk model (Raup 1977, Hunt, 2007) is constrained at the lower end of sizes by physiological limits that induce a minimum viable size for every species. The minimum for Equidae is set to $M_{min} = 20$ kg based on empirical data.

On the upper end, the probability of species extinction rises with increasing size (Liow et al. 2008, Davidson et al. 2012), which compactly summarizes risk contributions from all sources, including energetic requirements (McNab 2009), smaller populations (White et al. 2007), longer generation times (Martin and Palumbi 1993), and demographic stochasticity (Jeppsson and Forslund 2012). The net effect is a soft upper boundary on species sizes, in contrast to the hard limits typically derived from energetic constraints alone.

The resulting species mass distribution may be simulated directly (Clauset and Erwin 2008) or approximated analytically as the stationary or time-evolving solution to a constrained convection-reaction-diffusion equation (Clauset et al. 2009, Clauset and Redner 2009). Here, we use the analytic solution, which has a clean mathematical form and a small number of parameters that can be estimated directly from data.

We now sketch the main mathematical results of the CESR model that are necessary to conduct our comparison of the diversity and diffusion models in Equidae. Let $c(x, t)$ denote the fraction or density of observed species with mass $x = \ln M$ at time t. The value of $c(x, t)$ is then modeled using a modified form of the standard convection-diffusion-reaction equation (Berg 1993, Krapivsky et al. 2010):

$$\frac{\partial c}{\partial t} + v\frac{\partial c}{\partial x} = D\frac{\partial^2 c}{\partial x^2} + (k - A - Bx)c \qquad (4.1)$$

On the left-hand side, the first term models the density's time dynamics, while the second models the impact of the average change in size from ancestor to descendant, i.e., the strength of Cope's rule, represented by $v = \langle \ln \lambda \rangle$. On the right, the first term models the impact of the variability in size changes from ancestor to descendant, quantified by $D = \langle (\ln \lambda)^2 \rangle$, while the second models the changes in density due to extinction and speciation; k denotes the mean

speciation rate, *A* the background or size-independent extinction rate ($k - A$ is the net background speciation rate) and *B* quantifies how quickly the extinction rate increases with size (Clauset et al. 2009, Clauset and Redner 2009).

We may then rewrite 4. (5.1) in the form of Airy's differential equation (Berg 1972) by changing variables to $\beta = B/D$, $\mu = v/D$, and $\alpha = (k - A)/D$, which normalizes these parameters by the variance of size changes. We then impose a boundary condition on the solution by requiring the density go through zero *c(x,t) = 0* at the minimum viable size $x = x_{min} = lnM_{min}$. The steady-state solution can then be shown to be

$$C_i(x) \propto e^{\frac{\mu x}{2}} Ai[\beta^{\frac{1}{3}}(x - x_{min}) + z_0, \quad (4.2)$$

where Ai[.] is the Airy functions, and $z_0 = -2.3381\ldots$ is the location of its first zero (Clauset et al. 2009). The full time-evolving solution can also be derived from Eq. (4.1), using an eigenfunction expansion.

The resulting solution is a sum of eigenmodes

$$c(x,t) = \sum_i C_i(x_0)C_i(x)e^{-\gamma_i t}, \qquad (4.3)$$

where each eigenmode $C_i(x)$ has the form of Eq. (4.2) with z_0 replaced by $z_i = z_0 - \gamma_i/D\beta^{2/3}$ where γ_i denotes the decay rate for the *i*th eigenmode of the series, and where $x_0 = lnM_0$ is the size of the taxonomic group's founder species (Clauset and Redner 2009). The rates γ_i form an increasing sequence so that higher terms decay more quickly with time. In the long-time limit, all of the decaying eigenmodes with *i > 0* become negligible and the species mass distribution converges to the steady state in 4. (4.2). (Note: the parameter α is eliminated in both solutions by normalization.)

Given choices for parameters μ, β, and x_{min}, Eq. (4.2) fully specifies a steady-state species mass distribution. With the additional choice of $x_0 = x_{min}$, Eq. (4.3) fully specifies a

time-evolving distribution. Previous studies using this model estimated $\mu \approx 0.2$ and $\beta \approx 0.08$ for terrestrial mammals (Clauset and Redner 2009), and we use these values here. The lower end of the empirical horse size distribution remained close to the size of Hyracotherium, which has a mean estimated size of 20 kg (across multiple estimates found in the literature), until approximately 5 Ma. We choose this value for M_{min}.

Finally, this model is a deterministic approximation of an explicitly stochastic model (Clauset and Erwin 2008). The predicted distribution, however, agrees well with extant data for all terrestrial mammals (Clauset and Erwin 2008), all birds (Clauset et al. 2009), and all cetaceans (Clauset 2013). Furthermore, its temporal dynamics agree well with the expansion of terrestrial mammals as a whole in the late Cretaceous and early Paleogene (Clauset and Redner 2009). It thus provides a well-motivated and empirically reasonable mathematical framework by which to formalize the diversity- and diffusion-driven mechanisms.

4.2.4 Model Evaluation

The key period for evaluating these mechanisms is the rapid diversification around 24 Ma, during which both the species number and their maximum size increased dramatically. This period includes the expansion of browsing horses (*Parahippus, Anchitherium, Hypohippus, Anchitherium, and Archaeohippus*) at 24 Ma and the expansion of grazing horses in North America between 18 and 15 Ma (MacFadden and Hulbert 1988). We define the period before 24 Ma as "pre-diversification" and the period after as "post-diversification."

We measure the extent to which each model correctly predicts the empirically observed increase in maximum size over 56 My (Figure 4.2). Each model produces a probability distribution *c(x)* for Equidae species masses at each time point. For any such distribution, the

expected maximum species size M_* for *n* species is given mathematically by $1 - F(ln\ M_*) = {}^{1}/_{n}$, where $1 - F(M_*) = \int_{lnM_*}^{\infty} c(x)dx$, i.e. where the complementary cumulative distribution function (ccdf) crosses the horizontal line ${}^{1}/_{n}$. For a fixed distribution and increasing *n*, or for fixed *n* and a distribution with a lengthening right tail, the location of this intersection will shift toward larger sizes.

For the diversity-driven model, we fix the species mass distribution *c(x)* and let *n* vary according to the empirically observed species counts over time (Figure 4.1). We control the impact of distribution variance—niche space "width"—by testing two choices of *c(x)*: one fitted to the pre-diversification empirical mass distribution and one fitted to the broader post-diversification distribution. For the diffusion-driven model, we fix the number of species *n* and let *c(x)* evolve over time, reflecting the empirically observed expanding size distribution (Figure 4.2). We control the impact of species diversity by testing two choices of *n*, corresponding to the pre-and post-diversification species counts. For each model, the predicted maximum body mass was extracted for each 5 My period starting at 56 Ma and then compared to the observed maximum in the same period.

4.3 Results

4.3.1 Data Summary

From 56–24 Ma, horse diversity remained relative low (less than 30 species, up to 4 genera; Figure 4.1), and the maximum mass only approached 100kg toward the end of this period. However, during the early Miocene (24–12 Ma), both diversity and disparity increased dramatically, reaching a peak of 98 species with maximum mass of nearly 800 kg (Figure 4.2).

This increase in diversity represented the appearance of many new genera, with genus diversity growing to 17 distinct groups by 12 Ma.

Subsequently, however, both species and genus counts decreased dramatically. This trend continued into the Pleistocene extinction, reflecting the broader loss of diversity seen across mammals (Owen-Smith 1987, Guthrie 2006), during which roughly half of all mammalian genera with body masses over 5kg became extinct. For Equidae, this loss of diversity impacted mainly smaller-bodied species, rather than larger ones, as is typically expected (Liow et al. 2008). We observe no tendency for these emptied niches to be refilled from larger-bodied lineages, as we would expect from the reproductive-power hypothesis. To the contrary, the broad extinction of small-bodied lineages suggests high-level and long-term selection, possibly related to changing climate or reorganizing ecosystems, with better adapted species groups expanding into niche-space previously filled by Equidae.

The expansion of Equidae's body mass distribution was thus highly asymmetric, but consistent with expansion from minimum viable size (Stanley 1973, McShea 1994) at roughly 20kg. This pattern suggests the existence of a stable, and previously unidentified, physiological constraint at the lower end of the horse mass distribution. Furthermore, statistical tests indicate little evidence for either sampling bias in diversity data or non-stationary processes in the variation of body sizes over the study period (see Appendix 3).

4.3.2 Diversity or diffusion?

To extract the necessary distributions for our tests, we first fix the model parameters μ, β and x_{min}, as described above. For diversity-driven models, we divided the mass data into pre- and post-diversification periods from which we estimate the corresponding background mass

distributions. The diversity data were then converted into a time series of eleven 5 My periods, starting at 56 Ma. For diffusion-driven models, mass data were divided into the same sequence of 5 My periods, and pre- and post-diversification species averages were fixed at $n_{pre} = 15$ and $n_{post} = 69$, respectively. (Modest variations in the division date yield similar results in both cases.)

For each of the two model types, we fitted the time-evolving model to the respective sequence of distributions using the non-parametric method of Clauset and Redner (Clauset and Redner 2009), which chooses a mapping of model-time to real-time that minimizes the distributional distances between the evolving distribution and the sequence of empirical distributions. This approach yields good agreement with the empirical pattern (Figure 4.4).

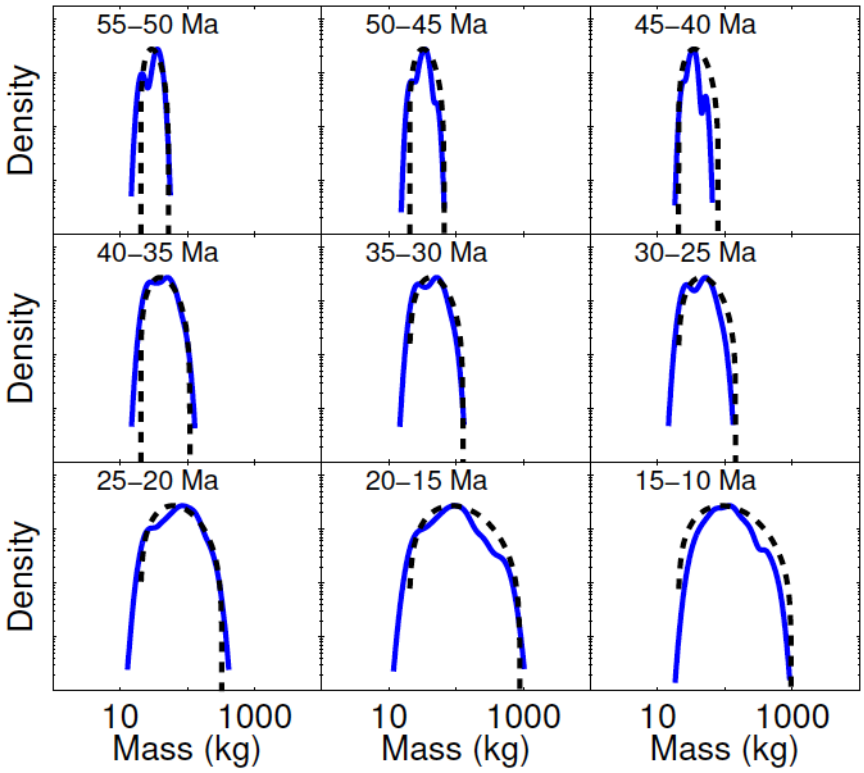

Figure 4.4 Comparison of empirical (blue; smoothed with a Gaussian kernel) and model-based (dashed, black) Equidae body mass distributions, in 5-million-year increments, showing good agreement.

For each 5 My period, we calculated the predicted maximum mass M_* under each model, which we compared to the observed maximum, smoothed using an exponential kernel. In both diversity-driven models, the empirical diversification pattern failed to produce a large increase in disparity (Figure 4.5a), even when the background distribution itself was broad. To quantify a model's prediction accuracy, we computed the sum of squared errors (SSE) between the diversity-driven prediction for ln (M_*) and the observed values. The pre-diversification diversity-driven model yielded the largest SSE across all models, with $R_{div,pre} = 35.42$, and failed to produce any species larger than 50 kg. The post-diversification model yielded a small

improvement, with $R_{div,post} = 22.05$, but this model dramatically overestimated the initial size disparity and produced very little increase in disparity over 50 My.

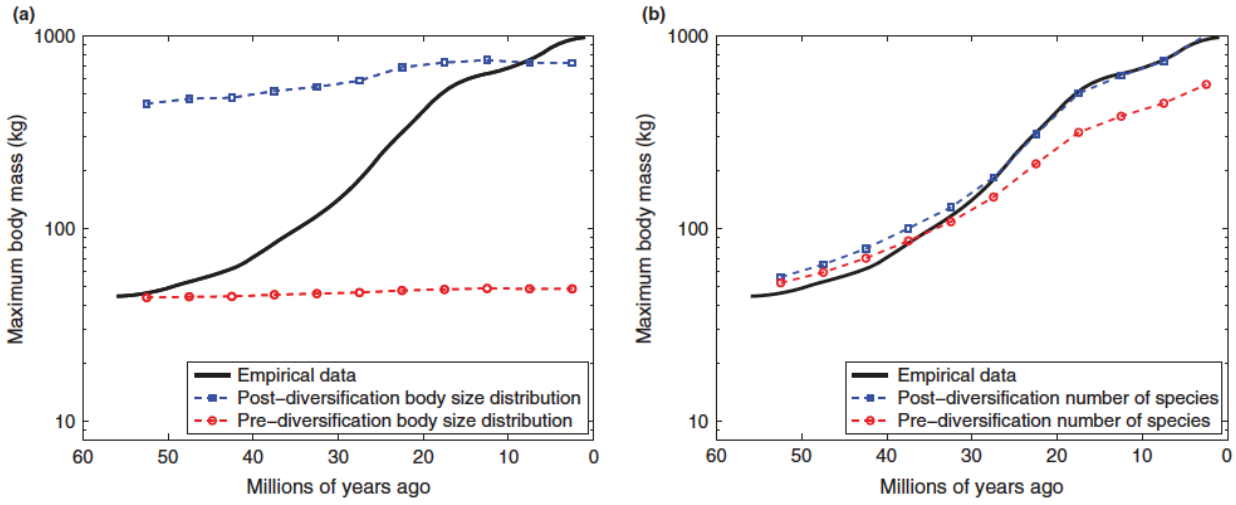

Figure 4.5 Evolution of species mass disparity in the Equidae lineage over 56 Ma, showing the empirical trend (bold line) and the predicted maximum sizes from (a) diversity-driven models, with background distributions fitted to pre- and post-diversification data, and (b) the diffusion-driven models, with a time-evolving distribution containing a number of species fixed at pre- or post-diversification levels. All models predict an increase in disparity, but diversity-driven disparity models show only modest increases, regardless of what background distribution is used, while diffusion-driven disparity accounts for 92% of the observed increase over this period, regardless of the number of species assumed.

In contrast, both diffusion-driven models accurately predict the observed increase in disparity (Figure 4.5b), with the post-diversification model performing slightly better over the last 20 My. The SSE for the pre-diversification diffusion prediction was $R_{diff,pre} = 1.29$, or about 27 times closer than $R_{div,pre}$, while the post-diversification model yielded $R_{diff,post} = 0.18$, or about 118 times closer. Overall, the post-diversification diffusion model (with $n = 69$) succeeds in explaining 92% of the observed increase in maximum size, from 39 kg to 1200 kg, over the 56 My expansion of Equidae.

4.4 Discussion

Previous studies (Stanley 1973, Maurer et al. 1992, Clauset and Erwin 2008, Smith et al. 2010) have advanced specific mechanistic explanations for the body size distributions within large taxonomic groups, particularly mammals. Here, we investigated the ability of two general hypotheses, formalized within a common mathematical framework, to explain the common pattern of increased disparity in an expanding lineage. Using the family Equidae as a model system, we found that macroevolutionary "diffusion," in which selective effects on species body size vary independently of the occupation status of nearby niches, explains substantially more of the observed changes in the Equidae body mass distribution over 56 My (Figure 4.4) than does a diversity-driven mechanism, in which niches closer to a preferred or optimal size are filled before less attractive and larger-bodied niches are filled. These results suggest that increases in disparity are not necessarily driven by macroecological competition for niches, as is commonly assumed. Instead, disparity may increase from neutral diffusion effects alone, even when small-sized niches are available and the niche space is sparsely occupied.

While some studies (Allen et al. 2002, Secord et al. 2012) have suggested a coupling between global temperatures and species body sizes, we found no such correlation with horse body sizes. However, global temperatures do appear to correlate with Equidae taxonomic diversity, which achieves its highest point during warm periods and low points during glaciation and cooler global temperatures (Figure 4.1). For instance, the first member of Equidae appeared at 56 Ma, during a thermal maximum. From 56–42 Ma, 18O isotope data show that average global temperatures were relatively cool (Zachos et al. 2001), and our data show that during this period both species and genera counts were low, with fewer than 30 species and 4 genera. Taxonomic counts increased substantially from 24–21 Ma and reached their peak during the

global warming period spanning the Oligocene-Miocene boundary to the mid-Miocene (Figure 4.1), which generated a loss of Antarctic ice and warmer deep water temperatures (Zachos et al. 2001).

This pattern suggests a climate-diversity coupling for Equidae in particular, and this pattern may also hold for other lineages. Although the evolutionary and ecological causes of the Equidae adaptive radiation remain unclear, the climatic connection provides a novel hypothesis, in which a warming climate drove changes in flora and the expansion of grassland ecosystems, which expanded the distribution of unoccupied niches, allowing the evolution of grazing horses and the corresponding increase in diversity (MacFadden and Hulbert 1988). Regardless of the cause of the radiation, our results suggest that Equidae disparity would have increased without any increase in species counts, and whatever mechanism caused the increase in diversity played only a minor role in the simultaneous increase in body size disparity.

The success of the diffusion-driven model in matching the observed tempo and magnitude of size disparity in Equidae over 56 My suggests that morphological disparity may generally be driven at the clade-level by diffusive processes rather than diversification processes. Such macroevolutionary diffusion is the natural consequence of randomly varying selective pressures on species sizes within fixed constraints on size (Clauset and Erwin 2008), and is entirely consistent with an expanding space of niches (Odling-Smee et al. 1996). For horses in particular, although both the distribution and diversity expanded during their adaptive radiation, diffusion appears to have played the dominant role in producing increasingly large-bodied species (Figure 4.5b), a point that is reinforced by the steady expansion of the mass distribution even with a roughly stable species number prior to 24 Ma (Figures 4.1 and 4.2).

A large role for diffusion does not undermine the general ecological importance of competition, but rather clarifies its role in generating broad-scale patterns for horses in particular, and for evolving systems in general. Macroevolutionary diffusion is an effective large-scale description of many roughly independent ecological interactions and evolutionary constraints on species size variation. Short-term selective effects on size for a particular species can stem from any number of specific mechanisms, including but not limited to competition over ecological niches. So long as the magnitude and direction of these effects, as defined at the species-level, are roughly independent across the taxonomic group, the large-scale pattern will be well-described by diffusion. Ecological competition may thus be crucial for individual species, but its effects are more diffuse at the large scale because competition is typically a local process.

In the body mass evolution and diversification of horses, competition between Equidae species appears to have played a minor role in driving the dramatic and sometimes rapid changes in species morphology observed over 56 My. Future work in which among-clade dynamics are additionally modeled could shed additional light on the relative roles of inter-clade (e.g., competition or predation) versus within-clade (e.g., diversification or diffusion) processes in structuring changes in the Equidae body-size distributions through time. Furthermore, understanding the ecological or evolutionary reason for the apparent coupling of climate and Equidae diversity and the apparent minimum viable size at roughly 20 kg, both identified here, may shed new light on Equidae evolution. Finally, diffusion-driven and diversity-independent increases in disparity may hold beyond Equidae, given the strong support for diffusion-type models in explaining the shape and dynamics of other species size distributions (Stanley 1973, McShea 1994, Clauset and Erwin 2008, Clauset and Redner 2009, Clauset 2013). Determining the generality of this pattern is an important direction for future work.

4.5 Acknowledgements

The authors thank Bruce MacFadden for insightful discussions and helpful suggestions. This work was supported in part by the Interdisciplinary Quantitative Biology (IQ Biology) program (NSF IGERT grant number 1144807) at the BioFrontiers Institute, University of Colorado, Boulder.

Chapter 5

Universal Processes Govern Body Mass Evolution in Marine and Terrestrial Environments

Lauren G. Shoemaker and Aaron Clauset

Extreme differences between marine and terrestrial environments are believed to drive divergent patterns in species morphology and ecosystem structure. Using comprehensive data on extant and extinct marine (cetacean) and terrestrial mammal species, we quantify the impact of environment on macroecological and macroevolutionary patterns of species body size, a fundamental biological variable. We show that the distribution of cetacean body sizes is indistinguishable from that of terrestrial mammals, except that sizes are 10^3 g times larger. This equivalence holds throughout the modern radiation of mammals, and is natural consequence of a universal cladogenetic diffusion process unfolding above a minimum viable body size. Environment thus appears to determine the location of the size distribution among mammals, while its shape follows a universal curve.

5.1 Introduction

Body mass is a fundamental species characteristic, as it correlates with physiological, ecological, and developmental traits, including metabolic rate, home range size, fecundity, and population size (Peters 1986, Brown 1995). Body mass is also relatively easy to measure for both extinct and extant species (MacFadden 1986, Smith et al. 2003), and thus represents a key

biological variable through which to develop general ecological and evolutionary theories that span large spatial and temporal scales. In terrestrial environments, extant species from large and evolutionarily distinct clades, such as mammals (Clauset and Erwin 2008), birds (John B Dunning 2007), lizards (Meiri 2008), and even insects (Stanley 1973), exhibit a common pattern in their mass (e.g. weight) or size (e.g. biovolume) distributions. It is unknown, however, what aspects of this pattern are shaped by environmental factors, or driven by endogenous biological dynamics.

Most research on body size distributions has focused on extant terrestrial species (Lomolino 1985, Brown 1995, Clauset and Erwin 2008, Shoemaker and Clauset 2014), showing a canonical, right-skewed distribution, such that the most common body size within a clade is only slightly larger than the smallest, but the largest size is orders of magnitude greater than the most common size (Clauset and Erwin 2008). Relatively little work, however, has focused on species size distributions in freshwater or marine environments. Terrestrial and marine ecosystems exhibit strong biotic and environmental differences that drive different macroecological patterns, and these differences should be reflected in species body mass distributions. For instance, marine systems have lower species diversity, lower average biomass and productivity, and conversely greater food chain length and more trophic interactions on average than in terrestrial systems (Cohen and Fenchel 1994). Additionally, marine systems exhibit decreased temporal variability (e.g. temperature fluctuations through time) as a result of the buffering capacity of water (Webb 2012). However, it is unknown the extent to which these or other environmental factors drive differences in species mass distributions across marine and terrestrial environments, in part because most extant animal groups are either fully terrestrial or fully aquatic. Using comprehensive data on extant and extinct members of a large animal clade

that contains both fully terrestrial species, and a monophyletic fully marine sub-clade, we construct a phylogenetically-controlled characterization of the impact of disparate environments on the evolution and distribution of species body size.

While unknown in marine systems, recent theory suggests the canonical right skewed distribution observed in terrestrial environments may be attributed to a neutral macroevolutionary random walk, or 'diffusion' process (e.g. the generalization of a random walk using continuous rather than discrete time) at each speciation event. This diffusion process for body mass evolution on land is constrained by the interactions of three well-understood mechanisms (Clauset and Erwin 2008, Clauset et al. 2009). The first—a minimum size—arises from metabolic constraints required for thermoregulation and sets the lower bound of the body mass distributions (Pearson 1948, West et al. 2002). The second—Cope's rule—is the widely observed macroecological pattern that, on average, lineages tend to increase in body size over time due to ecological advantages associated with larger sizes, such as escaping predation or foraging in larger home ranges (Stanley 1973, Alroy 1998). Cope's rule leads to increased species' sizes through time, and thus plays a critical role in forming the right-skew in body mass distributions. The third mechanism—a slight increased risk of extinction for larger species—occurs because larger species tend to have smaller population sizes and longer generation times (Hone and Benton 2005); they are therefore at higher risk of stochastic extinction events or extinction caused by large scale environmental disturbances (Cardillo et al. 2005, Liow et al. 2008). This final mechanism provides a soft upper-bound on body size distributions and constrains both the maximum size and the strength of the right skew.

Here, we test whether the commonly observed right-skewed body mass distributions, the evolution of body size, and the mechanisms hypothesized to create a right-skewed distribution

are environmentally driven or, alternatively, are conserved across marine and terrestrial environments. We do so by comparing mammalian body mass distributions and their evolution in marine and terrestrial systems. We further quantify the degree to which the three processes known to create the canonical distribution in terrestrial environments are present in marine systems. We test for the presence and strength of a minimum size constraint, Cope's rule, and a size-dependent extinction risk. We utilize this comparison—which controls for many confounding factors that would arise in comparing clades with more distant shared ancestry—to determine what governing effects the multitude of differences in environments have on extant body mass distributions and their evolution.

To conduct these tests, we constructed a novel and comprehensive database of extant and extinct cetacean body size. The infraorder Cetacea (whales, dolphins, and porpoises; originating from Artiodactyls—even-toed ungulates) is ideal to test the commonalities of mammalian body mass distributions because it has a long evolutionary history (originating 56 million years ago) and is sufficiently speciose to explore body size distributions, as the only other fully aquatic clade, Sirenia, only has four extant species. To construct the database, we recorded species-level first and last appearances and measurements of body length, occipital width, and condylobasal length from the primary literature (see Appendix 4 for a detailed description of data collection and methods). We then used allometric scaling of body length, occipital width, and condylobasal length to estimate body mass (g) from each fossil measurement and all potential combinations of measurements (see Appendix 4 Materials and Methods for details). This yielded mass estimates for 292 cetacean species. This is, to our knowledge, the largest current database of cetacean body sizes, giving us comparatively high resolution of both the extant body mass distribution, and the evolution of cetacean body mass through time. Using 4,002 extant terrestrial mammal species

(Smith et al. 2003, 2007) and 1,702 extinct North American species' mass estimates and first and last appearance dates (Clauset and Redner 2009), we then compared body mass distributions and governing mechanisms between marine and terrestrial ecosystems.

5.2 Extant Distributions

The extant cetacean body mass distribution closely matches that observed in multiple terrestrial clades (Figure 5.1). Across environments, we observe a canonical distribution skewed to the right, with the only major difference being a shift to larger sizes by ~3.5 orders of magnitude for marine mammals when compared to terrestrial mammals. As with terrestrial mammals, the median size of cetaceans (356 kg) is only slightly larger than the smallest (37.5 kg, *Pontoporia blainvillei*), but nearly 500 times smaller than the largest (175,000 kg, *Balaenoptera musculus*). Thus, given the extreme physical differences between marine and terrestrial environments and previously observed biotic differences (e.g. average food chain length, primary production) we would *a priori* expect different selection pressures in marine and terrestrial environments. Yet, we find that the shape of extant mammalian body mass distributions follows the same macroecological pattern and exhibits a highly right skewed distribution regardless of environmental differences.

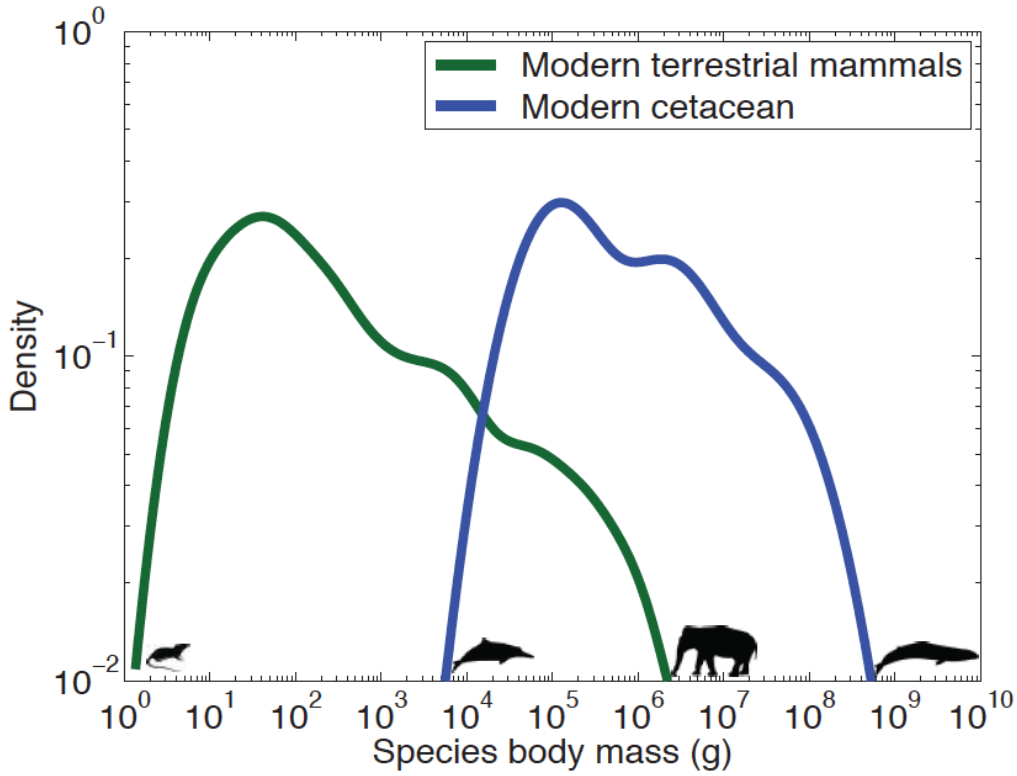

Figure 5.1 Cetacean and terrestrial body mass distributions.
Empirical body mass distributions for terrestrial mammals (green) and cetaceans (blue) show similar right-skewed patterns with the cetacean distribution shifted to larger sizes by ~3.5 orders of magnitude. For both terrestrial and marine environments, the median size is close to the smallest observed size, while relatively few species are much larger than the smallest or median size.

The canonical, right-skewed body mass distribution observed for mammals in both marine and terrestrial environments may be a product of: (*i*) the same macroecological mechanisms operating at the same strength in marine environments as terrestrial environments, (*ii*) the same mechanisms operating at different, but complementary, strengths in marine environments compared to terrestrial environments, producing a universal pattern via complementary processes, or (*iii*) different mechanisms operating in marine environments which create a marine body mass distribution convergent to that observed for terrestrial environments. To discriminate among these hypotheses, we first tested for the effects of a minimum size,

Cope's rule, and a size-dependent extinction risk in marine environments; support for these mechanisms have previously been shown in terrestrial environments for mammals (Clauset and Erwin 2008). Evidence for these three mechanisms in marine environments would corroborate hypothesis (*i*) or (*ii*), where the same evolutionary mechanisms in marine and terrestrial environments yield a similar shape in extant body mass distributions; determining the relative strength of the three processes subsequently allows us to differentiate between hypothesis (*i*) versus (*ii*). Alternatively, if we find no evidence for a minimum size, Cope's rule, nor a size-dependent extinction risk, we can infer that hypothesis (*iii*) is correct, and alternate mechanisms created convergent extant body mass distributions in marine and terrestrial environments.

5.3 Macroecological Principles

The first mechanism, a minimum viable size, is known both theoretically and empirically to occur at 2 g in terrestrial environments (Pearson 1948, Ahlborn 2000). Below 2 g, an individual's heat loss in air is too great to maintain its required internal temperature. In comparison, the convective heat loss in water is 90.8 times greater than in air (Downhower and Blumer 1988), pushing the theoretical minimum size in marine ecosystems orders of magnitude higher to 6.8-10 kg (Downhower and Blumer 1988, Ahlborn 1999, 2000) (Table 5.1). This range closely matches the weight (7-9 kg) of a newborn *Pontoporia blainvillei*, the smallest extant cetacean, providing both theoretical and empirical evidence for a minimum physical size in marine environments. This increase in minimum size due to greater heat loss in water creates a hard left-boundary for the marine body mass distribution. This, in turn, must shift the entire body mass distribution rightward to larger sizes (Figure 5.1). It also suggests a larger median and maximum size solely due to the increased minimum size, although increases in the median and

maximum size are also mediated by the number of species in a clade, Cope's rule, and the strength of a size-dependent extinction risk.

Process	Parameter Estimate (Marine)	Range (Marine)	Parameter Estimate (Terrestrial)	Range (Terrestrial)
Minimum Size	6.8 kg	6 – 10 kg	1.8 g	1.5-2.0 g
Cope's Rule	-0.021	-0.049 – 0.007	0.103	0.095 – 0.110
Size-Dependent Extinction Risk	0.045	0.037 – 0.053	0.040	0.039 – 0.042

Table 5.1 Comparison of the strength of macroevolutionary processes in marine versus terrestrial environments.

The second proposed mechanism is Cope's rule, or the tendency for species body mass to increase as a lineage evolves. Larger sizes have been shown to benefit mating success, provide a greater range of acceptable foods, increase survival via increased defense against predation, increase intra- and inter-specific competitive abilities, and extend longevity (Hone and Benton 2005). For an evolutionary advantage of increasing sizes during speciation events, these benefits have to outweigh negative fitness effects associated with larger sizes, such as increased food and water requirements, lower fecundity, and increased pre- and post-natal development times (Hone and Benton 2005). While there are multiple definitions of Cope's rule in the literature, we follow Alroy's method (Alroy 1998), which restricts our estimates of the strength of Cope's rule to the species level, where we compare masses of species within a single genus. This approach is robust to confounding factors such as increased variance in body size through time and expansion from a minimum size. We additionally minimize the effect of ghost-lineages (i.e. ancestors without estimated masses or currently unknown ancestors) in our calculations, and test

for the strength of Cope's rule at the smallest possible taxonomic level (within genera), giving us a conservative and unbiased estimate of the strength of Cope's rule (Alroy 1998).

While we find terrestrial mammals are on average 10% larger than older congeneric species (range: 0.095 to 0.110), agreeing with previous results (Alroy 1998, Clauset and Erwin 2008), cetaceans are on average 2% smaller than older congeneric species (range: -0.049 to + 0.007). Cetaceans therefore exhibit an absence or slight negative strength of Cope's rule (Table 5.1) and are thus not expected to become larger during speciation events. Rather, they exhibit a slight tendency to decrease in size during speciation. We demonstrate the first published example, to our knowledge, of a zero, or slightly negative strength of Cope's rule for marine mammals (Table 5.1).

While in terrestrial environments, Cope's rule is the outcome of short-term selective advantages for larger sized organisms (Hone and Benton 2005, Clauset and Erwin 2008), this finding implies the presence of different selective pressures in marine systems which mitigate the effect of terrestrial selective pressures and, rather, select for smaller sizes. One potential explanation for this pattern is that the distribution of resources in marine environments leads to a slight negative strength of Cope's rule for marine mammals. The most productive waters in marine systems are near-shore, while the open ocean can be considered a caloric desert (Field 1998). As cetaceans increase in size, they are more constrained to the offshore, poor-quality open ocean. This may select for smaller sizes as cetaceans evolve, negating the selective pressures that, most generally, leads to a moderately positive strength of Cope's rule. This hypothesis is consistent with previous literature, showing positive strength for Cope's rule in gastropods (Hunt and Roy 2006), crustaceans (Klompmaker et al. 2015), or when aggregating over 17,000 genera of marine animals (Heim et al. 2015); the negative pressures opposing Cope's rule would not be

predicted to be as strong in small sized marine organisms (though, see (Arnold et al. 1995, Jablonski 1997), but rather only present at the size distribution where individuals with large mass would no longer be able to utilize inshore resources.

The third and final mechanism we test is a size-dependent extinction risk. Extinction risk is predicted to be greater for larger species for multiple reasons. Larger species have smaller populations, making them more vulnerable to demographic stochasticity, and correspondingly higher extinction risk (Hone and Benton 2005, Cardillo et al. 2005). They also require more food, making them more susceptible to environmental disturbances, and have longer generation times, making it difficult for them to rapidly evolve in response to changing environments (Hone and Benton 2005) or recover from demographic fluctuations in population size. We estimate the strength of a size-dependent extinction risk by minimizing the distance between extant body mass distributions and the stationary distribution of a macroevolutionary diffusion model (see Appendix 4 Materials and Methods) (Massey 1951) that incorporates a minimum size, Cope's Rule, and a size-dependent extinction risk as parameters (Clauset and Erwin 2008, Clauset and Redner 2009, Clauset et al. 2009, Shoemaker and Clauset 2014). Size-dependent extinction risk is present in both environments and at a similar strength (marine: 0.045 ± 0.008; terrestrial: 0.040 ± 0.002), implying that this macroecological mechanism is common across environments at a universal strength. While marine environments have different food web structures, distribution of resources, and other ecological characteristics, this does not affect the relationship between body size and extinction risk at the macroecological scale. This result has striking implications for the relative roles of stochastic and deterministic structure in macroevolutionary patterns, implying that demographic stochasticity at small population sizes (Melbourne 2012)

may play a larger role than deterministic signatures created by environmental differences in predicting extinction risk and its relation to body size.

Across marine and terrestrial clades, the fundamental body size distribution is shaped by the clade's minimum size, Cope's rule, and extinction risk. The clade's minimum size provides a hard left bound on the distribution, while the asymmetrical right-skew to the distribution is the outcome of the size-dependent extinction risk. In terrestrial environments, Cope's rule accentuates the asymmetrical right-skew to the distribution, which is mitigated by the size-dependent extinction risk. The realized body size distribution also results from the number of species within a clade, as these represent random draws from the fundamental body size distribution. The more species within a clade, the more likely it is that the fundamental maximum size is observed in the dataset. Therefore, as there are 4,002 terrestrial mammals versus 78 cetaceans in our databases, the size range in terrestrial environments spans 6 orders of magnitude but only 5 in marine environments, and, correspondingly, the right tail of the cetacean body mass distribution has a slightly steeper slope than in terrestrial environments (Figure 5.1).

Incorporating these mechanisms into a constrained macroecological diffusion model, we accurately predict both marine and terrestrial mammalian extant body mass distributions using the model's steady state distribution (Figure 5.2). This lends support to hypothesis (*ii*), where the same macroecological principles operating at complementary strengths produce a similar body mass pattern in marine environments compared to terrestrial environments.

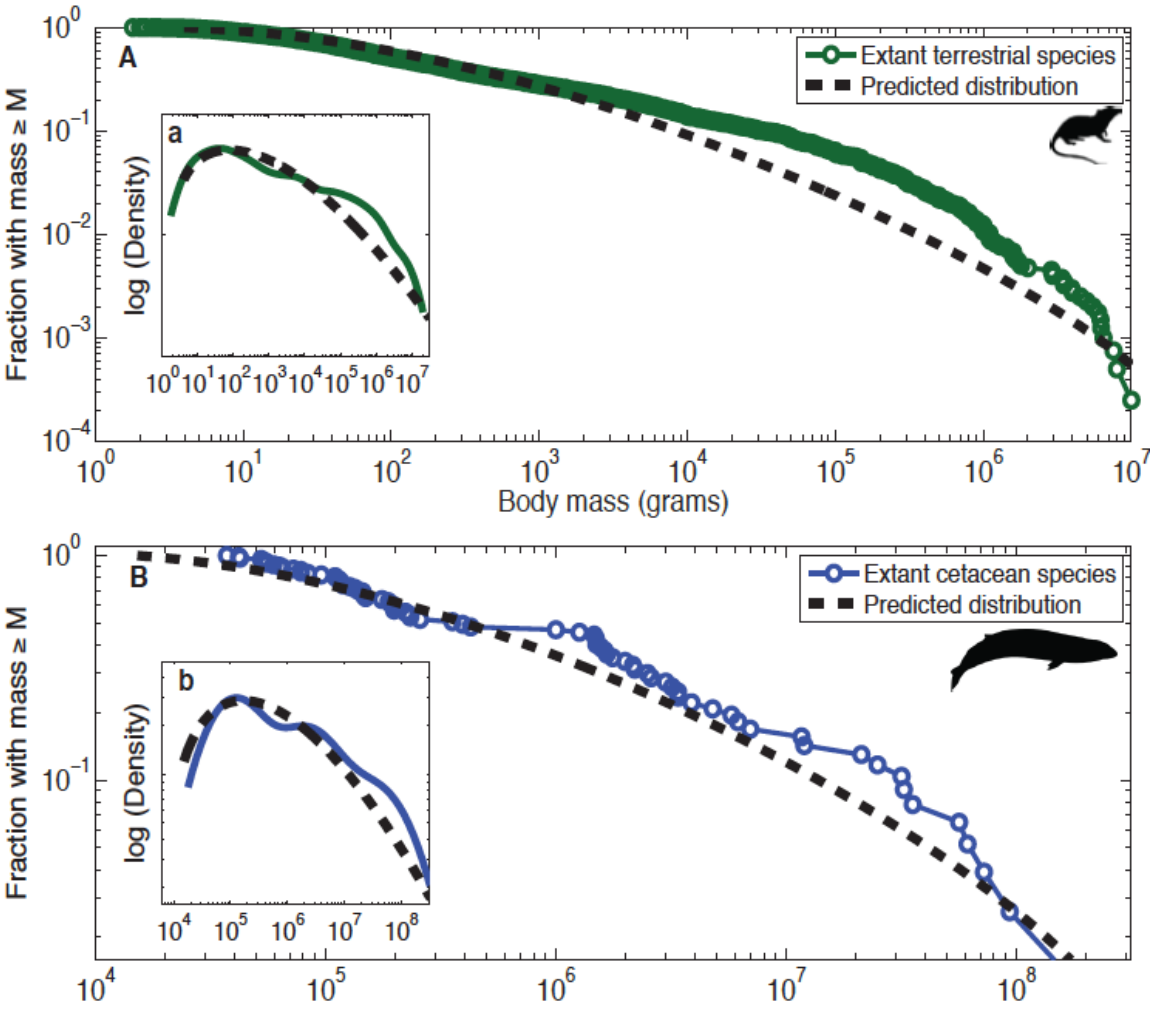

Figure 5.2 Macroecological model fit to extant body mass distributions.
Comparison of empirical body mass distributions (blue for cetaceans and green for terrestrial mammals) and model fits (dashed, black lines) for cetaceans (A, a) and terrestrial mammals (B, b). A and B show the percentage of species larger than a given size; a and b show the density of species with a given mass.

5.4 Evolution of body size

While the three macroecological mechanisms are sufficient to produce the extant body mass distribution in marine and terrestrial environments, with extant data alone, we cannot rule out the possibility that their similarity is a recent convergence, and that different mechanisms governed their evolution over time. Thus, we subsequently conduct two tests of the universality

of these mechanisms and their ability to accurately predict the evolution of marine and terrestrial body sizes. First, we test if these mechanisms accurately predict maximum size and frequency of body sizes over 56 Ma for cetaceans and 100 Ma for terrestrial mammals. Second, we examine if the strength of these processes appears constant across time, using the previous estimates of minimum size, Cope's Rule, and the size-dependent extinction risk.

To do so, we use the time-dependent macroevolutionary diffusion model (Clauset and Redner 2009) (see Appendix 4 Materials and Methods for details), rather than the steady-state distribution used previously. We model predicted body size distributions and the corresponding frequency of body mass through time at every 5 million-year increment using the mechanism estimates described previously, and thus assuming a constant strength through time. We additionally solve for the expected maximum body mass, M_{max}, at each million year increment. The expected maximum size depends on both the underlying distribution at a given period of time and the species-level diversity estimate (Appendix 4). If the same three macroevolutionary mechanisms are present at relatively constant strengths through time and are the primary mechanisms at play, then our model should predict the most commonly observed body size through time as well as provide an upper bound on the maximum size. If, alternatively, the similarity of marine and terrestrial body mass distributions is a recent convergence, then we would expect that the model would be unable to recover the most common body sizes in marine environments nor an upper bound on maximum size through time.

A constrained macroevolutionary 'diffusion' of body sizes (i.e. a random walk in continuous time) does indeed accurately predict maximum terrestrial and marine mammalian mass across evolutionary timescales. For terrestrial mammals, these processes are sufficient to replicate the small maximum size of 10^2–10^3 g observed from 100 million years ago (Ma) to 80

Ma, followed by the rapid increase in maximum size from 70 Ma to 55 Ma, where maximum size increased by three orders of magnitude (Figure 5.3A). The macroevolutionary model then produces a relatively constant maximum size, in good agreement with the observed fossil data. Thirteen terrestrial species (0.76% of the dataset) fall outside of the expected maximum size for their lifespan, while 99.24% of terrestrial species fall within the mass range predicted using macroevolutionary diffusion constrained by the three mechanisms. This slight deviation between model predictions and observed masses through time may be explained by: (i) temporal variation in the strength of Cope's Rule or the size-dependent extinction risk or (ii) higher species-level diversity than currently estimated.

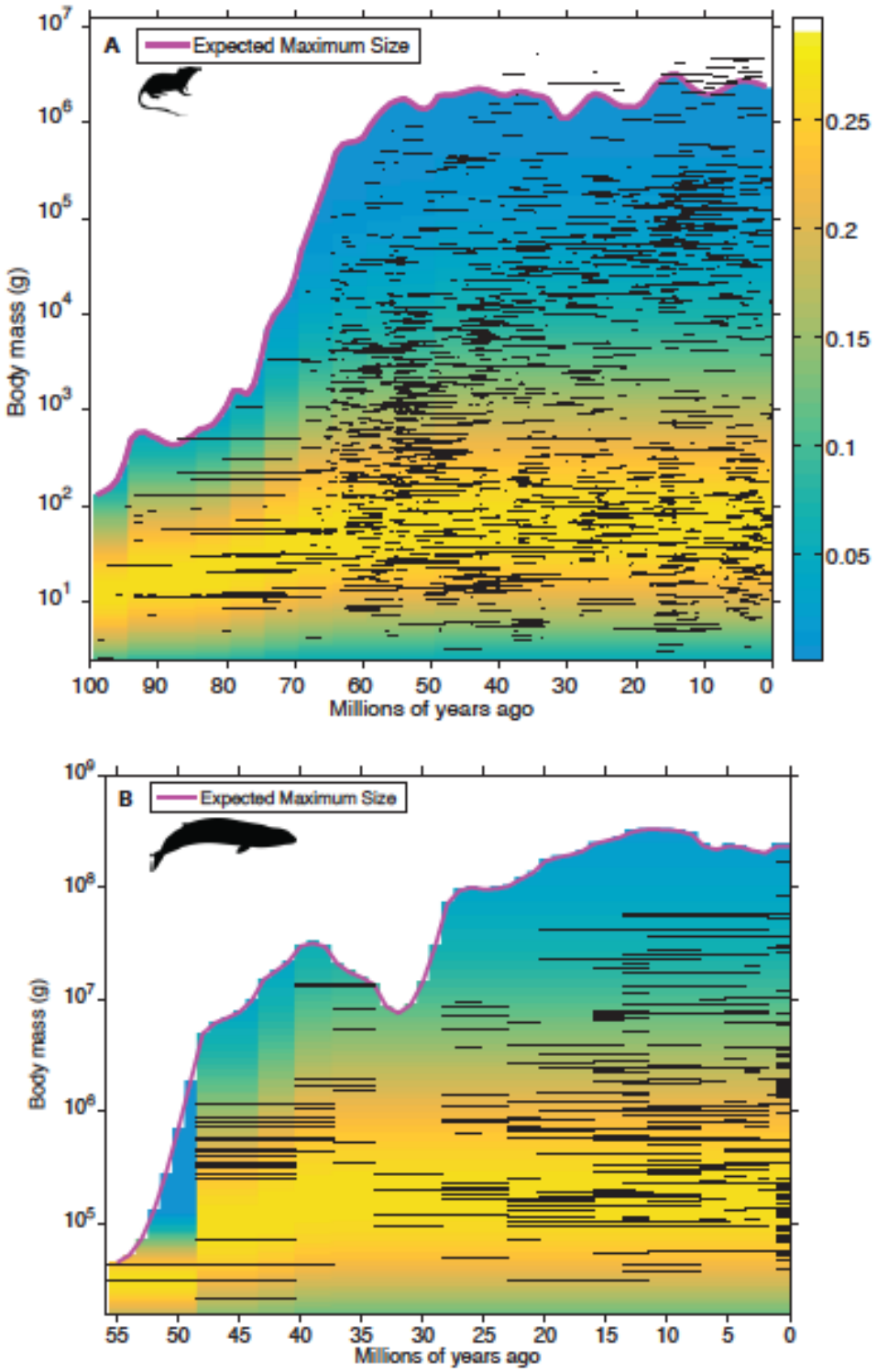

Figure 5.3 Cetacean and terrestrial body mass evolution.

Comparison of empirical terrestrial mammal (A) and cetacean (B) body masses through time against model predictions. Black horizontal lines show body mass and first and last appearance

for individual species. The yellow-to-blue heatmap depicts predicted density of species with a given body mass using the diffusion model with parameter estimates from Table 5.1. The maroon line shows the model predicted maximum size given mammalian and cetacean diversity through time.

In marine environments, the time-dependent macroecological diffusion model accurately predicts a maximum expected size as large or larger than any species observed in our database, with 100% of cetacean species falling within the mass range predicted by constrained macroevolutionary diffusion. The model therefore provides an upper bound on maximum size (Figure 5.3B). Consistent with the fossil record, maximum size is predicted to increase rapidly from 56 Mya to 40 Mya. Subsequently, maximum size is then predicted to decrease during the early Oligocene because maximum size correlates with taxonomic diversity, which decreases at the beginning of this epoch. Maximum size then increases again as taxonomic diversity recovers 28 Mya, and stays relatively consistent around ~ 10^8 g until present day. Thus, maximum cetacean size during the past 56 Ma is well predicted by a constrained macroevolutionary diffusion model that utilizes our previously estimated mechanism strengths.

Comparing the expected body mass distributions through time to observed cetacean body masses (Figure 5.3B), we demonstrate that the most commonly observed body masses match the range predicted with a constant strength of the three macroecological principles. Additionally, in data-poor periods, the observed body sizes are consistent with the most likely sizes predicted by the model. For example, during the origination of cetaceans 55 Mya-50 Mya (Uhen 2010), there are only two known species, but both exhibit body masses predicted by the three universal macroecological processes. The same holds for 35 Mya-30 Mya, during which known cetacean diversity fell to only eight known genera (Uhen and Pyenson 2007). It is currently possible to estimate masses for only four species during this time period using our methods, but all four

have masses predicted to occur with the highest frequency. We find that, just as in the terrestrial environment (Clauset and Redner 2009, Clauset et al. 2009), the evolution of cetacean body mass distributions and maximum size is controlled by three macroecological processes with relatively constant strengths across evolutionary time, lending support to the universality of body size evolution regardless of environmental differences.

5.5 Conclusion

We demonstrate that the ubiquitous right-skewed distribution of body mass observed for terrestrial mammals (Clauset and Erwin 2008), birds (John B Dunning 2007), lizards (Meiri 2008), and even insects (Stanley 1973) appears robust to environmental differences between marine and terrestrial ecosystems. Marine mammals exhibit a strikingly similar distribution despite enormous differences in ecosystem structure, resource distribution, and environmental conditions. The main exception we find is thermoregulation, which sets the size scale at which these universal processes unfold, where marine mammals display the same distribution as terrestrial mammals, but shifted toward larger sizes. The extant body mass distributions, as well as the evolution of body mass distributions and maximum size, appear to be the outcome of three macroecological mechanisms that constrain diffusion (i.e. a continuous time random walk) of cladogenesis. While ecological and evolutionary selective forces vary greatly across environments, clades, and time, their contributions to body size evolution through time in mammals can be summarized by three relatively simple macroecological mechanisms.

Here, we compared fully marine and fully terrestrial species within a single clade. Future work should extend this comparison to other marine clades, mirroring past work examining

diverse terrestrial clades (Meiri 2008). Further, we would expect more complex dynamics for clades that exhibit partially marine and terrestrial lifestyles, as individuals would experience unique, and more likely complex, ecological and thermoregulatory constraints when allocating their time between different environments. A broad examination of body size evolution across environments and clades will allow us to better disentangle the relative importance of environmental constraints versus general processes, as evidenced here, in shaping body size distributions, macroevolutionary patterns, and their corresponding mechanisms.

5.6 Acknowledgements

LGS was supported by an NSF GRFP 1144083. LGS and AC conceived of the project and wrote the manuscript. AC collected cetacean data and performed allometric scaling and LGS quantified the strength of macroevolutionary mechanisms and macroecological patterns in body mass. Silhouette pictures are reproduced without modification from PhyloPic; cetacean pictures from Chris Huh, shrew from Sarah Werning, and elephant from T. Michael Keesey. All images available for reuse under Creative Commons Attribution 3.0 Unported license.

Chapter 6

Conclusions

My dissertation combines analytical models, simulations, statistical methods used in empirical community ecology, and novel databases of extinct and extant species, all with the aim of understanding how equalizing and stabilizing mechanisms contribute to diversity across both space and time. Ecological communities are highly complex systems, with a multitude of biotic interactions, environmental filtering, feedbacks, and stochasticity, making it difficult to understand the relative importance of processes that maintain diversity (Vellend 2016). This difficulty is compounded by the fact that multiple mechanisms may yield similar community composition patterns, or alternatively, that a single set of mechanisms may produce divergent patterns depending on their strength and inherent stochasticity (Mackey and Currie 2001, Mayfield and Levine 2010). In my dissertation, I used the equalizing and stabilizing coexistence framework (Chesson 2000b) to compare patterns in diversity across multiple communities with varied ecological mechanisms maintaining diversity, ranging from two and twenty-five-species simulated metacommunities to mammalian communities spanning the paleobiology record.

Coexistence theory was originally formulated for communities, and the importance of stabilizing and equalizing mechanisms has disproportionately been examined across short temporal scales (i.e. several years, with a focus on the temporal storage effect) (Sears and Chesson 2007; Angert et al. 2009; Kraft et al. 2015). In my dissertation, I instead examined how spatial coexistence theory (Chesson 2000a) elucidates underlying community assembly mechanisms (e.g. dispersal, competitive strength, habitat heterogeneity) in metacommunities, providing an avenue for connecting coexistence theory and metacommunity theory (Leibold et al. 2004; Holyoak et al. 2005). I also extended the equalizing and stabilizing framework beyond

community ecology to macroecology, allowing me to use a parallel framework for exploring patterns in diversity in the paleobiology record. I compared diversity in body size of terrestrial mammals and the Equidae (horse) sub-clade, and explored the relative importance of stochastic processes and taxonomic diversity in predicting body size diversity. I also examined the universality of mammalian body size distributions and the role of environmental filtering by comparing the evolution of body size in terrestrial and marine environments.

At the metacommunity scale, as expected, I found that neutral metacommunities comprise only equalizing mechanisms, and therefore do not exhibit stable coexistence. Additional community structuring mechanisms, such as habitat heterogeneity, dispersal, and trait-tradeoffs stabilize metacommunities disproportionately via the fitness-density covariance mechanism (Shoemaker and Melbourne 2016; Chapter 2). In my thesis, I also highlight the versatility of coexistence theory, and I show how it allows comparisons of more complex metacommunities within a single framework. Furthermore, the coexistence framework successfully differentiates between diverse community structuring mechanisms, while the beta-null deviation metric, commonly used for determining community structure, fails to connect process with pattern. Similar patterns in beta-null deviation arise for metacommunities with different underlying structuring processes; stochasticity makes the underlying structuring processes even more difficult to detect (Tucker, Shoemaker, et al. 2016; Chapter 3).

I extended the equalizing and stabilizing framework of coexistence theory beyond communities to explore patterns in size diversity in mammals. In chapters four and five, I showed that primarily equalizing mechanisms predict current mammalian body size distributions and the evolution of body size. I do so using a model of ‘diffusion’ of body sizes (i.e. a random walk in continuous time) constrained by a physiological minimum size, Cope’s rule, and a single

stabilizing mechanism—a size-dependent extinction risk. These mechanisms accurately predict body mass evolution across mammals, a mammalian subclade (Equidae; Shoemaker and Clauset 2014; Chapter 4), and across both terrestrial and marine environments (Chapter 5). Thus, while stabilizing mechanisms maintain coexistence in metacommunities, across evolutionary time equalizing mechanisms play a critical role in the evolution of diversity. There are multiple potential explanations for this difference when comparing scales. One likely explanation is that, by extending the equalizing and stabilizing framework from communities to macroecological patterns, we average over large spatial and temporal scales. While stabilizing mechanisms likely are still critical at smaller temporal and spatial scales, the average of these stabilizing mechanisms can be well-represented using almost solely equalizing mechanisms when examining macroecological patterns over millions of years.

Across chapters, a unifying theme is the importance of stochasticity in structuring communities. For example, even in highly competitive metacommunities, where abundances are largely unaffected by demographic stochasticity, I showed that demographic stochasticity decreases coexistence strength. Environmental stochasticity, in comparison, increases the strength of coexistence by increasing available niche space. Both of these effects arise because stochasticity, regardless of its origin, disproportionately affects stabilizing mechanisms (Shoemaker and Melbourne 2016; Chapter 2). Stochasticity additionally obfuscates patterns in beta-null deviation, making it difficult to infer processes structuring communities from abundance patterns alone. Instead, I advocate for directly measuring the processes of interest, whether competitive strength, environmental stochasticity, or the role of dispersal (Tucker, Shoemaker et. al. 2016; Chapter 3); these processes can then be directly connected to the equalizing and stabilizing framework of coexistence.

When examining the relative importance of equalizing and stabilizing mechanisms at macroevolutionary temporal scales, stochasticity still plays a critical role. In fact, the constrained random walk of body size evolution explains over 90% of the increase in Equidae maximum size through time, while taxonomic diversity, surprisingly, plays only a minor role (Shoemaker and Clauset 2014; Chapter 4). Furthermore, while we would expect environmental differences to yield variation in body size distributions across marine and terrestrial environments, we find that the patterns in body size evolution are remarkably similar. Body size distributions, and their evolution, are indistinguishable across environments, except that environmental filtering sets the minimum size above which equalizing mechanisms along with a size-dependent extinction risk operate to produce right-skewed distributions (Chapter 5).

In summary, community coexistence is the outcome of interactions between stabilizing and equalizing mechanisms; the relative importance of these opposing mechanisms depends on species' competitive strengths, dispersal, stochasticity, and environmental effects. In general, my dissertation research suggests that stabilizing mechanisms are critical across relatively small spatial scales, but that equalizing mechanisms may effectively predict macroecological patterns across longer temporal scales. Stochasticity plays a critical, and currently understudied, role across scales and in its contribution to coexistence. I suggest that future work should continue to incorporate stochasticity and examine its effects, beyond its role in neutral drift (Vellend et al. 2014), in structuring community and macroecological patterns of diversity. Additionally, a fruitful direction forward would be to continue integrating community ecology and macroecology concepts and frameworks, and specifically by examining the interaction of spatial and temporal coexistence mechanisms in maintaining biodiversity across scales. In my thesis, I focused on relatively small spatial scales and, in contrast, large temporal scales. More work is

needed to bridge this gap across scales (e.g. Beck et al. 2012) and to synthesize across both spatial and temporal variation.

Additional studies are also needed to see if the pattern I observe—where diversity in body size can be well-described using primarily equalizing mechanisms—holds when examining additional clades as well as other forms of biological diversity. Mammalian body size diversity is fairly well studied, yet it is unknown if the general patterns I observe hold for other clades, in particular when comparing across environments. These patterns could be further explored across scales. I show that the right-skewed distribution is observed within the Equidae sub-clade, but this pattern should also be examined for smaller scales, such as within species or even populations.

Finally, empirical tests of my theoretical predictions in metacommunities—specifically examining the role of environmental and demographic stochasticity and the relative importance of the spatial storage effect versus fitness-density covariance—are needed, both to test theory, and to further integrate experimental and theoretical studies across spatial scales. Continuing to examine coexistence and the relative importance of equalizing and stabilizing mechanisms across spatial and temporal scales will allow us to better understand community structure and to more fully integrate community and macroecology with the goal of predicting patterns in biodiversity on our changing planet.

Bibliography

Adler, P. B., J. HilleRisLambers, and J. M. Levine. 2007. A niche for neutrality. Ecology Letters 10:95–104.

Adler, P. B., A. Fajardo, A. R. Kleinhesselink, and N. J. B. Kraft. 2013. Trait-based tests of coexistence mechanisms. Ecology Letters 16:1294–1306.

Ahlborn, B. K. 1999. Lower size limit of aquatic mammals. American Journal of Physics 67:920.

Ahlborn, B. K. 2000. Thermodynamic limits of body dimension of warm blooded animals. Journal of Non-Equilibrium Thermodynamics 25:87–102.

Alberdi, M. T., J. L. Prado, and E. Ortiz-Jaureguizar. 1995. Patterns of body size changes in fossil and living *Equini* (Perissodactyla). Biological Journal of the Linnean Society 54: 349–370.

Allen, G. M. 1921. A new fossil cetacean. Bulletin of the Museum of Comparative Zoology 45:1–14.

Allen, A. P., J. Brown, and J. Gillooly. 2002. Global biodiversity, biochemical kinetics, and the energetic-equivalence rule. Science 297: 1545–1548.

Alroy, J. 1998. Cope's rule and the dynamics of body mass evolution in North American fossil mammals. Science 280: 731–734.

Amano, M., N. Miyazaki, and K. Kureha. 1992. A morphological comparison of skulls of the finless orpoise *Neophocaena phocaenoides* from the Indian Ocean, Yangtze River and Japanese waters. Journal of the Mammalogical Society of Japan 17:59–69.

Amarasekare, P. 2003. Competitive coexistence in spatially structured environments: a synthesis. Ecology Letters 6:1109–1122.

Amarasekare, P. and R. M. Nisbet. 2001. Spatial heterogeneity, source-sink dynamics, and the local coexistence of competing species. The American Naturalist 158: 572-584.

Amarasekare, P., M. F. Hoopes, N. Mouquet, and M. Holyoak. 2004. Mechanisms of coexistence in competitive metacommunities. The American Naturalist 164: 310–326.

Armstrong, R. A. and R. McGehee. 1980. Competitive exclusion. The American Naturalist 115: 151–170.

Angert, A. L., T. E. Huxman, P. Chesson, and D. L. Venable. 2009. Functional tradeoffs determine species coexistence via the storage effect. Proceedings of the National Academy of Sciences 106: 11641-11645.

Archer, F. I. and W. F. Perrin. 1999. Mammalian species *Stenella coeruleoalba*. American Society of Mammalogists 603:1–9.

Arnold, A. J., D. C. Kelly, and W. C. Parker. 1995. Causality and Cope's rule: evidence from the planktonic foraminifera. Journal of Paleontology 69: 203-210.

Aslanova, S. M. 1977. Noviy rod kitoobraznykh (Atropatenocetus posteocenicus gen. et sp. nov.) iz oligotsena Azerbaydzhana. Pages 160–164. Doklady - Akademiya Nauk Azerbaydzjanskoy SSR.

Azeria, E. T., J. Ibarzabel, J. Boucher, and C. Hébert. 2011. Towards a better understanding of beta diversity: deconstructing composition patterns of saproxylic beetles breeding in recently burnt boreal forests. In: Research in biodiversity: models and applications. InTech, Open Access Publisher, Rijeka, pp. 75–94.

Azzaroli, A. 1998. The genus Equus in North America. The Pleistocene species. Palaeontographia Italica 85: 1–60.

Bajpai, S., and G. M. Johannes. 2000. A new, diminutive Eocene whale from Kachchh (Gujarat, India) and its implications for locomotor evolution of cetaceans. Current Science 79: 1478–1482.

Bajpai, S., and P. D. Gingerich. 1998. A new Eocene archaeocete (Mammalia, Cetacea) from India and the time of origin of whales. Proceedings of the National Academy of Sciences 95: 15464–15468.

Barnes, L. G. 1976. Outline of eastern North Pacific fossil cetacean assemblages. Systematic Biology 25:321–343.

Barnes, L. G. 1984. Fossil *Odontocetes* (Mammalia: Cetacea) from the Almejas Formation, Isla Cedros, Mexico. Natural History Museum of Los Angeles County.

Barnes, L. G. 1985a. Fossil *Pontoporiid* Dolphins (Mammalia, Cetacea) from the Pacific Coast of North America. Natural History Museum of Los Angeles County.

Barnes, L. G. 1985b. The Late Miocene Dolphin Pithanodelphis Abel, 1905 (Cetacea, Kentriodontidae) from California. Natural History Museum of Los Angeles County.

Barnes, L. G., D. P. Domning, and C. E. Ray. 1985. Status of studies on fossil marine mammals. Marine Mammal Science 1:15–53.

Barwick, A. R. 1939. Miocene porpoise (Delphinodon dividum) from southern Maryland. The American Midland Naturalist 22:154–159.

Beck, J., et al. 2012. What's on the horizon for macroecology? Ecography 35: 673-683.

Beck, J., J. D. Holloway, and W. Schwanghart. 2013. Undersampling and the measurement of beta diversity. Methods in Ecology and Evolution 4: 370–382.

Bell, G. 2000. The distribution of abundance in neutral communities. The American Naturalist 155: 606–617.

Benham, W. B. 1937. Fossil Cetacea of New Zealand. III. The skull and other parts of the skeleton of *Prosqualodon hamiltoni* n. sp. Transactions of the Royal Society of New Zealand 67: 8-14.

Berg, H. C. 1993. Random Walks in Biology. Princeton University Press, Princeton.

Berta, A. and T. A. Demere. 2009. Mysticetes, Evolution. Pages 1–5 *in* W. F. Perrin, B. Wursig, and J. G. M. Thewissen, editors. Encyclopedia of Marine Mammals. Second edition. Elsevier Inc.

Berta, A., J. L. Sumich, and K. M. Kovacs. 2006. Marine Mammals. Second edn. Academic Press, San Diego.

Best, R. C., and V. M. Silva. 1993. Mammalian species *Inia geoffrensis*. American Society of Mammalogists 426: 1–8.

Beverton, R. and S. J. Holt. 1957. On the dynamics of exploited fish populations. Ministry of Agriculture, Fisheries and Food, London, UK.

Bianucci, G. 2001. A new genus of kentriodontid (Cetacea: Odontoceti) from the Miocene of South Italy. Journal of Vertebrate Paleontology 21: 573–577.

Bianucci, G., and W. Landini. 2002. Change in diversity, ecological significance and biogeographical relationships of the Mediterranean Miocene toothed whale fauna. Geobios 35:19–28.

Bianucci, G. and W. Landini. 2006. Killer sperm whale: a new basal *physeteroid* (Mammalia, Cetacea) from the Late Miocene of Italy. Zoological Journal of the Linnaean Society 148: 103–131.

Bianucci, G., O. Lambert, and K. Post. 2007. A high diversity in fossil beaked whales (Mammalia, *Odontoceti, Ziphiidae*) recovered by trawling from the sea floor off South Africa. Geodiversitas 29: 561-618.

Bilal, S. O. and I. L. Bamy. 2004. Distribution, status, and biology of the Atlantic humpback dolphin, *Sousa teuszii* (Kükenthal, 1892). Aquatic Mammals 30: 56–83.

Bisconti, M. 2005. Skull morphology and phylogenetic relationships of a new diminutive balaenid from the Lower Pliocene of Belgium. Palaeontology 48: 793–816.

Bisconti, M. 2006. *Titanocetus*, a new baleen whale from the Middle Miocene of northern Italy (Mammalia, Cetacea, Mysticeti). Journal of Vertebrate Paleontology 26: 344–354.

Bisconti, M. 2008. Morphology and phylogenetic relationships of a new *eschrichtiid* genus (Cetacea: Mysticeti) from the Early Pliocene of northern Italy. Zoological Journal of the Linnean Society 153: 161–186.

Bisconti, M. 2009. Taxonomy and evolution of the Italian Pliocene Mysticeti (Mammalia, Cetacea): a state of the art. Bollettino della Società Paleontologica Italiana 48: 147–156.

Blondel, C. 1998. Etude morphologique du squelette appendiculaire des ruminants de l'Oligocene d'Europe occidentale; implications environnementales. Comptes Rendus de l'Academie des Sciences 326: 527–532.

Borsa, P. 2006. Marine mammal strandings in the New Caledonia region, Southwest Pacific. Comptes Rendus Biologies 329: 277–288.

Bouetel, V. and C. de Muizon. 2006. The anatomy and relationships of *Piscobalaena nana* (Cetacea, Mysticeti), a Cetotheriidae ss from the early Pliocene of Peru. Geodiversitas 28:v319–395.

Brännström, A., and D. J. T. Sumpter. 2005a. The role of competition and clustering in population dynamics. Proceedings of the Royal Society B: Biological Sciences 272: 2065–2072.

Brännström, Å. and D. J. T. Sumpter. 2005b. Coupled map lattice approximations for spatially explicit individual-based models of ecology. Bulletin of Mathematical Biology. 67: 663–682.

Brown, J. H. 1995. Macroecology. University of Chicago Press, Chicago.

Brownell, R. L. 1975. Mammalian species *Phocoena dioptrica*. The American Society of Mammalogists 193: 1–3.

Brownell, R. L. 1983. Mammalian species *Phocoena sinus*. The American Society of Mammalogists 198: 1–3.

Brownell, R. L., and E. S. Herald. 1972. Mammalian species *Lipotes vexillifer*. The American Society of Mammalogists:1–4.

Brownell, R. L., and P. R. 1984. Mammalian species *Phocena spinipinnis*. The American Society of Mammalogists 10: 1–4.

Buchholtz, E. A. 2007. Modular evolution of the cetacean vertebral column. Evolution and Development 9: 278–289.

Cabrera, A. 1926. Cetáceos fósiles del Museo de la Plata. Revista del Museo de La Plata 29: 363–411.

Caballero, I., J. M. Olano, A. Escudero, and J. Loidi. 2007. Seed bank spatial structure in semi-arid environments: beyond the patch-bare area dichotomy. Plant Ecology 195: 215–223.

Cardillo, M., G. M. Mace, K. E. Jones, J. Bielby, O. R. P. Bininda-Emonds, W. Sechrest, C. D. L. Orme, and A. Purvis. 2005. Multiple causes of high extinction risk in large mammal species. Science 309: 1239–1241.

Cadotte, M. W. 2006. Metacommunity influences on community richness at multiple spatial scales: a microcosm experiment. Ecology 87:1008–1016.

Cadotte, M. W. 2007. Competition-colonization trade-offs and disturbance effects at multiple scales. Ecology 88: 823–829.

Calcagno, V., N. Mouquet, P. Jarne, and P. David. 2006. Coexistence in a metacommunity: the competition–colonization trade-off is not dead. Ecology Letters 9: 897–907.

Caley, M. J., K. A. Buckley, and G. P. Jones. 2001. Separating ecological effects of habitat fragmentation, degradation, and loss on coral commensals. Ecology 82: 3435–3448.

Carroll, I., B. J. Cardinale, and R. M. Nisbet. 2011. Niche and fitness differences relate the maintenance of diversity to ecosystem function. Ecology 92: 1157–1165.

Chase, J. M. and M. A. Leibold. 2003. Ecological niches: linking classical and contemporary approaches. University of Chicago Press.

Chase, J. M. and R. S. Shulman. 2009. Wetland isolation facilitates larval mosquito density through the reduction of predators. Ecological Entomology 34: 741–747.

Chase, J. M. 2010. Stochastic community assembly causes higher biodiversity in more productive environments. Science 328:1388–1391.

Chase, J. M. and J. A. Myers. 2011. Disentangling the importance of ecological niches from stochastic processes across scales. Proceedings of the Royal Society B 366: 2351–2363.

Chase, J. M., N. J. B. Kraft, K. G. Smith, M. Vellend, and B. D. Inouye. 2011. Using null models to disentangle variation in community dissimilarity from variation in alpha-diversity. Ecosphere 2: 1-11.

Chase, J. M. and T. M. Knight. 2013. Scale-dependent effect sizes of ecological drivers on biodiversity: why standardised sampling is not enough. Ecology Letters 16: 17-26.

Chave, J. and E. G. Leigh. 2002. A spatially explicit neutral model of β-diversity in tropical forests. Theoretical Population Biology 62: 153-168.

Chesson, P. 2000a. General theory of competitive coexistence in spatially-varying environments. Theoretical Population Biology 58: 211–237.

Chesson, P. 2000b. Mechanisms of maintenance of species diversity. Annual Review of Ecology and Systematics 31: 343–366.

Chesson, P. 2008. Quantifying and testing species coexistence mechanisms. Pages 119–164 in F. Valladares, A. Camacho, A. Elosegui, C. Gracia, M. Estrada, J. C. Senar, and J. M. Gili, editors. Unity in diversity: reflections on ecology after the legacy of Ramon Margalef. Fundacion BBCA, Bilbao, Spain.

Chesson, P., M. J. Donahue, B. A. Melbourne, and A. L. Sears. 2005. Scale transition theory for understanding mechanisms in metacommunities. Pages 279–306 in M. Holyoak, M. A. Leibold, and R. D. Holt, editors. Metacommunities: spatial dynamics and ecological communities. University of Chicago Press, Chicago, Illinois, USA.

Clapham, P. J. and J. G. Mead. 1999. Mammalian species *Megaptera novaeangliae*. American Society of Mammalogists 604:1–9.

Clauset, A. 2013. How large should whales be? Plos One 8: e53967.

Clauset, A. and D. H. Erwin. 2008. The evolution and distribution of species body size. Science, 321: 399–401.

Clauset, A. and S. Redner. 2009. Evolutionary model of species body mass diversification. Physical Review Letters 102: 038103.

Clauset, A., D. J. Schwab, and S. Redner. 2009. How many species have mass *M*? American Naturalist 173: 256–263.

Cohen, J. E. and T. Fenchel. 1994. Marine and continental food webs: three paradoxes? Philosophical Transactions: Biological Sciences 343: 57-59.

Colwell, R. K. and D. W. Winkler. 1984. A null model for null models in biogeography. Pp. 344–359 in Strong, D. R. et al. (eds), Ecological communities: conceptual issues and the evidence. Princeton Univ. Press.

Connor, E. F. and D. Simberloff. 1979. The assembly of species community: chance or competition? Ecology 60: 1132–1140.

Cottenie, K. 2005. Integrating environmental and spatial processes in ecological community dynamics. Ecology Letters 8: 1175–1182.

Crist, T. O., J. A. Veech, J. C. Gering, and K. S. Summerville. 2003. Partitioning species diversity across landscapes and regions: a hierarchical analysis of α, β, and γ diversity.

The American Naturalist 162: 734–743.

Cope, E. D. 1867. An addition to the vertebrate fauna of the Miocene period, with a synopsis of the extinct Cetacea of the United States. Proceedings of the Academy of Natural Sciences of Philadelphia 19: 138-156.

Cope, E. D. 1890. The Cetacea. The American Naturalist 24: 599-616.

Cranford, T. W. 1999. The sperm whale's nose: sexual selection on a grand scale? Marine Mammal Science 15: 1133–1157.

Culik, B. M., U. N. E. Programme, and C. O. M. S. Secretariat. 2004. Review of small cetaceans. United Nations Environment Programme.

Czyzewska, T. and Z. Ryziewicz. 1976. *Pinocetus polonicus* gen. n. sp. n.(Cetacea) from the Miocene limestones of Pinczow, Poland. Acta Palaeontologica Polonica 21: 259-291.

Dalebout, M. L., C. S. Baker, and R. C. Anderson. 2003. Appearance, distribution, and genetic distinctiveness of Longman's beaked whale, *Indopacetus pacificus*. Marine Mammal Science 19: 421–461.

Damuth, J. and B. J. MacFadden. 1990. Body Size in mammalian paleobiology: estimation and biological implications. Cambridge University Press, Cambridge, UK.

Davidson, A. D., A. G. Boyer, H. Kim, S. Pompa-Mansilla, M. J. Hamilton, D. P. Costa, G. Ceballos, and J. H. Brown. 2012. Drivers and hotspots of extinction risk in marine mammals. Proceedings of the National Academy of Science 109: 3395–3400.

Davies, K. F., B. A. Melbourne, C. R. Margules, and J. F. Lawrence. 2005. Metacommunity structure influences the stability of local beetle communities. Pages 170–188 in M. Holyoak, M. A. Leibold, and R. D. Holt, editors. Metacommunities: spatial dynamics and ecological communities. University of Chicago Press, Chicago, Illinois, USA.

Dawson, S. D. 1996. A new kentriodontid dolphin (Cetacea; Delphinoidea) from the middle Miocene Choptank Formation, Maryland. Journal of Vertebrate Paleontology 16: 135–140.

Debout, G. D. G., A. Dalecky, A. N. Ngomi, and D. B. McKey. 2009. Dynamics of species coexistence: maintenance of a plant-ant competitive metacommunity. Oikos 118: 873–884.

de Muizon, C., D. P. Domning, and D. R. Ketten. 2002. *Odobenocetops peruvianus*, the walrus-convergent delphinoid (Mammalia: Cetacea) from the Early Pliocene of Peru. Smithsonian Contributions to Paleobiology 93: 223-261.

de Muizon, C., D. P. Domning, and M. Parrish. 1999. Dimorphic tusks and adaptive strategies in

a new species of walrus-like dolphin (Odobenocetopsidae) from the Pliocene of Peru. Comptes Rendus de l'Académie des Sciences-Series IIA-Earth and Planetary Science 329: 449-455.

Demere, T. A. 1986. The fossil whale, *Balaenoptera davidsonii* (Cope 1872), with a review of other Neogene species of Balaenoptera (Cetacea: Mysticeti). Marine Mammal Science 2: 277–298.

Demere, T. A. and A. Berta. 2008. Skull anatomy of the Oligocene toothed mysticete *Aetioceus weltoni* (Mammalia; Cetacea): implications for mysticete evolution and functional anatomy. Zoological Journal of the Linnean Society 154: 308-352.

Demere, T. A. and R. A. Cerutti. 1982. A Pliocene shark attack on a cethotheriid whale. Journal of Paleontology 56: 1480-1482.

Dooley, A. C. 2005. A new species of Squalodon (Mammalia, Cetacea) from the Middle Miocene of Virginia. Virginia Museum of Natural History.

Dooley, A. C., Jr, N. C. Fraser, and Z. X. Luo. 2004. The earliest known member of the rorqual—gray whale clade (Mammalia, Cetacea). Journal of Vertebrate Paleontology 24: 453–463.

Downhower, J. F. and L. S. Blumer. 1988. Calculating just how small a whale can be. Nature 335: 675–675.

Dornelas, M., S. R. Connolly, and T. P. Hughes. 2006. Coral reef diversity refutes the neutral theory of biodiversity. Nature 440: 80-82.

Dunning, J. 2007. CRC Handbook of Avian Body Masses, Second Edition. CRC Press.

Economo, E. P. and T. H. Keitt. 2007. Species diversity in neutral metacommunities: a network approach. Ecology Letters 11: 52–62.

Eisenmann, V. and P. Sondaar. 1998. Pliocene vertebrates locality of, Alta, Ankara, Turkey. 7. Hipparion. Godiversitas 20: 409–439.

Eisenmann, V. 2003. Gigantic horses. Paleontology 50: 57–73.

Ellis, A. M., L. P. Lounibos, and M. Holyoak. 2006. Evaluating the long-term metacommunity dynamics of tree hole mosquitoes. Ecology 87: 2582–2590.

Emry, R. J. 2002. Cenozoic mammals of land and sea: Tributes to the career of Clayton E. Ray. Pages 1–384 (R. J. Emry, Ed.). Smithsonian Contributions to Paleobiology, Washington, D.C.

Erwin, D. H. 2007. Disparity: morphological pattern and developmental context. Paleontology

50: 57–73.

Ferrenberg, S. et al. 2013. Changes in assembly processes in soil bacterial communities following a wildfire disturbance. The ISME Journal 7: 1102:1111.

Field, C. B. 1998. Primary production of the biosphere: integrating terrestrial and oceanic components. Science 281: 237–240.

Fitzgerald, E. M. G. 2006. A bizarre new toothed mysticete (Cetacea) from Australia and the early evolution of baleen whales. Proceedings of the Royal Society B: Biological Sciences 273: 2955–2963.

Fitzgerald, E. M. 2009. The morphology and systematics of *Mammalodon colliveri* (Cetacea: Mysticeti), a toothed mysticete from the Oligocene of Australia. Zoological Journal of the Linnean Society 158: 367–476.

Foote, M. 1993. Discordance and concordance between morphological and taxonomic diversity. Paleobiology 19: 185–204.

Fordyce, R. E. 2002. *Simocetus rayi* (Odontoceti: Simocetidae, New Family): a bizarre new archaic Oligocene dolphin from the eastern North Pacific. Smithsonian Contributions to Paleobiology.

Fordyce, R. E. 2003. Cetacean evolution and Eocene-Oligocene oceans revisited. Pages 154 to 171 in From greenhouse to icehouse: the marine Eocene-Oligocene transition..

Fordyce, R. E., P. G. Quilty, and J. Daniels. 2002. *Australodelphis mirus*, a bizarre new toothless ziphiid-like fossil dolphin (Cetacea: Delphinidae) from the Pliocene of Vestfold Hills, East Antarctica. Antarctic Science 14: 37-54.

Forsten, A. 2002. Latest Hipparion Christol, 1832 in Europe. A review of the Pliocene Hipparion crassum Gervais Group and other finds (Mammalia, Equidae). Geodiversitas 24: 465–486.

Fuller, A. J. and S. J. Godfrey. 2007. A late Miocene ziphiid (*Messapicetus sp*.: Odontoceti: Cetacea) from the St. Marys Formation of Calvert Cliffs, Maryland. Journal of Vertebrate Paleontology 27: 535–540.

Gavrilets, S. and J. B. Losos. 2009. Adaptive radiation: contrasting theory with data. Science 323: 732–737.

Germain, R. M., L. Johnson, S. Schneider, K. Cottenie, E. A. Gillis, and A. S. MacDougall. 2013. Spatial variability in plant predation determines the strength of stochastic community assembly. The American Naturalist 182: 169–179.

Gittleman, J. L. 1985. Carnivore body size: ecological and taxonomic correlates. Oecologia 67:

540–554.

Gingerich, P. D.1991. Systematics and evolution of early Eocene Perissodactyla (Mammalia) in the Clarks Fork Basin. Wyoming Contributions from the Museum of Paleontology, the University of Michigan 28: 181–213.

Gingerich, P. D. 2001. Origin of whales from early Artiodactyls: hands and feet of Eocene Protocetidae from Pakistan. Science 293: 2239–2242.

Gingerich, P. D. and D. E. Russell. 1981. *Pakicetus inachus*, a new archaeocete (Mammalia, Cetacea) from the early-middle Eocene Kuldana Formation of Kohat (Pakistan). Contributions from the Museum of Paleontology The University of Michigan.

Gingerich, P. D. and M. D. Uhen. 1996. *Ancalecetus simonsi*, a new dorudontine archaeocete (Mammalia, Cetacea) from the early late Eocene of Wadi Hitan, Egypt. Contributions from the Museum of Paleontology The University of Michigan 29: 359–401.

Gingerich, P. D., B. H. Smith, and E. L. Simons. 1990. Hind limbs of eocene basilosaurus: evidence of feet in whales. Science 249: 154–157.

Gingerich, P. D., I. S. Zalmout, M. Ul-Haq, and M. A. Bhatti. 2005. *Makaracetus bidens*, a new protocetid archaeocete (Mammalia, Cetacea) from the early middle Eocene of Balochistan (Pakistan). Contributions from the Museum of Paleontology The University of Michigan 31: 197–210.

Gingerich, P. D., M. Arif, M. A. Bhatti, H. A. Raza, and S. M. Raza. 1995. Protosiren and Babiacetus (Mammalia, Sirenia and Cetacea) from the middle Eocene Drazinda Formation, Sulaiman Range, Punjab (Pakistan). Contributions from the Museum of Paleontology The University of Michigan 29: 331–357.

Gingerich, P. D., M. Arif, M. A. Bhatti, M. Anwar, and W. J. Sanders. 1997. *Basilosaurus drazindai* and *Basiloterus hussaini*, new Archaeoceti (Mammalia, Cetacea) from the middle Eocene Drazinda Formation. Contributions from the Museum of Paleontology The University of Michigan 30: 55–81.

Gingerich, P. D., W. von Koenigswald, W. J. Sanders, B. H. Smith, and I. S. Zalmout. 2009. New Protocetid whale from the middle Eocene of Pakistan: birth on land, precocial development, and sexual dimorphism. PLoS ONE 4: e4366.

Gingerich, P. D., S. M. Raza, M. Arif, M. Anwar, and X. Y. Zhou. 1994. New whale from the Eocene of Pakistan and the origin of cetacean swimming. Nature 368: 844-847.

Godfrey, S. J. 2009. Fossil beaked whale skull donated to the Calvert Marine Museum. Pages 1–2 in The Ecphora.

Godfrey, S. J. and L. G. Barnes. 2008. A new genus and species of late Miocene pontoporiid

dolphin (Cetacea: Odontoceti) from the St. Marys Formation in Maryland. Journal of Vertebrate Paleontology 28: 520–528.

Gotelli, N. J. and G. R. Graves. 1996. Null models in ecology. Smithsonian Institution Press. Washington D.C.

Gould, G. C. and B. J. MacFadden. 2004. Gigantism, dwarfism, and Cope's Rule: nothing in evolution makes sense without a phylogeny. Bulletin of the American Museum of Natural History 285: 219–237.

Grman, E. and L. A. Brudvig. 2014. Beta diversity among prairie restorations increases with species pool size, but not through enhanced species sorting. Journal of Ecology 102: 1017–1024.

Guthrie, R. D. 2006. New carbon dates link climatic change with human colonization and Pleistocene extinctions. Nature 441: 207–209.

Gutstein, C. S., M. A. Cozzuol, and A. O. Vargas. 2009. Patterns of skull variation of Brachydelphis (Cetacea, Odontoceti) from the Neogene of the Southeastern Pacific. Journal of Mammalogy 90: 504–519.

Guo, H., K. Więski, Z. Lan, and S. C. Pennings. 2013. Relative influence of deterministic processes on structuring marsh plant communities varies across an abiotic gradient. Oikos 123: 173–178.

Hammersley, J. M. and D. C. Handscomb. 1964. Monte Carlo methods. Fletcher and Son Ltd. Great Britain.

Hampe, O. 2006. Middle/late Miocene hoplocetine sperm whale remains (Odontoceti: Physeteridae) of North Germany with an emended classification of the Hoplocetinae. Fossil Record 9: 61–86.

Hastings, A. 1980. Disturbance, coexistence, history, and competition for space. Theoretical Population Biology 18: 363–373.

Hay, O. P. 1917. Description of a new species of extinct horse, *Equus lambei*, from the Pleistocene of Yukon Territory. Proceedings of the U.S. National Museum 53: 435–443.

Heim, N. A., M. L. Knope, E. K. Schaal, S. C. Wang, and J. L. Payne. 2015. Cope's rule in the evolution of marine animals. Science 347: 867–870.

Henry-Stamper, A. 2006, October 26. Cave slowly revealing its nautral history secrets. Springfield's Community Free Press.

Heyning, J. E., and M. E. Dahlheim. 1988. Mammalian species *Orcinus orca*. The American Society of Mammalogists 304: 1–9.

Hiebeler, D. 1997. Stochastic spatial models: from simulations to mean field and local structure approximations. Journal of Theoretical Biology 187: 307–319.

Hirota, K. and L. G. Barnes. 1994. A new species of Middle Miocene sperm whale of the genus Scaldicetus (Cetacea; Physeteridae) from Shiga-mura, Japan. The Island Arc 3: 453–472.

Holyoak, M., M. A. Leibold, and R. D. Holt. 2005. Metacommunities: spatial dynamics and ecological communities. University of Chicago Press, Chicago, Illinois, USA.

Hone, D., and M. J. Benton. 2005. The evolution of large size: how does Cope's Rule work? Trends in Ecology and Evolution 20: 4-6.

Hubbell, S. P. 2001. The unified neutral theory of biodiversity and biogeography. Princeton University Press, Princeton, New Jersey, USA.

Hubbell, S. P. 1997. A unified theory of biogeography and relative species abundance and its application to tropical rain forests and coral reefs. Coral Reefs 16: S9-S21.

Hulbert, R. C. J. 1993. Late Miocene Nannippus (Mammalia: Perissodactyla) from Florida, with a description of the smallest Hipparionine horse. Journal of Vertebrate Paleontology 13: 350–366.

Hunt, G., and K. Roy. 2006. Climate change, body size evolution, and Cope's Rule in deep-sea ostracodes. Proceedings of the National Academy of Science 103: 1347-1352.

Hunt, G. 2007. The relative importance of directional change, random walks, and stasis in the evolution of fossil lineages. Proceedings of the National Academy of Science 104: 18404–18408.

Hutchinson, G. E. 1959. Homage to Santa Rosalia or why are there so many kinds of animals? The American Naturalist 93: 145-159.

Huxley, J. 1932. Problems of relative growth. Methuen, London, UK.

Huxley, T. H. 1864. On the Cetacean Fossils termed “Ziphius” by Cuvier, with a notice of a new species (*Belemnoziphius compressus*) from the Red Crag. Quarterly Journal of the Geological Society 20: 388–396.

Ichishima, H., and M. Kimura. 2000. A new fossil porpoise (Cetacea; Delphinoidea; Phocoenidae) from the early Pliocene Horokaoshirarika Formation, Hokkaido, Japan. Journal of Vertebrate Paleontology 20:561–576.

Ichishima, H. and M. Kimura. 2005. *Haborophocoena toyoshimai*, a new early Pliocene porpoise (Cetacea; Phocoenidae) from Hokkaido, Japan. Journal of Vertebrate Paleontology 25: 655–664.

Ichishima, H., L. G. Barnes, R. E. Fordyce, and M. Kimura. 1994. A review of kentriodontine dolphins (Cetacea; Deiphinoidea; Kentriodontidae): systematics and biogeography. Island Arc 3: 486-492.

Jablonski, D. 1997. Body-size evolution in Cretaceous molluscs and the status of Cope's rule. Nature 385: 250–252.

Jabot, F., R. S. Etienne, and J. Chave. 2008. Reconciling neutral community models and environmental filtering: theory and an empirical test. Oikos 117: 1308–1320.

Janis, C. 1982. Evolution of horns in ungulates: ecology and paleoecology. Biological Reviews 57: 261–318.

Janis, C., I. J. Gordon. and A. W. Illus. 1994. Modelling equid/ruminant competition in the fossil record. Historical Biology 8: 15–29.

Janis, C. M. 2007. The horse series. In Icons of Evolution. (ed Regal, B.) Greenwood Press, Westport, USA.

Jefferson, T. A. 1998. Mammalian species *Phocoenoides dalli*. American Society of Mammalogists 319: 1–7.

Jefferson, T. A. and B. E. Curry. 2003. Mammalian species *Stenella clymene*. American Society of Mammalogists 726: 1–5.

Jefferson, T. A. and L. Karczmarski. 2001. Mammalian species *Sousa chinensis*. American Society of Mammalogists 655: 1–9.

Jefferson, T. A. and M. W. Newcomer. 1993. Mammalian species *Lissodelphis borealis*. American Society of Mammalogists 425: 1–6.

Jefferson, T. A. and M. W. Newcomer. 1994. Right whale dolphins *Lissodelphis borealis* (Peale, 1848) and *Lissodelphis peronii*.. Handbook of marine mammals 5: 335-362.

Jefferson, T. A. and N. B. Barros. 1997. Mammalian species *Peponocephala electra*. American Society of Mammalogists 553: 1–6.

Jefferson, T. A. and S. K. Hung. 2004. Mammalian species *Neophocaena phocaenoides*. American Society of Mammalogists 746: 1–12.

Jefferson, T. A., M. A. Webber, and R. L. Pitman. 1993. Marine mammals of the world. United Nations Environment Programme, Food and Agriculture Organization of the United Nations.

Jeppsson, T. and P. Forslund. 2012. Can life history predict the effect of demographic

stochasticity on extinction risk? American Naturalist 179: 706–720.

Jost, L. 2007. Partitioning diversity into independent alpha and beta components. Ecology 88: 2427–2439.

Kazár, E. and D. Grigorescu. 2005. Revision of *Sarmatodelphis moldavicus* Kirpichnikov, 1954 (Cetacea: Delphinoidea), from the Miocene of Kishinev, Republic of Moldavia. Journal of Vertebrate Paleontology 25: 929–935.

Kellogg, A. R. 1923. Description of two squalodonts recently discovered in the Calvert Cliffs, Maryland; and notes on the shark-toothed cetaceans. Proceedings of the United States National Museum 62: 1–69.

Kellogg, A. R. 1924. A fossil porpoise from the Calvert formation of Maryland. Proceedings of the United States National Museum 63: 1–39.

Kellogg, A. R. 1925. On the occurrence of remains of fossil porpoises of the genus Eurhinodelphis in North America. Proceedings of the United States National Museum 66: 1–40.

Kellogg, A. R. 1936. A Review of the Archaeoceti. Carnegie Institution of Washington, Washington D.C. USA.

Kellogg, A. R. 1957. Two additional Miocene porpoises from the Calvert Cliffs, Maryland. Proceedings of the United States National Museum 107: 279–337.

Kellogg, A. R. 1965. Fossil marine mammals from the Miocene Calvert Formation of Maryland and Virginia. Part 2. The Miocene Calvert sperm whale Oryclerocetus. United States National Museum Bulletin 247: 47–63.

Kellogg, A. R. 1966. A new odontocete from the Calvert Miocene of Maryland. Bulletin United States National Museum of Natural History 247: 99–101.

Kellogg, A. R. 1968. Fossil marine mammals from the Miocene Calvert Formation of Maryland and Virginia, Part 7: A sharp-nosed cetothere from the Miocene Calvery. Bulletin United States National Museum of Natural History 247: 163–173.

Kellogg, R. 1928. The history of whales-their adaptation to life in the water. The Quarterly Review of Biology 3: 29-76.

Kellogg, R. 1929. A new fossil toothed whale from Florida. American Museum Novitates 389: 1-10.

Kembel, S. W. 2009. Disentangling niche and neutral influences on community assembly: assessing the performance of community phylogenetic structure tests. Ecology Letters 12: 949–960.

Kimura, T. and T. Ozawa. 2002. A new cetothere (Cetacea: Mysticeti) from the early Miocene of Japan. Journal of Vertebrate Paleontology 22: 684–702.

Klompmaker, A. A., C. E. Schweitzer, R. M. Feldmann, and M. Kowalewski. 2015. Environmental and scale-dependent evolutionary trends in the body size of crustaceans. Proceedings of the Royal Society B 282: 20150440.

Koehler, E., E. Brown, and S. J. P. A. Haneuse. 2009. On the assessment of Monte Carlo error in simulation-based statistical analyses. The American Statatistician 63: 155–162.

Kozwski, J. and A. T. Gawelczyk. 2002. Why are species' body size distributions usually skewed to the right? Functional Ecology 16: 419–432.

Kraft, N. J. et al. 2011. Disentangling the drivers of beta-diversity along latitudinal and elevational gradients. Science 333: 1755–1758.

Kraft, N. J., O. Godoy, and J. M. Levine. 2015. Plant functional traits and the multidimensional nature of species coexistence. Proceedings of the National Academy of Sciences, 112: 797-802.

Krapivsky, P. L., S. Redner, and E. Ben-Naim. 2010. A kinetic view of statistical physics. Cambridge University Press, Cambridge, England.

Lambert, O. 2005a. Phylogenetic affinities of the long-snouted dolphin Eurhinodelphis (cetacea, odontoceti) from the Miocene of Antwerp, Belgium. Palaeontology 48: 653–679.

Lambert, O. 2005b. Systematics and phylogeny of the fossil beaked whales *Ziphirostrum du Bus*, 1868 and *Choneziphius Duvernoy*, 1851 (Mammalia, Cetacea, Odontoceti), from the Neogene of Antwerp (North of Belgium). Geodiversitas 27: 443-497.

Lambert, O. 2008. A new porpoise (Cetacea, Odontoceti, Phocoenidae) from the Pliocene of the North Sea. Journal of Vertebrate Paleontology 28: 863–872.

Lambert, D. W. 2006. Functional convergence of ecosystems: evidence from body mass distributions of North American late Miocene mammal faunas. Ecosystems 9: 97–118.

Lambert, O. and S. Louwye. 2006. *Archaeoziphius microglenoideus*, a new primitive beaked whale (Mammalia, Cetacea, Odontoceti) from the Middle Miocene of Belgium. Journal of Vertebrate Paleontology 26: 182-191.

Lambert, O., G. Bianucci, and C. de Muizon. 2008. A new stem-sperm whale (Cetacea, Odontoceti, Physeteroidea) from the Latest Miocene of Peru. Comptes Rendus Palevol 7: 361–369.

Lambert, O., G. Bianucci, and K. Post. 2009. A new beaked whale (Odontoceti, Ziphiidae) from

the middle Miocene of Peru. Journal of Vertebrate Paleontology 29: 910-922.

Legendre, S. and C. Roth. 1988. Correlation of carnassial tooth size and body weight in recent carnivores (Mammalia). Historical Biology 1: 85–98.

Leibold, M. A., et al. 2004. The metacommunity concept: a framework for multi-scale community ecology. Ecology Letters 7: 601–613.

Leibold, M. A. and M. A. McPeek. 2006. Coexistence of the niche and neutral perspectives in community ecology. Ecology 87: 1399–1410.

Leslie, P. H. and J. C. Gower. 1960. The properties of a stochastic model for the predator–prey type of interaction between two species. Biometrica 47: 219–234.

Levins, R. 1969. Some demographic and genetic consequences of environmental heterogeneity for biological control. Bulletin of the Ecological Society of America 15: 237–240.

Liow, L. H., M. Fortelius, E. Bingham, K. Lintulaakso, H. Mannila, L. Flynn, and N. C. Stenseth. 2008. Higher origination and extinction rates in larger mammals. Proceedings of the National Academy of Science 105: 6097–6102.

Loeuille, N. and M. A. Leibold. 2008. Evolution in metacommunities: on the relative importance of species sorting and monopolization in structuring communities. The American Naturalist 171: 788–799.

Logue, J. B., N. Mouquet, H. Peter, and H. Hillebrand. 2011. Empirical approaches to metacommunities: a review and comparison with theory. Trends in Ecology and Evolution 26: 482–491.

Lomolino, M. V. 1985. Body size of mammals on islands: the island rule reexamined. The American Naturalist 125:310–316.

Long, C. A. 1968. An analysis of patterns of variation in some representative Mammalia. Part I. A review of estimates of variability in selected measurements. Transactions of the Kansas Academy of Science. 71: 201–227.

Loughlin, T. R. and M. A. Perez. 1985. Mammalian Species *Mesoplodon stejnegeri*. American Society of Mammalogists 250:1–6.

Lucas, P., P. Constantino, B. Wood, and B. Lawn. 2008. Dental enamel as a dietary indicator in mammals. BioEssays 30: 374–385.

Lydekker, R. 1894. Contributions to a knowledge of the fossil vertebrates of Argentina. Pages 1–118. Anales del Museo de La Plata, Paleontologia Argentina.

MacFadden, B. J. 1986. Fossil horses from ‘Eohippus’ (Hyracotherium) to Equus: scaling,

Cope's Law, and the evolution of body size. Paleobiology 12: 355–369.

MacFadden, B. J. and R. C. Jr Hulbert. 1988. Explosive speciation at the base of the adaptive radiation of Miocene grazing horses. Nature 336: 466–468.

MacFadden, B. J. 1992. Fossil horses: systematics, paleobiology, and evolution of the family *Equidae*. Cambridge University Press, Cambridge, England.

MacFadden, B. J. and T. E. Ceding. 1994. Fossil horses, carbon isotopes and global change. Trends in Ecology and Evolution 9: 481–486.

MacFadden, B. J. 1998. Equidae. Pages 537-550 in Evolution of tertiary mammals of North America. Eds Janis, C. M., K. S. Scott, L. L. Jacobs. Cambridge University Press, Cambridge.

MacFadden, B. J., N. Solounias, and T. E. Cerling. 1999. Ancient diets, ecology, and extinction of 5-million-year-old horses from Florida. Science 283: 824–827.

MacFadden, B. J. 2001. Three-toed browsing horse *Anchitherium clarencei* from the early Miocene (Hemingfordian) Thomas Farm, Florida. Bulletin of the Florida Museum of Natural History 43: 79–109.

Mackey, R. L. and D. J. Currie. 2001. The diversity–disturbance relationship: is it generally strong and peaked? Ecology 82: 3479–3492.

Madar, S. I. 2007. The postcranial skeleton of early Eocene pakicetid cetaceans. Journal of Paleontology 81: 176-200.

Manger, P. R. 2006. An examination of cetacean brain structure with a novel hypothesis correlating thermogenesis to the evolution of a big brain. Biological Reviews 81: 293-338.

Marino, L., D. W. McShea, and M. D. Uhen. 2004. Origin and evolution of large brains in toothed whales. The Anatomical Record 281:1247–1255.

Marino, L., M. D. Uhen, B. Frohlich, and J. M. Aldag. 2000. Endocranial volume of mid-late Eocene archaeocetes (Order: Cetacea) revealed by computed tomography: implications for cetacean brain evolution. Journal of Mammalian Evolution 7: 81–94.

Marples, B. J. 1956. Cetotheres (Cetacea) from the Oligocene of New Zealand. Journal of Zoology 126: 565-580.

Martin, A. P. and S. R. Palumbi. 1993. Body size, metabolic rate, generation time, and the molecular clock. Proceedings of the National Academy of Science 90: 4087–4091.

Massey, F. J., Jr. 1951. The Kolmogorov-Smirnov test for goodness of fit. Journal of the

American statistical Association, 46: 68-78.

Maurer, B., J. H. Brown, and R. Rusler. 1992. The micro and macro in body size evolution. Evolution 46: 939–953.

Mayfield, M. M. and J. M. Levine. 2010. Opposing effects of competitive exclusion on the phylogenetic structure of communities. Ecology Letters 13: 1085–1093.

Mazin, J.-M., and V. de Buffrénil. 2001. Secondary adaptation of tetrapods to life in water. Proceeding of the International Meeting, Potiers.

Matthiessen, B., and H. Hillebrand. 2006. Dispersal frequency affects local biomass production by controlling local diversity. Ecology Letters 9:652–662.

McNab, B. K. 2009. Resources and energetics determine dinosaur maximal size. Proceedings of the National Academy of Science 106: 12184–12188.

McShea, D. W. 1994. Mechanisms of large-scale evolutionary trends. Evolution 48: 1747–1763.

Mead, J. G., W. A. Walker, and W. J. Houck. 1982. Biological observations on *mesoplodon carlhubbsi* (Cetacea, Ziphiidae). Smithsonian Institution Press, Washington D.C., USA.

Meiri, S. 2008. Evolution and ecology of lizard body sizes. Global Ecology and Biogeography 17: 724–734.

Melbourne, B. A., et al. 2007. Invasion in a heterogeneous world: resistance, coexistence or hostile takeover? Ecology Letters 10: 77–94.

Melbourne, B. A. and A. Hastings. 2008. Extinction risk depends strongly on factors contributing to stochasticity. Nature 454: 100–103.

Melbourne, B. A. 2012. Demographic Stochasticity. Page 848 In A. Hastings and L. Gross, editors. Encyclopedia of Theoretical Ecology. Univ of California Press, California USA.

Mendoza, M., C. M. Janis, and P. Palmquist. 2006. Estimating the body mass of extinct ungulates: a study on the use of multiple regression. Journal of Zoology 270: 90–101.

Miller, A. D., S. H. Roxburgh, and K. Shea. 2011a. How frequency and intensity shape diversity–disturbance relationships. Proceedings of the National Academy of Sciences of the United States of America 108: 5643–5648.

Miller, A. D., S. H. Roxburgh, and K. Shea. 2011b. Timing of disturbance alters competitive outcomes and mechanisms of coexistence in an annual plant model. Theoretical Ecology 5: 419–432.

Mori, A. S., S. Fujii, R. Kitagawa, and D. Koide. 2015. Null model approaches to evaluating the

relative role of different assembly processes in shaping ecological communities. Oecologia 178: 261–273.

Moritz, C., C. N. Meynard, V. Devictor, K. Guizien, C. Labrune, J. M. Guarini, and N. Mouquet. 2013. Disentangling the role of connectivity, environmental filtering, and spatial structure on metacommunity dynamics. Oikos 122: 1401–1410.

Mouquet, N. and M. Loreau. 2003. Community patterns in source-sink metacommunities. The American Naturalist 162: 544–557.

Mouquet, N., P. Munguia, J. M. Kneitel, and T. E. Miller. 2003. Community assembly time and the relationship between local and regional species richness. Oikos 103: 618–626.

Mustoe, G. E. 2002. Eocene bird, reptile, and mammal tracks from the Chuckanut Formation, Northwest Washington. Palaios 17: 403–413.

Myers, J. A. et al. 2013. Beta-diversity in temperate and tropical forests reflects dissimilar mechanisms of community assembly. Ecology Letters 16: 151–157.

Nagorson, D. 1985. Mammalian species *Kogia simus*. American Society of Mammalogists 239: 1–6.

Nee, S. and R. M. May. 1992. Dynamics of metapopulations: habitat destruction and competitive coexistence. Journal of Animal Ecology 61: 37–40.

Newcomer, M. W., T. A. Jefferson, and R. I. Brownell. 1996. Mammalian species *Lissodelphis peronii*. American Society of Mammalogists531: 1–4.

Norman, S. A. and J. G. Mead. 2001. Mammalian species *Mesoplodon europaeus*. American Society of Mammalogists 688: 1–5.

Odling-Smee, F. J., K.N. Laland, and M. W. Feldman. 1996. Niche construction. American Naturalist 147: 641–648.

Ostman, O., S. Drakare, E. S. Kritzberg, S. Langenheder, J. B. Logue, and E. S. Lindström. 2010. Regional invariance among microbial communities. Ecology Letters 13: 118–127.

Owen-Smith, N. 1987. Pleistocene extinctions: the pivotal role of megaherbivores. Paleobiology, 13: 351–362.

Paleobiology Database. 2012. Equidae. Available at: http://paleodb.org/. Last accessed 1 December 2012.

Pearson, O. P. 1948. Metabolism of small mammals, with remarks on the lower limit of mammalian size. Science 108: 44.

Perrin, W. F. 1998. Mammalian species *Stenella longirostris*. American Society of Mammalogists 599: 1–7.

Perrin, W. F. 2002. Mammalian species *Stenella frontalis*. American Society of Mammalogists 702: 1–6.

Perrin, W. F. 2009. Mammalian Species *Stenella attenuata*. American Society of Mammalogists 683:1–8.

Perrin, W. F., B. Wursig, and J. G. Thewissen. 2009. Encyclopedia of marine mammals. Second edition. Elsevier Inc.

Perrin, W. F., G. E. Zubtsova, and A. A. Kuz'min. 2004. Partial catalog of cetacean osteological specimens in Russian museums. NOAA Technical Memorandum NMFS.

Perrin, W. F., J. V. Kashiwada, Southwest Fisheries Center (U.S.). 1989. Catalog of the synoptic collection of marine mammal osteological specimens at the Southwest Fisheries Center. NOAA Technical Memorandum NMFS.

Pesquero, M. D., M. T. Alberdi, and L. Alcala. 2006. New species of Hipparion from La Roma 2 (late Vallesian; Turel, Spain): a study of the morphological and biometric variability of Hipparion Primigenium. Jouranl of Paleontology 80: 343–356.

Peters, R. H. 1986. The ecological implications of body size. Cambridge University Press, Cambridge, England.

Pledge, N. S. 2005. A new species of early Oligocene cetacean from Port Willunga, South Australia. Memoirs of the Queensland Museum 51: 123-133.

Pryor, T., K. Pryor, and K. S. Norris. 1965. Observations on a pygmy killer whale (*Feresa attenuata Gray*) from Hawaii. Journal of Mammalogy 46: 450–461.

Püttker, T., A. de Arruda Bueno, P. I. Prado, and R. Pardini. 2014. Ecological filtering or random extinction? Beta-diversity patterns and the importance of niche-based and neutral processes following habitat loss. Oikos 124: 206–215.

Radinsky, L. B. 1978. Evolution of brain size in carnivores and ungulates. American Naturalist 112: 815–831.

Raup, D. M. 1977. Probabilistic models in evolutionary paleobiology: a random walk through the fossil record produces some surprising results. American Scientist 65: 50–57.

Reeves, R. R., and S. Tracey. 1980. Mammalian species *Monodon monoceros*. The American Society of Mammalogists 127:1–7.

Ridgway, S. H. and R. H. Brownson. 1984. Relative brain sizes and cortical surface areas in

odontocetes. Acta Zool Fennica 172: 149–152.

Robineau, D., R. N. P. Goodall, F. Pichler, and C. S. Baker. 2007. Description of a new subspecies of Commerson's dolphin, *Cephalorhynchus commersonii* (Lacépède, 1804), inhabiting the coastal waters of the Kerguelen Islands. Mammalia 71: 172–180.

Robovský, J. and P. Benda. 2006. Catalogue of the cetaceans (Mammalia: Cetacea) in selected collections of the Czech Republic, with special respect to the collection of the National Museum. Journal of the National Museum, Natural History Series 175: 127–156.

Rocha-Ortega, M. and M. E. Favila. 2013. The recovery of ground ant diversity in secondary Lacandon tropical forests. Journal of Insect Conservation 17: 1161–1167.

Rosindell, J., Hubbell, S. P., He, F., Harmon, L. J., and R. S. Etienne. 2012. The case for ecological neutral theory. Trends in Ecology and Evolution 27: 203-208.

Roxburgh, S. H., K. Shea, and J. B. Wilson. 2004. The intermediate disturbance hypothesis: patch dynamics and mechanisms of species coexistence. Ecology 85: 359–371.

Sachs, R. 1967. Liveweights and body measurements of Serengeti game animals. African Journal of Ecology 5: 24–36.

Sanders, A. E., and L. G. Barnes. 2002. Paleontology of the Late Oligocene Ashley and Chandler Bridge formations of South Carolina, 1: Paleogene pinniped remains; the oldest known seal (Carnivora: Phocidae). Smithsonian Contributions to Paleobiology 93: 179-183.

Scott, R. S. and M. Maga. 2005. Paleoecology of the Akkaşdağı hipparions (Mammalia, Equidae), late Miocene of Turkey. Geodiversitas 27: 809–830.

Secord, R. et al. 2012. Evolution of the earliest horses driven by climate change in the Paleocene-Eocene thermal maximum. Science 335: 959–962.

Sears, A. L. and P. Chesson. 2007. New methods for quantifying the spatial storage effect: an illustration with desert annuals. Ecology 88: 2240–2247.

Segre, H., R. Ron, N. De Malach, Z. Henkin, M. Mandel, and R. Kadmon. 2014. Competitive exclusion, beta diversity, and deterministic vs stochastic drivers of community assembly. Ecology Letters 17: 1400–1408.

Shea, K. and P. Chesson. 2002. Community ecology theory as a framework for biological invasions. Trends in Ecology and Evolution 17: 170–176.

Shoemaker, L. G. and A. Clauset. 2014. Body mass evolution and diversification within horses (family *Equidae*). Ecology Letters 17: 211–220.

Shoemaker, L. G. and B. A. Melbourne. 2016. Linking metacommunity paradigms to spatial coexistence mechanisms. Ecology 97: 2436-2446.

Siepielski, A. M. and M. A. McPeek. 2012. Niche versus neutrality in structuring the beta diversity of damselfly assemblages. Freshwater Biology 58: 758–768.

Silva, M. and J. A. Downing. 1995. Mammalian Body Masses. CRC Press Inc., Boca Raton, USA.

Silva, V. M. and R. C. Best. 1996. Mammalian species *Sotalia fluviatilis*. American Society of Mammalogists 527: 1–7.

Smith, F. A., J. H. Brown, J. Haskell, S. Lyons, J. Alroy, and E. Charnov. 2002. Similarity of mammalian body size across the taxonomic hierarchy and across space and time. American Naturalist 163: 672–691.

Smith, F. A., S. K. Lyons, S. Ernest, and K. E. Jones. 2003. Body mass of late quaternary mammals: Ecological Archives E084-094.

Smith, F. A., S. K. Lyons, S. Ernest, and K. E. Jones. 2007. Macroecological database of mammalian body mass. MOM version.

Smith, F. A. et al. 2010. The evolution of maximum body size of terrestrial mammals. Science 330: 1216–1219.

Smith, F. A. and S. K. Lyons. 2011. How big should a mammal be? A macroecological look at mammalian body size over time and space. Philosophical Transactions of the Royal Society B 366: 2364–2378.

Snyder, R. E. and P. Chesson. 2003. Local dispersal can facilitate coexistence in the presence of permanent spatial heterogeneity. Ecology Letters 6: 301–309.

Snyder, R. E., E. T. Borer, and P. Chesson. 2005. Examining the relative importance of spatial and nonspatial coexistence mechanisms. The American Naturalist 166: E75–E94.

Souza, S. P., S. Siciliano, and S. Cuenca. 2005. A True's beaked whale (*Mesoplodon mirus*) on the coast of Brazil: adding a new beaked whale species to the Western Tropical Atlantic and South America. Latin American Journal of Aquatic Mammals 4: 129–136.

Spoor, F., S. Bajpai, S. T. Hussain, and K. Kumar. 2002. Vestibular evidence for the evolution of aquatic behaviour in early cetaceans. Nature 417: 163-166.

Stacey, P. J. and P. W. Arnold. 1999. Mammalian species *Orcaella brevirostris*. American Society of Mammalogists 616:1–8.

Stacey, P. J., S. Leatherwood, and R. W. Baird. 1994. Mammalian species *Pseudorca crassidens*.

American Society of Mammalogists 456: 1–6.

Stanley, S. M. 1973. An explanation for Cope's rule. Evolution 27: 1–26.

Stegen, J. C., X. Lin, A. E. Konopka, and J. K. Fredrickson. 2012. Stochastic and deterministic assembly processes in subsurface microbial communities. The ISME Journal 6: 1653–1664.

Stegen, J. C. et al. 2013. Stochastic and deterministic drivers of spatial and temporal turnover in breeding bird communities. Global Ecology and Biogeography 22: 202–212.

Stewart, B. E. and R. E. A. Stewart. 1989. Mammalian species *Delphinapterus leucas*. American Society of Mammalogists 333:1–8.

Storer, J. E. and H. N. Bryant. 1993. Biostratigraphy of the cypress hills formation (Eocene to Miocene), Saskatchewan: equid types (Mammalia: Perissodactyla) and associated faunal assemblages. Journal of Paleontology 67: 660–669.

Tanentzap, A. J., W. G. Lee, and K. A. C. Schulz. 2013. Niches drive peaked and positive relationships between diversity and disturbance in natural ecosystems. Ecosphere 4: 1-28.

Thewissen, J. G. M. 1998. The emergence of whales: evolutionary patterns in the origin of cetacea. Springer Science and Business Media. Berlin, Germany.

Thewissen, J. G. M., S. I. Madar, and S. T. Hussain. 1996. *Ambulocetus Natans*, an Eocene Cetacean (Mammalia) from Pakistan. Cour Forschungsinst Senckenb 191: 1-86.

Thewissen, J. G., E. M. Williams, L. J. Roe, and S. T. Hussain. 2001. Skeletons of terrestrial cetaceans and the relationship of whales to artiodactyls. Nature 413: 277–281.

Thewissen, J. and E. M. Williams. 2002. The early radiations of Cetacea (Mammalia): evolutionary pattern and developmental correlations. Annual review of Ecology and Systematics 33: 73–90.

Thewissen, J. and S. Bajpai. 2001. Whale origins as a poster child for macroevolution fossils collected in the last decade document the ways in which Cetacea (whales, dolphins, and porpoises) became aquatic, a transition that is one of the best documented examples of macroevolution in mammals. BioScience 51: 1037-1049.

Thewissen, J., and S. Bajpai. 2009. New skeletal material of Andrewsiphius and Kutchicetus, two Eocene cetaceans from India. Journal of Paleontology. 83: 635-663.

Tilman, D. 1982. Resource competition and community structure. Princeton University Press. Princeton, USA.

Tilman, D. 1994. Competition and biodiversity in spatially structured habitats. Ecology 75: 2–16.

Ting, S., G. J. Bowen, P. L. Koch, W. C. Clyde, Y. Wang, Y. Wang, and M. C. McKenna. 2003. Biostratigraphic, chemostratigraphic, and magnetostratigraphic study across the Paleocene-Eocene boundary in the Hengyang Basin, Hunan, China. Geological Society of America 369: 521–535.

True, F. W. 1907. Remarks on the type of the fossil cetacean *Agorophius pygmaeus* (Müller). Smithsonian Institution. Washington D.C. USA.

True, F. W. 1910. Description of a skull and some vertebrae of the fossil cetacean *Diochoticus vanbenedeni* from Santa Cruz, Patagonia. Bulletin American Museum of Natural History 28: 1–5.

Tucker, C. M., L. G. Shoemaker, K. F. Davies, D. Nemergut, and B. A. Melbourne. 2016. Differentiating between niche and neutral assembly in metacommunities using null models of β-diversity. Oikos 125: 778–789.

Tuomisto, H. 2010. A diversity of beta diversities: straightening up a concept gone awry. Part 1. Defining beta diversity as a function of alpha and gamma diversity. Ecography 33: 2–22.

Turelli, M. 1981. Niche overlap and invasion of competitors in random environments I. Models without demographic stochasticity. Theoretical Population Biology 20: 1–56.

Uhen, M. D. 1996. An evaluation of clade-shape statistics using simulations and extinct families of mammals. Paleobiology 22: 8–22.

Uhen, M. D., R. E. Fordyce, and L. G. Barnes. 1998. Mysticeti. Pages 607–628 In C. M. Janis, G. F. Gunnell, and M. D. Uhen, editors. Evolution of Tertiary Mammals of North America: Volume 2, Small Mammals, Xenarthrans, and Marine Mammals. Cambridge University Press. Cambridge, England.

Uhen, M. D. 2005. A new genus and species of archaeocete whale from Mississippi. Southeastern Geology 43: 157–172.

Uhen, M. D., and N. D. Pyenson. 2007. Diversity estimates, biases, and historiographic effects: resolving cetacean diversity in the Tertiary. Palaeontologia Electronica 10: 1–22.

Uhen, M. D. 2008a. New protocetid whales from Alabama and Mississippi, and a new cetacean clade, Pelagiceti. Journal of Vertebrate Paleontology 28: 589-593.

Uhen, M. D. 2008b. A new xenorophus-likeodontocete cetacean from the oligocene of North Carolina and a discussion of the basal odontocete radiation. Journal of Systematic Palaeontology 6: 433–452.

Uhen, M. D. 2010. The origin(s) of whales. Annual Review of Earth and Planetary Sciences 38: 189–219.

Ulrich, W. and N. Gotelli. 2007. Disentangling community patterns of nestedness and species co-occurrence. Oikos 116: 2053–2061.

Valladares, F. et al. 2008. Unity in diversity: reflections on ecology after the legacy of Ramon Margalef. Fundacion BBVA.

Vellend, M. 2010. Conceptual synthesis in community ecology. The Quarterly Review of Biology 85: 183–206.

Vellend, M. et al. 2014. Assessing the relative importance of neutral stochasticity in ecological communities. Oikos 123: 1420–1430.

Vellend, M. 2016. The theory of ecological communities. Princeton University Press. Princeton, USA.

Volkov, I., J. R. Banavar, S. P. Hubbell, and A. Maritan. 2007. Patterns of relative species abundance in rainforests and coral reefs. Nature 450: 45-49.

Yu, D. W., and H. B. Wilson. 2001. The competition-colonization trade-off is dead; long live the competition-colonization trade-off. The American Naturalist 158: 49–63.

Yu, D. W., H. B. Wilson, and N. E. Pierce. 2001. An empirical model of species coexistence in a spatially structured environment. Ecology 82: 1761–1771.

Wiegand, T., Huth, A., Getzin, S., Wang, X., Hao, Z., Gunatilleke, C. S., and I. N. Gunatilleke. 2012. Testing the independent species' arrangement assertion made by theories of stochastic geometry of biodiversity. Proceedings of the Royal Society B 279: 3312-3320.

Weiher, E. and P.A. Keddy. 1999. Ecological assembly rules: perspectives, advances, retreats. Cambridge University Press. Cambridge, England.

Webb, T. J. 2012. Marine and terrestrial ecology: unifying concepts, revealing differences. Trends in Ecology and Evolution 27: 535–541.

West, G. B., W. H. Woodruff, and J. H. Brown. 2002. Allometric scaling of metabolic rate from molecules and mitochondria to cells and mammals. Proceedings of the National Academy of Science 99: 2473–2478.

White, E. P., M. Ernest, A. J. Kerkhoff, and B. J. Enquist. 2007. Relationships between body size and abundance in ecology. Trends in Ecology and Evolution 22: 323–330.

Whitmore, F. C., and A. E. Sanders. 1976. Review of the Oligocene cetacea. Systematic Biology 25: 304-320.

Wikimedia Foundation. accessed 2016. Wikipedia: The Free Encyclopedia. Wikipedia.

http://en.wikipedia.org/wiki/Wikipedia.

Williams, R. J., A. Anandanadesan, and D. Purves. 2010. The probabilistic niche model reveals the niche structure and role of body size in a complex food web. Plos One 5: e12092.

Zachos, J., M Pagani, L. Sloan, E. Thomas, and K. Billups. 2001. Trends, rhythms, and aberrations in global climate 65 Ma to present. Science 292: 686–693.

Appendix 1

Chapter 2: Derivation of Spatial Coexistence Mechanisms

Local dynamics

Local dynamics of species *j* within patch *x* are Beverton-Holt:

$$N_{t+1,jx} = R_{jx} N_{t,jx} \frac{1}{1+\sum_k \alpha_k N_{t,kx}} \tag{S1}$$

where *k* indexes all of the species, including the focal species *j*.

Growth Rate

Using (S1), the growth rate for a single time step for a given species, *j*, is:

$$\lambda_{jx} = R_{jx} \frac{1}{1+\sum_k \alpha_k N_{t,kx}} . \tag{S2}$$

We now define the competitive term as:

$$C_x = 1 - \frac{1}{1+\sum_k \alpha_k N_{t,kx}} . \tag{S3}$$

In this choice, C_x increases as a function of species' densities, which meets our intuitive relationship between competition and density. In other words, as density in a given patch increases, the effect of competition on growth rate increases as well. Additionally, the effect of competition is zero when densities are zero, as we would intuitively expect.

Using (S3),

$$\lambda_{jx} = R_{jx}(1 - C_x), \tag{S4}$$

which is an exact quadratic form, allowing for an exact solution to our model rather than a quadratic approximation.

Furthermore, we define the effect of environment on fitness as:

$E_{jx} = \frac{R_{jx}}{\overline{R_j}}$, so that the growth rate is

$$\lambda_{jx} = \overline{R_j} E_{jx}(1 - C_x), \tag{S5}$$

where the overbar indicates the spatial average across patches.

Natural Scaling Unit

The natural scaling unit, b_j is the rate that the growth rate for *j* in a patch changes in response to changes in the magnitude of competition (Chesson and Valladares 2008). The natural scaling unit is always positive (Chesson and Valladares 2008).

For our model, we want to choose b_j such that linear terms in $\overline{C}$ disappear when we compare average lambda's across space. This allows us to compare both species on the same scale (i.e. when accounting for intrinsic metacommunity level differences in growth rates). Additionally, we choose b_j such that, since the linear terms in $\overline{C}$ disappear, we can directly solve for each coexistence mechanism, rather than using a quadratic approximation, as is commonly done (Chesson 2000a). For this, we define

$b_j = \overline{R_j}$.

Metacommunity dynamics

We want to know the fitness of species *i* (the invader) at the metacommunity scale, which we will denote $\widetilde{\lambda}_i$ (Chesson 2000a, 2000b). We will here develop a full spatial equation to calculate $\widetilde{\lambda}_i$ scaled by the natural units. Since we want to examine fitness at the community level, we need to compare the scaled values of $\widetilde{\lambda}_i$ (invader) and $\widetilde{\lambda}_r$ (resident), i.e. we want to determine

$$\widetilde{\lambda}_i - \widetilde{\lambda}_r. \tag{S6}$$

For ease of future calculations, we subtract 1 from each fitness in (S6) to achieve:

$$\tilde{\lambda}_i - \tilde{\lambda}_r = \tilde{\lambda}_i - 1 - (\tilde{\lambda}_r - 1). \tag{S7}$$

We then divide both the invader's and resident's growth rates by their natural scaling units (i.e. their intrinsic growth rates) so that we are comparing the invader and resident on the same scale. Thus, we wish to solve:

$$\frac{\tilde{\lambda}_i - 1}{\overline{R}_i} - \frac{\tilde{\lambda}_r - 1}{\overline{R}_r}. \tag{S8}$$

Scaling From Individual Patch Growth Rate to Metacommunity Level

Growth Rate

The fitness at the metacommunity scale is the fitness averaged across all individuals in the metapopulation, that is:

$$\tilde{\lambda}_j = \frac{\bar{N}_{t+1,j}}{\bar{N}_{t,j}} \tag{S9}$$

which follows from the metacommunity scale dynamics given by

$$\sum_x N_{t+1,jx} = \tilde{\lambda}_j \sum_x N_{t,jx} \Rightarrow \bar{N}_{t+1,j} = \tilde{\lambda}_j \bar{N}_{t,j} .$$

The metacommunity scale fitness is related to the average patch level fitness $\bar{\lambda}_i$ in the following way.

$$N_{t+1,jx} = \lambda_{jx} N_{t,jx}$$

$$\begin{aligned} \bar{N}_{t+1,j} &= \overline{\lambda_j N_{t,j}} \\ &= \bar{\lambda}_j \bar{N}_{t,j} + \mathrm{Cov}\left(\lambda_{jx}, N_{t,jx}\right) \end{aligned} \tag{S10}$$

$$\tilde{\lambda}_j = \frac{\bar{N}_{t+1,j}}{\bar{N}_{t,j}} = \bar{\lambda}_j + \mathrm{Cov}\left(\lambda_{jx}, v_{t,jx}\right), \tag{S11}$$

where

$$v_{t,jx} = \frac{N_{t,jx}}{\bar{N}_{t,j}} \tag{S12}$$

is the relative abundance of species *j* in patch *x*.

Derivation: Fitness–density Covariance

We solve (S8) using equation (S11). Thus,

$$\begin{aligned} \frac{\tilde{\lambda}_i - 1}{\overline{R_i}} - \frac{\tilde{\lambda}_r - 1}{\overline{R_r}} &= \frac{\frac{\bar{N}_{t+1,i}}{\bar{N}_{t,i}} - 1}{\overline{R_i}} - \frac{\frac{\bar{N}_{t+1,r}}{\bar{N}_{t,r}} - 1}{\overline{R_r}} \\ &= \frac{\bar{\lambda}_i + \mathrm{Cov}\left(\lambda_{ix}, v_{t,ix}\right) - 1}{\overline{R_i}} - \frac{\bar{\lambda}_r + \mathrm{Cov}\left(\lambda_{rx}, v_{t,rx}\right) - 1}{\overline{R_r}} \\ &= \frac{\bar{\lambda}_i - 1}{\overline{R_i}} - \frac{\bar{\lambda}_r - 1}{\overline{R_r}} + \frac{\mathrm{Cov}\left(\lambda_{ix}, v_{t,ix}\right)}{\overline{R_i}} - \frac{\mathrm{Cov}\left(\lambda_{rx}, v_{t,rx}\right)}{\overline{R_r}} \end{aligned} \tag{S13}$$

where

$$\frac{\mathrm{Cov}\left(\lambda_{ix}, v_{t,ix}\right)}{\overline{R_i}} - \frac{\mathrm{Cov}\left(\lambda_{rx}, v_{t,rx}\right)}{\overline{R_r}} \tag{S14}$$

is a comparison of the fitness–density covariance between invader and resident and quantifies the fitness–density covariance mechanism.

To generalize our model for more than one resident species (i.e. more than two species present in the community) (S14) would be modified as follows:

$$\frac{\mathrm{Cov}(\lambda_{ix}, v_{t,ix})}{\overline{R_i}} - \left\langle \frac{\mathrm{Cov}(\lambda_{rx}, v_{t,rx})}{\overline{R_r}} \right\rangle, \tag{S15}$$

where $\langle x \rangle$ indicates an average across all resident species.

Derivation: Storage Effect

We will now continue by parsing $\frac{\overline{\lambda_i} - 1}{\overline{R_i}} - \frac{\overline{\lambda_r} - 1}{\overline{R_r}}$ to find the other spatial components for our model. First, we compare the lambda values of the invader and resident:

$$\begin{aligned} \frac{\lambda_{ix} - 1}{\overline{R_i}} - \frac{\lambda_{rx} - 1}{\overline{R_r}} &= \frac{\overline{R_i} E_{ix}(1 - C_x) - 1}{\overline{R_i}} - \frac{\overline{R_r} E_{rx}(1 - C_x) - 1}{\overline{R_r}} \\ &= E_{ix}(1 - C_x) - \frac{1}{\overline{R_i}} - E_{rx}(1 - C_x) + \frac{1}{\overline{R_r}} \\ &= \frac{1}{\overline{R_r}} - \frac{1}{\overline{R_i}} + (E_{ix} - E_{rx})(1 - C_x) \end{aligned} \tag{S16}$$

Now, taking (S16) and averaging in space:

$$\begin{aligned}\frac{\bar{\lambda}_i - 1}{\bar{R}_i} - \frac{\bar{\lambda}_r - 1}{\bar{R}_r} &= \frac{\overline{\bar{R}_i E_{ix}(1-C_x)} - 1}{\bar{R}_i} - \frac{\overline{\bar{R}_r E_{rx}(1-C_x)} - 1}{\bar{R}_r} \\ &= \frac{1}{\bar{R}_r} - \frac{1}{\bar{R}_i} + \overline{E_i(1-C_x)} - \overline{E_r(1-C_x)} \\ &= \frac{1}{\bar{R}_r} - \frac{1}{\bar{R}_i} + \bar{E}_i \cdot \overline{(1-C_x)} + \mathrm{Cov}(E_{ix}, (1-C_x)) - (\bar{E}_r \cdot \overline{(1-C_x)} + \mathrm{Cov}(E_{rx}, (1-C_x))) \\ &= \frac{1}{\bar{R}_r} - \frac{1}{\bar{R}_i} + (\bar{E}_i - \bar{E}_r) \cdot \overline{(1-C_x)} + \mathrm{Cov}((E_{ix} - E_{rx}), (1-C_x)).\end{aligned} \tag{S17}$$

From here, recall $E_{jx} = \frac{R_{jx}}{\bar{R}_j}$, which we use to simplify (S17) as follows:

$$\begin{aligned}\frac{\bar{\lambda}_i - 1}{\bar{R}_i} - \frac{\bar{\lambda}_r - 1}{\bar{R}_r} &= \frac{1}{\bar{R}_r} - \frac{1}{\bar{R}_i} + (\frac{\bar{R}_i}{\bar{R}_i} - \frac{\bar{R}_r}{\bar{R}_r})\overline{(1-C_x)} + \mathrm{Cov}((E_{ix} - E_{rx}), (1-C_x)) \\ &= \frac{1}{\bar{R}_r} - \frac{1}{\bar{R}_i} + 0 \cdot \overline{(1-C_x)} + \mathrm{Cov}((E_{ix} - E_{rx}), (1-C_x))\end{aligned} \tag{S18}$$

showing that there is no nonlinear competitive variance for this model, since $\overline{(1-C_x)}$ is multiplied by zero.

We can further simplify (S18), and find

$$\begin{aligned}\frac{\bar{\lambda}_i - 1}{\bar{R}_i} - \frac{\bar{\lambda}_r - 1}{\bar{R}_r} &= \frac{1}{\bar{R}_r} - \frac{1}{\bar{R}_i} + \mathrm{Cov}((E_{ix} - E_{rx}), (1-C_x)) \\ &= \frac{1}{\bar{R}_r} - \frac{1}{\bar{R}_i} + \mathrm{Cov}((E_{ix} - E_{rx}), 1) + \mathrm{Cov}((E_{ix} - E_{rx}), -C_x) \\ &= \frac{1}{\bar{R}_r} - \frac{1}{\bar{R}_i} - \mathrm{Cov}((E_{ix} - E_{rx}), C_x)\end{aligned} \tag{S19}$$

where

$$-\mathrm{Cov}((E_{ix} - E_{rx}), C_x) \tag{S20}$$

quantifies the spatial storage-effect mechanism.

Furthermore

$$\frac{1}{\overline{\overline{R_r}}} - \frac{1}{\overline{\overline{R_i}}} \tag{S21}$$

quantifies the non-spatial fitness mechanism.

The derivation above follows Chesson and Valladares (2008). It is possible to verify the results and directly calculate Chesson's γ_j, the sub-additivity term of the effects of the environment and competition on growth rate (Chesson 2000a), by taking the cross partial derivative of λ_{jx}in E_{jx} and C_{jx}. This yields $\gamma_j = -\overline{R_J}$, so $\frac{\gamma_j}{b_j} = -1$, as we find above.

To generalize (S18) to more than two species, i.e., more than one resident species, (S18) becomes instead:

$$\begin{aligned}\frac{\lambda_i - 1}{\overline{R_\iota}} - \frac{\lambda_r - 1}{\overline{R_r}} &= \langle\frac{1}{\overline{\overline{R_r}}}\rangle - \frac{1}{\overline{R_\iota}} + \mathrm{Cov}(E_{ix}, 1 - C_{ix}) - \langle\mathrm{Cov}(E_{rx}, 1 - C_{rx})\rangle \\ &= \langle\tfrac{1}{\overline{\overline{R_r}}}\rangle - \tfrac{1}{\overline{R_\iota}} + \mathrm{Cov}(E_{ix}, 1 - C_{ix}) - \mathrm{Cov}(\langle E_{rx}\rangle, 1 - C_{rx}).\end{aligned} \tag{S22}$$

Then, since for our model, $C_{ix} = C_{rx}$ we can simplify further:

$$= \langle\frac{1}{\overline{\overline{R_r}}}\rangle - \frac{1}{\overline{R_\iota}} + \mathrm{Cov}(E_{ix} - \langle E_{rx}\rangle, 1 - C_x)$$

$$= \langle\frac{1}{\overline{\overline{R_r}}}\rangle - \frac{1}{\overline{R_\iota}} + \mathrm{Cov}(E_{ix} - \langle E_{rx}\rangle, -C_x)$$

$$= \langle \frac{1}{\overline{R_r}} \rangle - \frac{1}{\overline{R_i}} - \mathrm{Cov}(E_{ix} - \langle E_{rx} \rangle, C_X) \tag{S23}$$

where

$$-\mathrm{Cov}(E_{ix} - \langle E_{rx} \rangle, C_X) \tag{S24}$$

is the spatial storage effect and

$$\langle \frac{1}{\overline{R_r}} \rangle - \frac{1}{\overline{R_i}} \tag{S25}$$

is the non-spatial fitness.

Thus, taken together we combine (S14), (S20), and (S21) to find that the metacommunity spatial coexistence mechanisms for a two species system are:

$$\frac{\tilde{\lambda}_i - 1}{\overline{R_i}} - \frac{\tilde{\lambda}_r - 1}{\overline{R_r}} = \underbrace{\frac{1}{\overline{R_r}} - \frac{1}{\overline{R_i}}}_{\substack{\text{non-spatial} \\ \text{fitness}}} - \underbrace{\mathrm{Cov}((E_{ix} - E_{rx}), C_x)}_{\substack{\text{storage} \\ \text{effect}}} + \underbrace{\frac{\mathrm{Cov}\left(\lambda_{ix}, v_{t,ix}\right)}{\overline{R_i}} - \frac{\mathrm{Cov}\left(\lambda_{rx}, v_{t,rx}\right)}{\overline{R_r}}}_{\substack{\text{fitness-density} \\ \text{covariance}}}. \tag{S26}$$

For the general case of an arbitrary number of species, the metacommunity spatial coexistence mechanisms are:

$$\langle \frac{1}{\overline{R_r}} \rangle - \frac{1}{\overline{R_i}} - \mathrm{Cov}(E_{ix} - \langle E_{rx} \rangle, C_X) + \frac{\mathrm{Cov}(\lambda_{ix}, v_{t,ix})}{\overline{R_i}} - \langle \frac{\mathrm{Cov}(\lambda_{rx}, v_{t,rx})}{\overline{R_r}} \rangle \tag{S27}$$

where

$$\langle \frac{1}{\overline{R_r}} \rangle - \frac{1}{\overline{R_i}} \tag{S28}$$

is the non-spatial fitness,

$$\mathrm{Cov}(E_{ix} - \langle E_{rx} \rangle, C_X) \tag{S29}$$

is the storage effect,

$$\frac{\mathrm{Cov}(\lambda_{ix}, v_{t,ix})}{\overline{R_i}} - \langle \frac{\mathrm{Cov}(\lambda_{rx}, v_{t,rx})}{\overline{R_r}} \rangle \tag{S30}$$

is the fitness–density covariance and there is no non-linear competitive variance.

Appendix 2

Chapter 3: Effect of dispersal on beta-diversity metrics

Local dispersal results

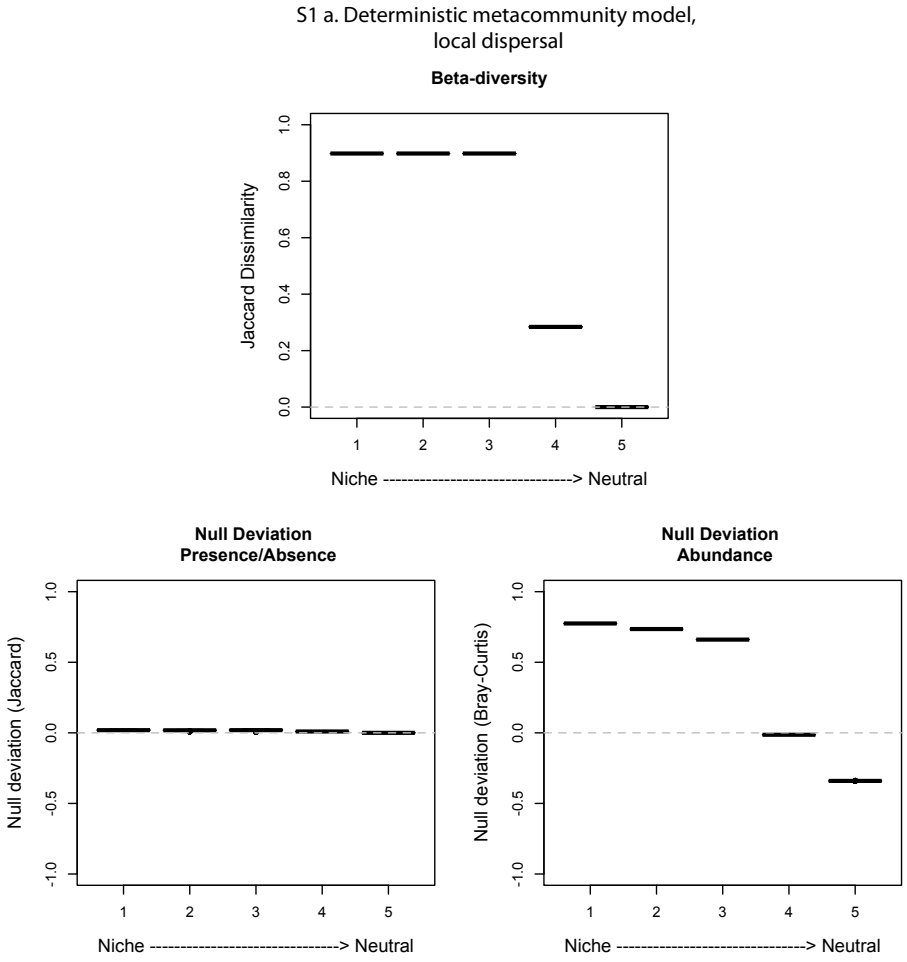

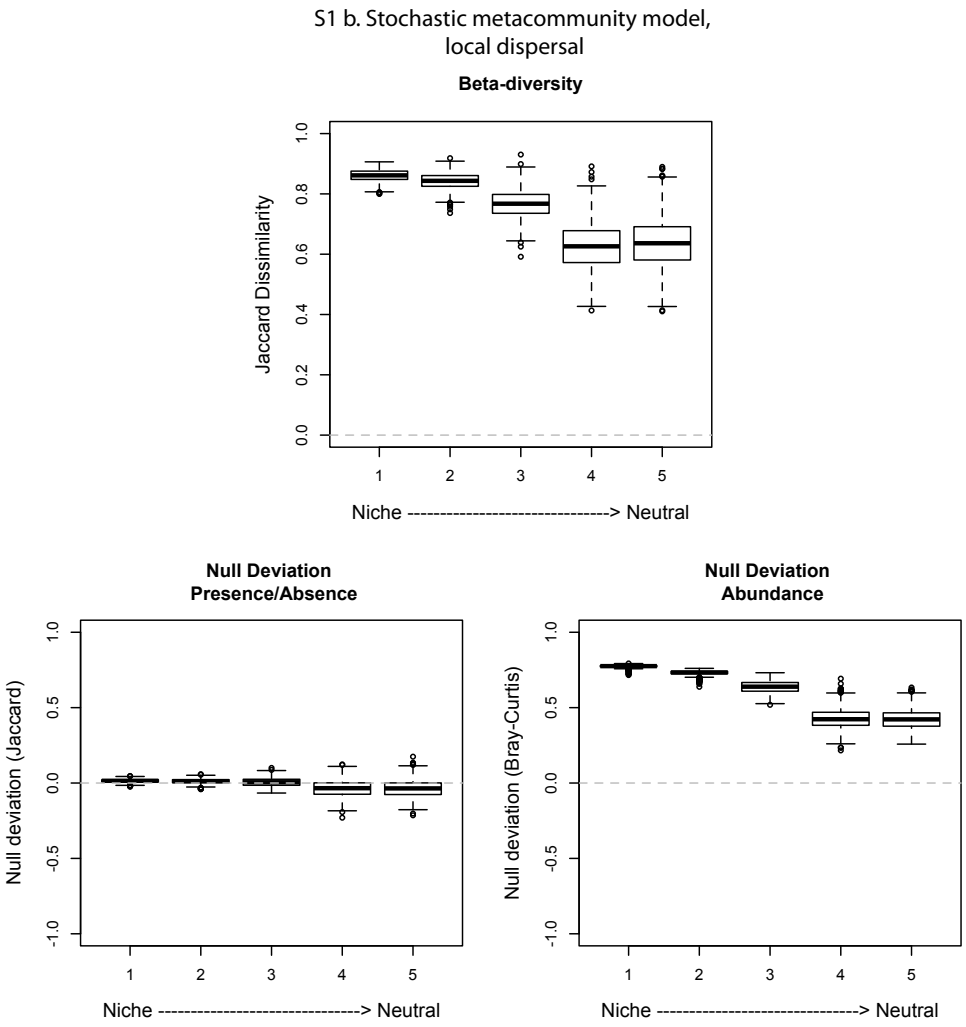

Figure S1 Null deviation results from simulations of deterministic and stochastic metacommunity models with local dispersal for 5 community types. β-diversity presence/absence, and abundance β-null deviation values for A) deterministic metacommunity models and B) stochastic metacommunity models. Results for both metacommunity types are shown for each of metacommunity types 1-5, and represent 50 replicates (see *Methods*).

Variation in dispersal rates

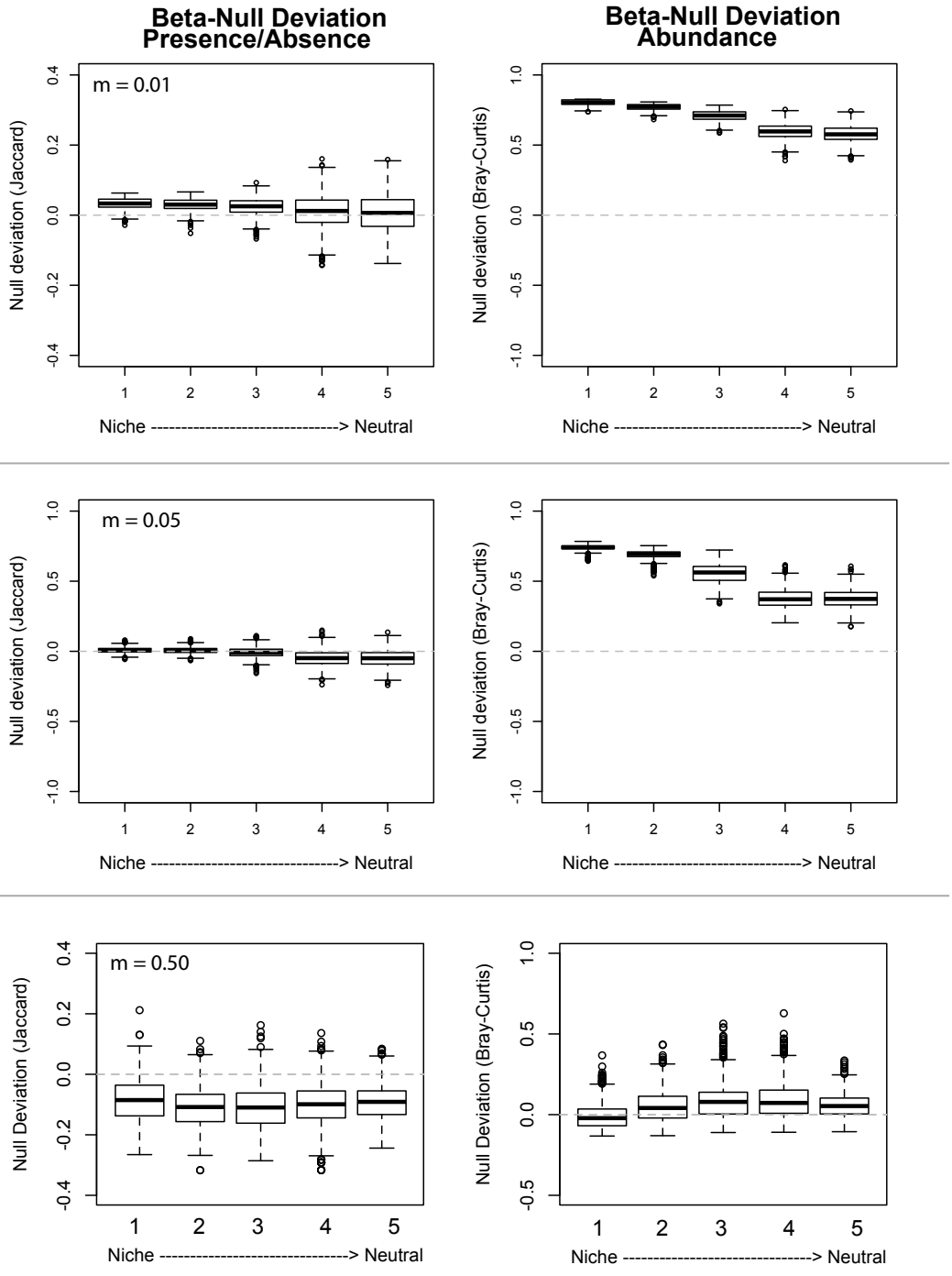

Figure S2 Comparison of the effect of dispersal rate (*m*) on β-null deviation values from simulated metacommunity models, for 5 assembly types representing a gradient from niche to neutral. Subplots show β-diversity (Jaccard), presence/absence β-null deviation values, and abundance β-null deviation values for stochastic metacommunity models. Results represent 50 replicate metacommunities. Note that y-axes differ for presence/absence and abundance β-null deviation results.

Appendix 3

Chapter 4: Equidae Data Collection and Data Consistency

Data Collection Methods

Species names and durations were derived from the list of all Equidae species contained within the Paleobiology Database (Paleobiology Database, 2012). Using the mass estimation methods described below, we estimated body sizes for 225 (91%) of these 246 known species.

Estimation method 1: All independent estimates of species body size from the literature were included without modification. If multiple estimates were found in the literature, these were averaged together.

Estimation method 2: MacFadden's estimating technique for Equidae body size (MacFadden, 1986). For all species with upper molar measurements, we multiplied reported upper molar length (mm) by width (mm), to find upper first molar area *m* (in mm^2). Following (MacFadden, 1986), head-body length (mm) *L*, was related to upper first molar area by $L = 2{:}49m + 579{:}38$ $(r^2 = 0.99)$, estimated via maximum likelihood from extant data. We then convert head-body length *L* measurements or estimates into a species body mass *M* using MacFadden's exponential model (MacFadden, 1986), $\ln M = 0.00158L + 2.21$ $(r^2 = 0.92)$.

Estimation method 3: Modifying the second method, we used a similar concept for our third estimation method of body size. Lower first molar area was calculated as lower first molar length (mm) multiplied by width (mm). We then converted lower first molar measurements into head-body length estimates yielding $L = 4.22m + 666.3$ $(r^2 = 0.93)$. This model was estimated using the dataset of lower molar measurements and body size estimates from methods one or two (see Figure S3). The linear model was then utilized for all species with lower first molar

measurements.

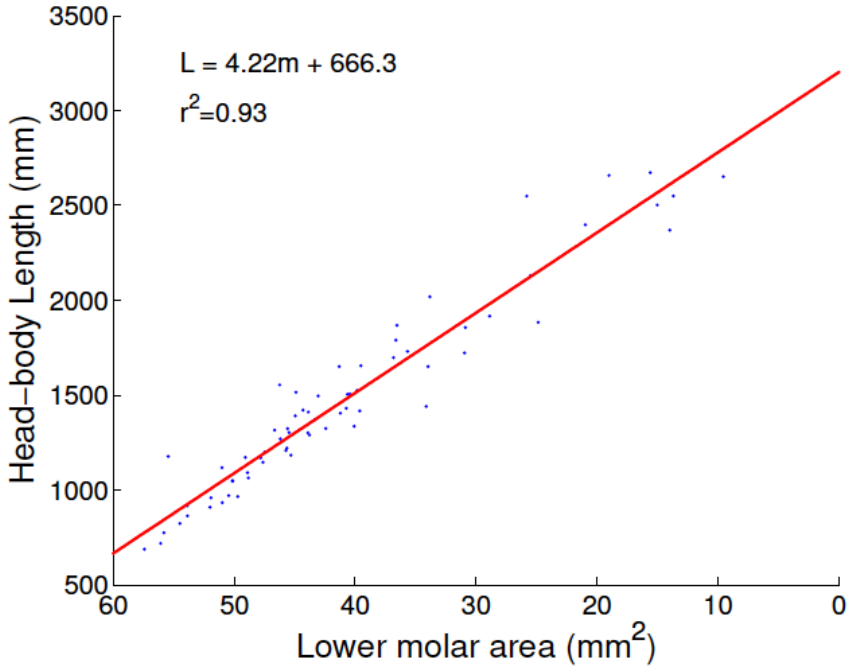

Figure S3 Linear model for converting lower first molar measurements into head-body length estimates. Model is fit to data where lower molar measurements and body size estimates from methods one or two are available.

Combining multiple estimates: If multiple estimates were produced for a single species from method one, two, or three, we averaged the estimates from each for a single body mass average for each species. Together, these methods produced estimates for 152 species (62%).

Estimation method 4: This method was only utilized for species lacking specific body mass estimates from the above methods (73 species), but for whom a genus-level size range was available. In some case, several species in the same genus were known, but no size estimates were available for them. Size estimates for such species can thus be derived from the size ranges, but we note that such estimates should not be considered as accurate as estimates derived from

other three methods.

To assign a rough size estimate to such a species, we first aligned a Normal distribution to the genus-level size range, placing the 5 and 95% quantiles at the reported lower and upper values. We then drew a random value from the fitted Normal distribution for each species in the genus without a size estimate.

Notably, these species include none of the maximum sizes in our study, which are the main focus of our analysis. Including estimates derived via this method provides (i) a more reliable estimate of minimum size through time, which is more susceptible to biases within the fossil record, and (ii) a more complete picture of the Equidae body mass distribution that would be presented if this information were excluded.

Data consistency

We test for potential bias in our fossil data, e.g., due to sampling effects (Foote and Sepkoski, 1999), by comparing the observed species counts over time with a range derived from a non-parametric estimate. This estimate is produced by first smoothing the genus counts via an exponential kernel and then multiplying by 0.5 and 1.5 times the average number of species per genus. The resulting envelope—lower and upper estimated species counts—agrees well with the observed counts, suggesting reasonably even sampling rates across time and taxonomic level.

We test the assumption of a stationary size-variation mechanism by comparing the estimated strength of Cope's rule in pre- and post-diversification periods. Here, we use the modern, species-level definition of Cope's rule (Alroy, 1998), the average change in size from ancestor to descendent species, which is equivalent to v (see Eq. 4.1). Using Alroy's method

(Alroy, 1998), we estimate v among all species whose durations intersect the pre- and post-diversification period, and for the entire study period. The corresponding estimates are $\nu_{pre} \approx 0.103$, $\nu_{post} \approx 0.117$, and $\nu_{avg} \approx 0.112$ which are statistically indistinguishable (ANOVA, $p = 0.14$) and span the estimated value for all terrestrial mammals, $v = 0.109$ (Clauset and Redner, 2009), in agreement with a stationary size-variation mechanism.

Appendix 4

Chapter 5: Supplementary Materials and Methods

Data Collection

To compare within-clade body mass distributions between terrestrial and marine environments, we first constructed a novel database of extinct and extant cetacean body mass measurements. To do so, we downloaded a complete list of all known cetacean species (56 million years ago to present) from the Paleobiology Database. Body mass was estimated for extinct cetacean species using the allometric scaling relationship $y = kx^a$ (Huxley 1932), derived from 78 extant cetaceans. When expressed using a log-log scale, this is equivalent to $\log y = a \log x + \log k$, where y is estimated body mass (g) and x is the skeletal measurement (m). We estimated body mass (g) from body length (Figure S4), condylobasal length (i.e. skull length, measured from the anterior premaxilla points to the occipital condyles' posterior surface; Figure S5), and occipital condyle width (the width of rounded nodes on the occipital bone, forming a joint with the first cervical vertebra; Figure S6). These measurements are most commonly reported for cetaceans, and thus provided a large enough sample size for allometric scaling. All skeletal measurements and body mass estimates were collected from the primary literature and the Paleobiology Database (Huxley 1864, Cope 1867, 1890, Lydekker 1894, True 1907, 1910, Allen 1921, Kellogg 1923, 1924, 1925, Cabrera 1926, Kellogg 1928, 1929, 1936, Benham 1937, Barwick 1939, Marples 1956, Kellogg 1957, 1965, Pryor et al. 1965, Kellogg 1966, Long 1968, Kellogg 1968, Brownell and Herald 1972, Brownell 1975, Czyzewska and Ryziewicz 1976, Whitmore and Sanders 1976, Barnes 1976, Aslanova 1977, Reeves and Tracey 1980, Gingerich and Russell 1981, Demere and Cerutti 1982, Mead et al. 1982, Brownell 1983,

Barnes 1984, Ridgway and Brownson 1984, Brownell and R 1984, Barnes 1985a, 1985b, Barnes et al. 1985, Nagorson 1985, Loughlin and Perez 1985, Demere 1986, Heyning and Dahlheim 1988, Perrin et al. 1989, Stewart and Stewart 1989, Gingerich et al. 1990, Amano et al. 1992, Jefferson et al. 1993, Best and Silva 1993, Jefferson and Newcomer 1993, Gingerich et al. 1994, Hirota and Barnes 1994, Ichishima et al. 1994, Jefferson and Newcomer 1994, Stacey et al. 1994, Gingerich et al. 1995, Dawson 1996, Gingerich and Uhen 1996, Thewissen et al. 1996, Uhen 1996, Silva and Best 1996, Newcomer et al. 1996, Gingerich et al. 1997, Jefferson and Barros 1997, Uhen et al. 1998, Jefferson 1998, Perrin 1998, Thewissen 1998, Bajpai and Gingerich 1998, Clapham and Mead 1999, Cranford 1999, de Muizon et al. 1999, Archer and Perrin 1999, Stacey and Arnold 1999, Ichishima and Kimura 2000, Marino et al. 2000, Bajpai and Johannes 2000, Bianucci 2001, Mazin and de Buffrénil 2001, Thewissen and Bajpai 2001, Gingerich 2001, Thewissen et al. 2001, Jefferson and Karczmarski 2001, Norman and Mead 2001, Bianucci and Landini 2002, de Muizon et al. 2002, Fordyce 2002, Fordyce et al. 2002, Kimura and Ozawa 2002, Sanders and Barnes 2002, Spoor et al. 2002, Thewissen and Williams 2002, Emry 2002, Perrin 2002, Dalebout et al. 2003, Fordyce 2003, Smith et al. 2003, Jefferson and Curry 2003, Bilal and Bamy 2004, Culik et al. 2004, Dooley et al. 2004, Marino et al. 2004, Perrin et al. 2004, Jefferson and Hung 2004, Bisconti 2005, Dooley 2005, Gingerich et al. 2005, Ichishima and Kimura 2005, Kazár and Grigorescu 2005, Lambert 2005a, 2005b, Pledge 2005, Souza et al. 2005, Uhen 2005, Bianucci and Landini 2006, Bisconti 2006, Bouetel and de Muizon 2006, Hampe 2006, Lambert and Louwye 2006, Berta et al. 2006, Manger 2006, Borsa 2006, Henry-Stamper 2006, Fitzgerald 2006, Bianucci et al. 2007, Buchholtz 2007, Fuller and Godfrey 2007, Madar 2007, Demere and Berta 2008, Godfrey and Barnes 2008, Lambert 2008, Uhen 2008a, 2008b, Lambert et al. 2008, Bisconti 2008, 2009, Gutstein et al. 2009, Lambert et

al. 2009, Perrin et al. 2009, Thewissen and Bajpai 2009, Gingerich et al. 2009, Berta and Demere 2009, Perrin 2009, Godfrey 2009, Fitzgerald 2009, Robineau et al. 2007, Robovský and Benda. 2006, Wikimedia Foundation). When a range in sizes or measurements were found, we used the midpoint of the range for our estimates, and we used all combinations of the three measurements when possible, such that no data was excluded (Table S1). For all allometric models, R^2 ranged between 0.82 and 0.97. This provided estimated body mass measurements for 214 of the known 403 extinct cetaceans (53% coverage), spanning from 56 million years ago to present, yielding the most comprehensive database of cetacean sizes through time to date.

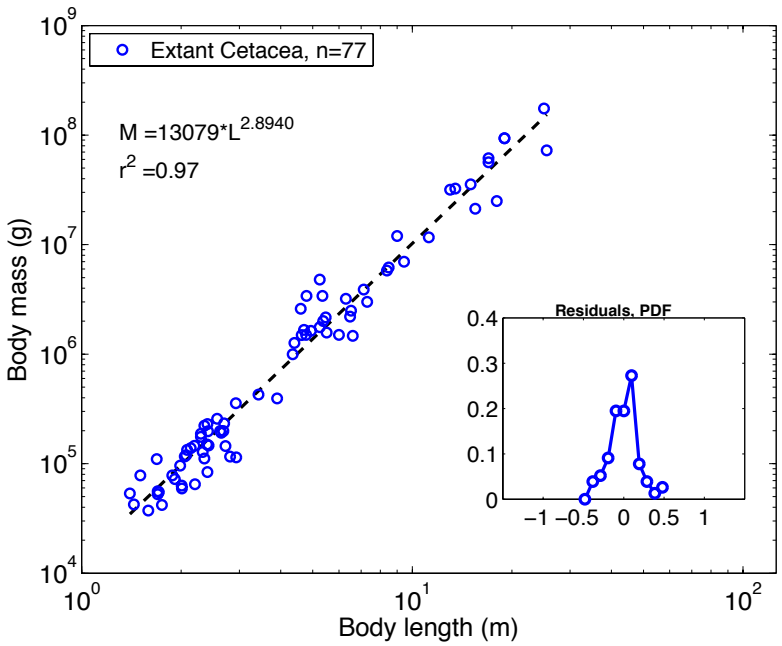

Figure S4 Allometric scaling model from body length to body mass.

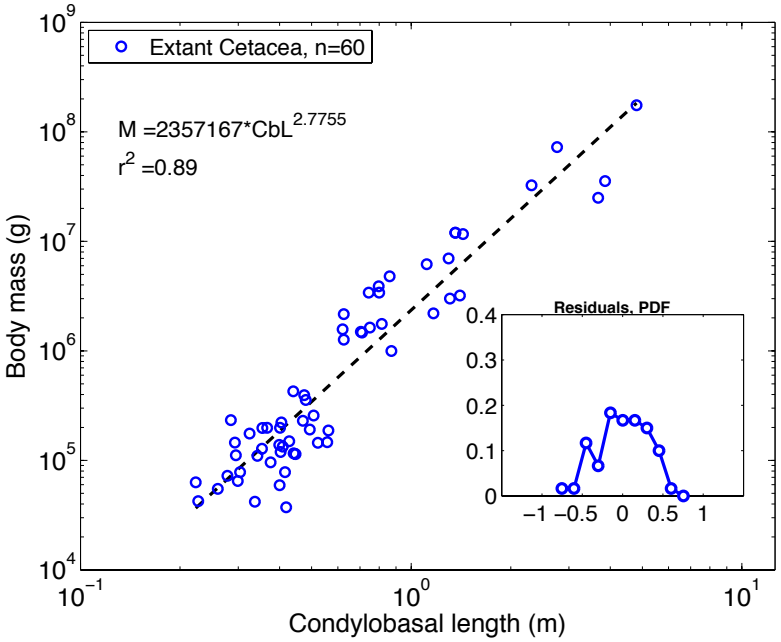

Figure S5 Allometric scaling model from condylobasal length to body mass.

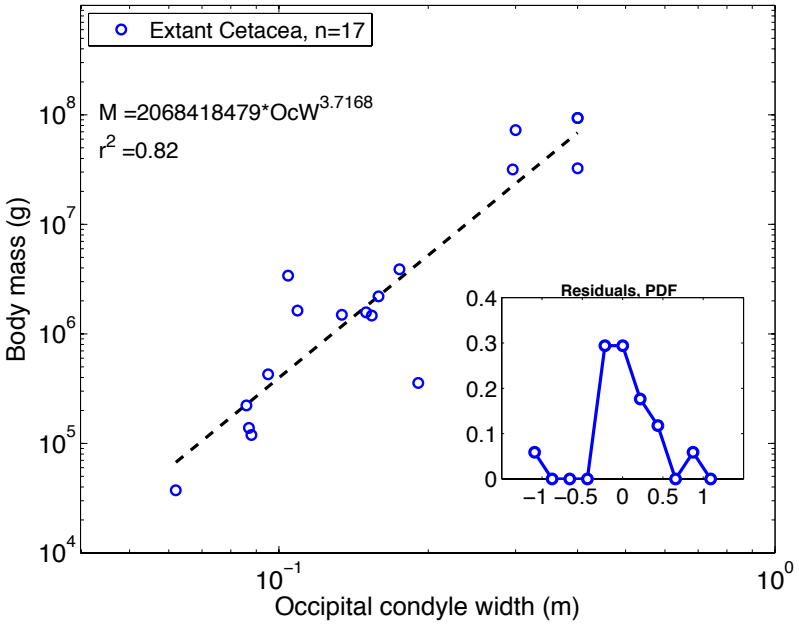

Figure S6 Allometric scaling model from occipital condyle width to body mass.

Model	Allometric Equation	R^2	Sample size (n)
OcW and L	$M = 52839L^{2.5637}OcW^{0.4190}$	0.97	17
CbL and L	$M = 24506L^{2.5355}CbL^{0.3481}$	0.96	60
CbL and OcW	$M = 17958136CbL^{2.4932}OcW^{0.9523}$	0.90	15
L and CbL and OcW	$M = 47.98L^{2.3768}CbL^{0.2718}OcW^{0.2027}$	0.97	15

Table S1 Allometric scaling for combined models.

M is mass, L is length, OcW is occipital condyle width, and CbL is condylobasal length. All skeletal measurements are in meters and body mass is in grams.

The terrestrial mammalian database includes both first and last appearance and estimated body mass for extinct species (Clauset and Redner 2009) and body mass for extant species (Smith et al. 2003, 2007). Combining three previous datasets (Smith et al. 2003, 2007, Clauset and Redner 2009) yielded 4,002 extant terrestrial mammals and 2,034 extinct North American species.

Diversity Through Time

To calculate our cetacean database's coverage through time, we assume that, on average, there are a uniform number of species per family through time. We estimated the number of species expected at each 1 million year increment as the number of known families multiplied by the number of species per family. As family is a higher taxonomic class, our estimate of family diversity is less likely to be prone to biases in the fossil record. Our database has high coverage of the estimated total number of cetaceans during most of the Eocene and the mid-Miocene to present (Figure S7), and low coverage of species from the Eocene/Oligocene transition into the

Oligocene/Miocene transition. Low coverage is due to a paucity of fossils from the late Eocoene and Oligocene. The Eocene/Oligocene transition experienced a drop in sea level that likely prevented cetacean fossil deposition and destroyed fossils via erosion, causing a underrepresentation of cetacean species in the fossil record for this time period (Fordyce 2003, Uhen and Pyenson 2007, Uhen 2010), consistent across the literature as well as our database.

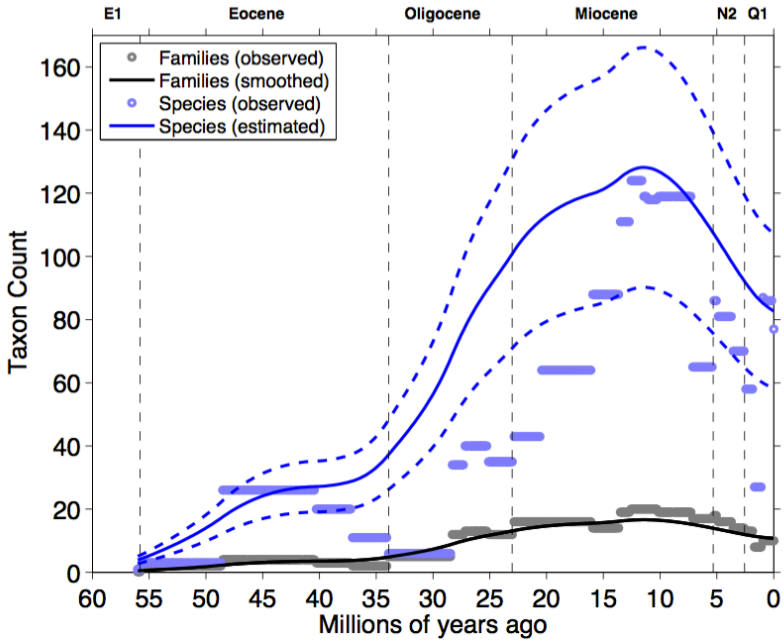

Figure S7 Cetacean taxon count from 55 million years to present.

The black solid line shows the estimated number of families; grey shows observed number of families. Blue lines are the expected number of species through time and light blue is the observed number of species in our dataset.

Modeling Body Mass Evolution Through Time

We estimated body mass distributions, and the relative density of body sizes through time, using a convection-diffusion-reaction model that follows a branching multiplicative

diffusion process of cladogenesis, constrained by three well-documented mechanisms: a clade-specific minimum size, M_{min}, Cope's rule, and size dependent extinction risk. Following (Clauset et al. 2009), we fit the steady state version of the model to the extant marine and terrestrial body mass distributions, while the time-dependent evolving model was subsequently compared to fossil estimates of body mass distributions over the past 100 million years (terrestrial) and 56 million years (marine) respectively. A full model description can be found in (Clauset and Redner 2009, Clauset et al. 2009). Here, we provide an overview of the analytical model that allows for mathematical analyses without relying on simulations.

Model Description

Let $c(x,t)$ denote the fraction, or density, of observed species with mass $x = ln\ M$ at a given time, t. Each species with a given mass, M, produces descendants according to a branching, multiplicative process through time. A given descendant's mass, M_D depends on its ancestor's mass such that $M_D = \lambda M_A$, where M is mass of the descendent (D) or ancestor (A) and λ is a random variable. The strength of Cope's rule, which is estimated independently of the model (see Estimating Cope's Rule, below), is $\langle ln\ \lambda \rangle$, where the brackets denote the mean value.

The number of descendant species produced is proportional to species' density, $c(x,t)$, as is the size-dependent extinction probability, $p(x)$. Here, the probability that a species goes extinct is represented as a loss term proportional to $c(x,t)$, but with a weak linear dependence on the species' mass, such that $p(x) = A + Bx$. The value of $c(x,t)$ is then modeled using a modified form of the standard convection-diffusion-reaction equation (Krapivsky et al. 2010):

$$\frac{\partial c}{\partial t} + v\frac{\partial c}{\partial x} = D\frac{\partial^2 c}{\partial x^2} + (k - A - Bx)c \quad (1).$$

On the left-hand side, the first term, $\frac{\partial c}{\partial t}$, models the density's time dynamics, while the second, $v\frac{\partial c}{\partial x}$, models the average change in size from ancestor to descendant. This change, Cope's rule, is represented by $v = \langle ln\ \lambda \rangle$ where λ is a random variable denoting bias towards either larger (positive values of λ) or smaller (negative values of λ) descendant body sizes compared to ancestors. On the right hand side of the equation, the first term, $D\frac{\partial^2 c}{\partial x^2}$, models the impact of the variability in size changes from ancestor to descendant, which is quantified by $D = \langle (ln\ \lambda)^2 \rangle$. The second term on the right hand side, $(k - A - Bx)c$, models changes in density of species that occurs from extinction and speciation events. Here, k denotes the mean speciation rate, A the background or size-independent extinction rate, and B quantifies the increase in extinction rate with body size. We normalize these parameters by the variance of size change to define: $\beta = B/D$, $\mu = v/D$, and $\alpha = (k - A)/D$, and require that the density go through zero at the minimum viable size, x_{min}.

After substituting the eigenfunction expansion $c(x,t) = \sum_i A_i C_i(x) e^{-\gamma_i t}$ in equation (1), the time-dependent solution is the sum of eigenmodes:

$$c(x,t) = \sum_i C_i(x_0) C_i(x) e^{-\gamma_i t} \qquad (2)$$

where each eigenmode $C_i(x) \propto e^{\frac{\mu x}{2}} Ai[\beta^{\frac{1}{3}}(x - x_{min}) + z_0 - \gamma_i / D\beta^{2/3}]$. Here, $x_0 = ln\ M_0$ is the size of the founder species, Ai[.] is the Airy functions, γ_i denotes the decay rate for the ith eigenmode of the series, and $z_0 = -2.3381$ is the location of the Airy zero (Clauset and Redner 2009) . The steady state solution for the species mass distribution is

$$c(x) \propto e^{\frac{\mu x}{2}} Ai[\beta^{\frac{1}{3}}(x - x_{min}) + z_0 \qquad (3).$$

Furthermore, we estimate the expected maximum species size, M_*, for n species as

$$\int_{\ln M_*}^{\infty} c(x)dx = 1/n \quad (4),$$

i.e. where the complementary cumulative distribution function crosses the horizontal line *1/n*. This yields predictions of increasing maximum observed size for a fixed distribution and increasing *n*, as well as for fixed *n* and a distribution with a lengthening right tail via diffusion.

Estimating Minimum Size

A minimum viable size is the result of metabolic constraints for maintaining body temperature in endotherms. We estimated the minimum viable size for both marine and terrestrial clades from a combination of empirical data and previous theoretical work—independent of the body mass evolution model described above. For terrestrial mammals, the empirically observed lower limit on body size is $x_{min} \cong 2$ g, matching the size of the bumblebee bat (C*raseonycteris thonglongyai*), Etruscan shrew (*Suncus etruscus*), and Remy's pygmy shrew (*Suncus remyi*). This lower limit is further supported by metabolic scaling theory, which suggests that the smallest mass of a terrestrial mammal is approximately 1 g (West et al. 2002). Finally, this limit appears constant in terrestrial mammals since at least the Cretaceous-Tertiary (K-T) boundary (Smith et al. 2003, 2007).

We estimated marine mammal minimum size as $x_{min} \cong 6.8$ kg, as heat loss in water is over 90 times higher than in air. This matches the newborn weight (7 – 9 kg) of the smallest marine mammal, the La Plata dolphin (*Pontoporia blainvillei*). This lower limit is further supported by theoretical calculations where endothermic heat production is balanced by convection and conductive heat loss (6.8 – 10 kg), below which an individual would be too small to generate sufficient heat to compensate for heat loss to water (Downhower and Blumer 1988, Ahlborn 1999, 2000).

Estimating Cope's Rule

Following the methods of (Alroy 1998), we estimated Cope's Rule as the average multiplicative change in body mass from ancestors to descendants. For each species, a possible ancestor was chosen from the set of all species within the same genus whose last appearance date overlaps with the first appearance date of the descendent. If no such species exists, a descendant was otherwise chosen from the set of species within the same genus that has the closest last appearance date. If multiple species fit this requirement, we randomly drew an ancestor with uniform probability for all potential ancestors. We estimated the strength of Cope's Rule, λ, such that $\langle \ln \lambda \rangle = \langle \ln M_D / M_A \rangle$, where M is mass of the descendent (D) or ancestor (A) and the brackets donate the average. We followed this process for all species, excluding genera with only a single species. We repeated this process 5,000 times and took the average strength of Cope's Rule across runs.

Estimating Extinction Risk

A predicted increased risk of extinction at larger body sizes provides a soft-upper bound on the body mass distribution, as larger species are more likely to go extinct. We first estimated the minimum physiological size and Cope's rule independently of the model. Using the independent estimates of the minimum size and Cope's rule, yielded one free model parameter—an increased risk of extinction with larger body sizes—which we estimated by minimizing the distance between the steady state model distribution and the empirical distribution using a weighted Kolmogorov-Smirnov (Massey 1951) test.